

THE UNIVERSITY OF MELBOURNE

**The Synchronisation Relationship  
Between Fetal and Maternal  
cardiovascular systems**

by

Qianqian Wang

Department of Electrical and Electronic Engineering  
Melbourne School of Engineering  
The University of Melbourne

Thesis submitted to University of Melbourne  
for the Degree of  
Master of Philosophy

September 2015

*Produced on Archival Quality Paper*

# Declaration of Authorship

*This is to certify that*

- (i) the thesis comprises only my original work towards the degree of Master of Philosophy except where indicated in the Preface,*
- (ii) due acknowledgment has been made in the text to all other material used,*
- (iii) the thesis is fewer than 50,000 words in length, exclusive of words in tables, maps, bibliographies and appendices.*

Signed: 王偉偉

---

Date: 16/09/2015

---

## *Abstract*

During pregnancy, the fetal physiological condition is carefully checked and monitored during the foetus' development. It is well known that the health of the foetus relies heavily on the nutrient and oxygen supply. The oxygen and nutrient supply is exchanged from the maternal vessel to the fetal vascular system via maternal placenta.

The hypothesis that this research is trying to prove is that there may exist a strong synchronised relationship between the maternal and fetal cardiac systems, and the relationship may also correlate to the gestation period. The focus of the research was to extract fECG and mECG using non-invasive abdominal recordings and analyse the relationship between the parameters derived from the ECG signals. The research used derived parameters from the abdominal recordings to analyse the relationship between the maternal and fetal cardiac systems.

To do this the fECG and mECG signals need to be separated from multiple abdominal and thoracic signals from open online source recordings. The principle of the ECG separation was based on independent component analysis (ICA) that considers multiple component signals statistically independent to each other.

The pairs of extracted fECG and mECG signals are analysed on the time scale to investigate the synchronisation relationship. Being able to extract the heart rate of fetus and the mother independently is the key to determining the existence of a synchronised relationship between the separate cardiac systems.

The findings from the fECG and mECG recordings at different gestational periods is that there is a direct relationship between the mother's cardiovascular system on the foetus, it may be caused by the nutritional influence during certain gestation periods.

## *Acknowledgements*

I would firstly like to thank Dr.Ahsan Khandoker and Prof. Marimuthu Swami Palaniswami for their guidance, encouragement and good advice. This thesis is a much work better thanks to their supervision.

My thanks must also go to Prof.Yoshitaka Kimura and his team from Kimura Laboratory Department of Gynecology and Obstetrics, Tohoku University Graduate School of Medicine, who, in spite of having practically no spare time, still managed to find time to provide patient data and clinical advice.

Finally, I would like to thank my family and friends for all their invaluable support.

# Contents

<b>Declaration of Authorship</b>	<b>i</b>
<b>Abstract</b>	<b>ii</b>
<b>Acknowledgements</b>	<b>iii</b>
<b>List of Figures</b>	<b>vii</b>
<b>List of Tables</b>	<b>ix</b>
<b>1 Introduction</b>	<b>1</b>
1.1 Physiological structure of fetal cardiovascular system . . . . .	1
1.2 Measurement of fetal cardiac function . . . . .	2
1.2.1 Electrocardiogram (ECG) . . . . .	3
1.2.2 Cardiotocography (CTG) . . . . .	3
1.3 Synchronisation . . . . .	3
1.3.1 Proposed synchronisation relationship between fetal and maternal cardiac system . . . . .	3
<b>2 Literature Review</b>	<b>5</b>
2.1 Blind source separation . . . . .	5
2.2 Empirical mode decomposition . . . . .	6
2.3 Singular value decomposition . . . . .	7
2.4 Adaptive filter . . . . .	7
2.5 Wavelet transform . . . . .	8
2.6 Clustering . . . . .	8
2.7 Neural network . . . . .	9
<b>3 Material and Method</b>	<b>10</b>
3.1 Recorded database . . . . .	10
3.1.1 The recording data . . . . .	10
3.1.2 The online database . . . . .	10
3.1.3 Heart sound . . . . .	11
3.1.4 Mouse data . . . . .	11
3.2 Measurement variables . . . . .	12

3.3	Synchronisation variables . . . . .	12
3.4	Signal processing . . . . .	14
3.4.1	Preprocessing . . . . .	14
3.4.1.1	Process data selection . . . . .	14
3.4.1.2	Resampling and modification . . . . .	15
3.4.1.3	Whitening . . . . .	17
3.4.1.4	Baseline wander . . . . .	17
3.4.2	Independent component analysis (ICA) . . . . .	18
3.4.3	Clustering . . . . .	21
3.4.3.1	K-mean clustering . . . . .	22
3.4.3.2	Fuzzy clustering . . . . .	23
3.4.4	Beamforming . . . . .	24
3.4.5	Transform of mECG signal in thoracic and abdominal signal . . . . .	25
3.4.6	Power spectral . . . . .	26
3.4.7	Learning iterative loop . . . . .	26
3.4.8	Template construction of ECG . . . . .	27
3.4.9	Empirical mode decomposition (EMD) . . . . .	28
3.4.10	Singular value decomposition (SVD) . . . . .	28
3.4.11	Mask for fECG . . . . .	29
3.4.12	Adaptive filter . . . . .	29
3.4.13	Frequency filter . . . . .	30
3.4.14	Other approaches . . . . .	30
3.4.15	Heart sound processing . . . . .	32
3.4.16	Mouse data . . . . .	33
<b>4</b>	<b>Result</b> . . . . .	<b>35</b>
4.1	Signal processing . . . . .	35
4.1.1	Noise . . . . .	36
4.1.2	Baseline wander . . . . .	36
4.1.2.1	Smooth . . . . .	36
4.1.3	Cross correlation variables . . . . .	37
4.1.4	Independent component analysis . . . . .	38
4.1.5	Frequency domain . . . . .	39
4.1.6	Clustering . . . . .	39
4.1.7	Singular value decomposition . . . . .	40
4.1.8	Empirical mode decomposition . . . . .	41
4.1.9	Adaptive filter . . . . .	41
4.1.10	Other approaches . . . . .	41
4.2	Heart rate . . . . .	41
4.2.1	<i>PhysioNet</i> recordings . . . . .	41
4.2.2	Subjects at various gestation period recordings . . . . .	43
4.3	Synchronisation . . . . .	45
4.3.1	Synchronisation ratio . . . . .	48
4.3.2	Phase locking value . . . . .	49
4.3.3	Synchronisation epoch . . . . .	52
4.3.4	Same subject . . . . .	54
4.4	Fetal heart sound . . . . .	54

4.5	Mouse data	56
<b>5</b>	<b>Discussion</b>	<b>58</b>
5.1	Signal selection	58
5.2	ECG pattern	58
5.2.1	Normalisation of ECG interval	60
5.3	Signal processing	60
5.3.1	Assumption	60
5.3.2	Error	61
5.3.3	Effect	61
5.3.3.1	Noise	61
5.3.3.2	Motion artifact	62
5.3.3.3	Cardiorespiratory	62
5.3.4	Independent component analysis	63
5.3.5	Clustering	63
5.3.6	Empirical mode decomposition	64
5.3.7	Adaptive filter	64
5.3.8	Learning algorithm	64
5.3.9	Wavelet transform	64
5.3.10	Frequency domain	65
5.3.11	Beamforming	65
5.3.12	Other approaches	66
5.3.13	Selection of the algorithms	66
5.3.14	Cross correlation	66
5.3.15	Very low frequency component	67
5.4	Demographic information	67
5.5	Synchronisation	68
5.5.1	Synchronisation ratio	69
5.5.2	Phase locking value	70
5.5.3	Same subject	70
5.5.4	Statistical comparison analysis across the gestation groups	71
5.6	Heart rate	71
5.7	Gestation period	71
5.8	Oxygenation level	72
5.9	Proposed relationship	72
5.10	Heart sound	73
5.11	Mouse data	73
<b>6</b>	<b>Conclusion</b>	<b>74</b>
6.1	fECG signal separation from abdominal signal	74
6.2	The synchronisation analysis between fetal and maternal cardiac system	75
	<b>Bibliography</b>	<b>77</b>
	<b>Appendix</b>	<b>88</b>

# List of Figures

1.1	The ultrasound image of fetal heart from online source [43] . . . . .	2
3.1	A pair of abdominal and thoracic recordings of one subjects from <i>PhysioNet</i> . . . . .	11
3.2	The abdominal recordings at two different abdominal electrodes . . . . .	12
3.3	The fetal and maternal ECG signal forms synchronisation points and phase locking value of corresponding synchronisation points . . . . .	14
3.4	The alignment of mECG QRS peak in both abdominal and thoracic recordings . . . . .	16
3.5	The first minute recording of heart sound with heart sound peaks . . . . .	32
3.6	The heart sound recording filtered by high and low frequency filters . . . . .	33
3.7	The fetal ECG from normal mouse including events of clipping and opening . . . . .	34
4.1	The gradient of abdominal signal after removal of white noise . . . . .	35
4.2	The three original abdominal recording with visible potential fECG peaks from <i>PhysioNet</i> . . . . .	36
4.3	The baseline wander signal and result abdominal signal after removal of baseline wander . . . . .	37
4.4	The extracted fECG is compared to the potential fECG peak in abdominal recording . . . . .	38
4.5	The ICA separated component corresponding to fECG signal (blue) and filtered signal for peak detection signal (red) . . . . .	39
4.6	The maternal heart rate in the overall analysis interval for subjects from <i>PhysioNet</i> . . . . .	42
4.7	The mean and standard deviation of fetal and maternal heart rate for subjects from <i>PhysioNet</i> . . . . .	42
4.8	The fHR at corresponding gestation period for subjects from <i>PhysioNet</i> . . . . .	43
4.9	The relationship between maternal and fetal heart rate at corresponding gestation period, red is low gestation period, blue is median and green is high . . . . .	44
4.10	The fECG and mECG extraction from abdominal and thoracic signals and synchronisation relationship between the two signals at various primary cycles . . . . .	45
4.11	The corresponding relationship between the number of synchronisation points and duration of synchronisation at synchronisation ratio 3:5 and 4:7 . . . . .	46
4.12	The synchronisation stability at corresponding heart rate ratio in log scale . . . . .	47
4.13	The effect on the variation of synchronisation by the variation of mHR . . . . .	47
4.14	The synchronisation of fECG at primary cycle 3 and 4 mECG cycles results various synchronisation ratio for 4 subjects from <i>PhysioNet</i> . . . . .	48

---

4.15	The synchronisation ratio with effect from heart rate variables at corresponding synchronisation epoch, red is low gestation period, blue is median and green is high . . . . .	49
4.16	The fetal and maternal heart rate, synchronisation phase locking value and gradient of phase locking value . . . . .	50
4.17	The gradient of phase locking value at primary cycle 2 and 3 . . . . .	51
4.18	The gradient of phase locking value at three different gestation groups of data in 120 seconds . . . . .	51
4.19	The gradient of phase locking value of subjects in individual gestation groups in 120 seconds (Top: Low gestation group, Middle: Median gestation group, Bottom: High gestation group) . . . . .	52
4.20	The normalised synchronisation epoch at major synchronisation ratio for the three gestation groups . . . . .	53
4.21	The normalised synchronisation epochs at corresponding synchronisation ratios . . . . .	53
4.22	The heart rate and synchronisation behaviour of same subject at different gestation period . . . . .	54
4.23	The preprocessing stage of heart sound recording to enhance the peaks of ECG signal . . . . .	55
4.24	The envelop of heart sound signal with manual selected potential heart sound region . . . . .	55
4.25	The ICA component of heart sound recording for best representation of heart sound signal . . . . .	56
4.26	The fetal ECG from low protein intake mouse including events of clipping and opening . . . . .	56
4.27	The fetal heart rate from normal mouse at individual event interval . . . .	57

# List of Tables

4.1	The mean and standard deviation of heart rate at three gestation groups, where red is low gestation period, blue is median and green is high . . . . .	44
4.2	The p-value of statistical property of synchronisation behaviour at 6 major synchronisation ratios between the three gestation groups . . . . .	52
5.1	The demographic information of recorded subjects . . . . .	67

# Chapter 1

## Introduction

### 1.1 Physiological structure of fetal cardiovascular system

The cardiovascular system supplies oxygen to the cells of body and is essential to foetal development. The foetal cardiovascular system works differently to the adult system it is derived by isolating air from the placenta. Due to the limited amount of oxygen that the foetus can extract from the placenta, the foetus exists in a state of relative hypoxia compared to an adult[28]. The oxygenated blood is supplied through umbilical cord from maternal cardiac system to the fetus. Once the oxygenated blood arrives at the foetus, the cardiac system takes the most highly oxygenated blood to heart through the inferior vena instead of the pulmonary veins [26].

The foetal heart has an additional foramen ovale that makes the blood flow to be different from adult's blood flow. The foramen ovale along with the Eustachian valve moves oxygenated blood from the right side of the heart into the left atrium, then via the left ventricle into the aorta to supply blood to the head [31]. The Eustachian valve is a separation barrier between the inferior and superior vena cava to block the blood to flow across in order to keep the relatively high saturated blood passing into the left atrium then to the brain [27].

The desaturated blood from fetal body returns to heart through the superior vena cava and passes the tricuspid valve into the right ventricle [33]. Then it goes into the pulmonary artery through the ductus arteriosus into the descending aorta. The fetus heart starts to beat and pump blood from gestation period of 7 weeks, the range of the fetal heart rate (fHR) is 120-180 beats/min (BPM)[43]. During the total pregnancy variations in foetal BPM can be caused by fetal motion or various maternal psychological states. Also some researchers believe that decreases of fHR can create variability with the hypoxigenation of the maternal arterial blood [28].

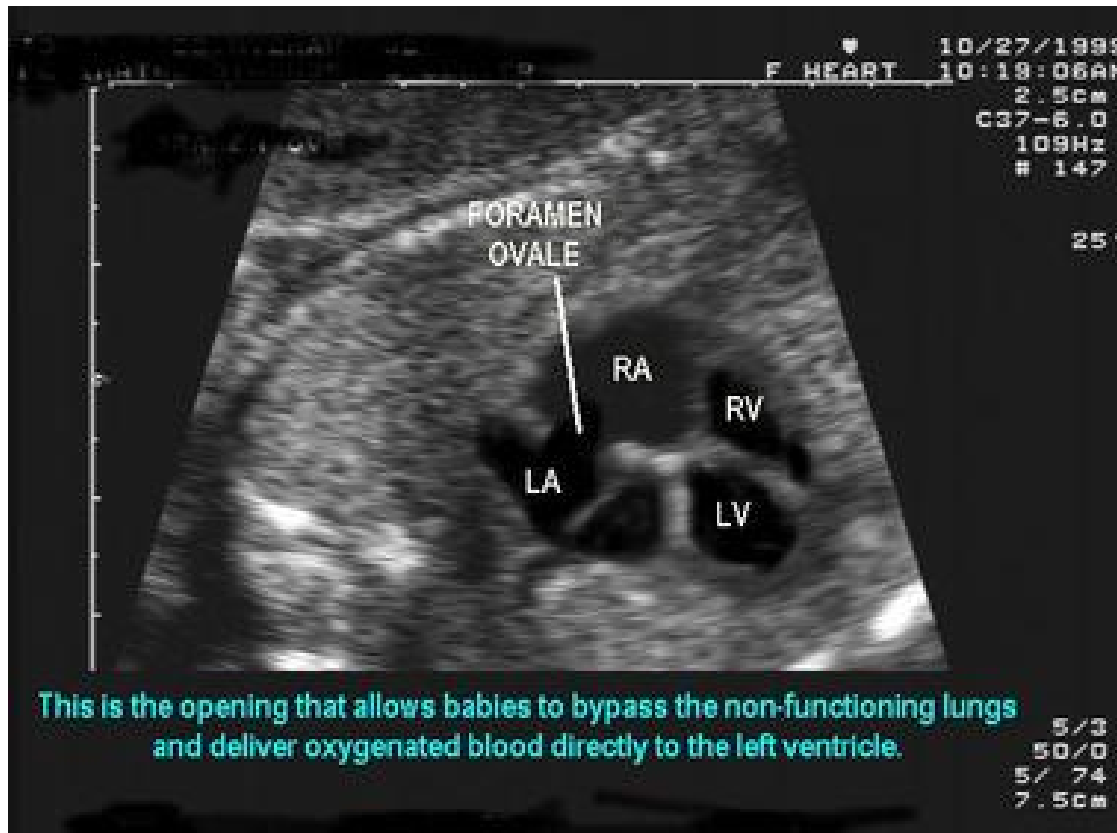


FIGURE 1.1: The ultrasound image of fetal heart from online source [43]

In general, the heart rates decrease with the increase of age, but fetus in longer gestational periods does not have faster heart rate.

## 1.2 Measurement of fetal cardiac function

The general feature of cardiac function is indicated by pressure, sound, flow and electrical potential. The pressure in the heart chamber includes the aortic pressure, left ventricular pressure and left atrial pressure. The recording of heart sound, the ventricular volume, the blood flow such as aortic flow and the electrical potential of myocardium polarisation and depolarisation by ECG, are the common approaches to measuring the functional behaviour of the heart [22]. The target variable measurement is the flow velocity related to the heart valve function which forms the turbulence of blood flow. The signal from cardiotocography (CTG) is in sound wave form which represents the frequency property at each stage of cardiac cycle. Tissue Doppler Imaging focuses on the movement of the myocardium including contraction and relaxation within the cardiac cycle [18].

### 1.2.1 Electrocardiogram (ECG)

The electrical propagation is the essential physiological activity that causes the contractions and relaxations that allows the heart to pump blood. The ECG is relevant to detecting the primary function of the heart

Lately, the non-invasive of fECG recording has been introduced for research purpose and it extracts the fECG from the multiple recordings collected by the electrodes at maternal abdomen. The major problem associated in the non-invasive approach is the low signal-to-noise ratio (SNR) caused by the weak fECG signal and strong mECG recorded from the surface of maternal abdomen.

### 1.2.2 Cardiotocography (CTG)

The heart sound is produced by valves opening and closing which means the sound of the heart only indicates the functionality of the valve. The ventricular contraction is when the mitral valve opens and the tricuspid valve closes - this creates the first sound heard with the second heart sound coming from the closure of the aortic and pulmonary valves.

The first heart sound follows R waves of ECG patterns which are formed by ventricular contraction. The second heart sound is at the end of the T-wave which is when the ventricles relax. The abnormal existence of third and fourth heart sounds are caused by sudden termination of ventricle and atrial systole.

## 1.3 Synchronisation

The synchronisation behaviour between two separate systems is caused by the interaction of a weak external force on each system and can be found between the cardiac and respiratory systems. It is known as the cardiorespiratory synchronisation, which sees the neural system act as the external force to balance the function of the two systems [9]. The synchronisation relationship is analysed by the synchronisation phase of the events in one system with respect to the cycle of the other one [23].

### 1.3.1 Proposed synchronisation relationship between fetal and maternal cardiac system

The hypothesis of this research paper is to investigate the existence of the synchronisation relationship between the fetal and the maternal cardiac system using ECG recordings.

The possible synchronisation relationship between fECG and mECG is analysed in two individual biological systems. The analysis principle is adopted from the cardiorespiratory synchronisation, which uses similar mathematical equations to calculate the synchronisation phase. The difference is that the fetal signal is analysed as the time point of QRS peak instead of the entire ECG cycle, which is used for cardiac signal in cardiorespiratory synchronisation.

The physical connection of oxygen supply for the fetal system is the hypothesized mechanism of the synchronisation relationship. The oxygen supply for the fetal system totally relies on the oxygenated level in the maternal cardiovascular system, which indirectly links the maternal cardiac functionality to the fetal cardiac system.

During the fetal development, the growth of the fetal myocardium may change the heart function behaviour, leading to various synchronisation behaviours during different gestation periods. The extended theoretical hypothesis is about the relationship between the saturation level of blood oxygen and heart rate of the maternal heart rate and if this relates to the fetal heart function because of the oxygen exchange.

The gestation period is proposed to link the synchronisation relationship between the fetal and the maternal cardiac cycle in a reciprocal relation and as the gestation period grows longer, this leads to a weaker synchronisation relationship especially towards labour time when the two cardiac systems would separate entirely.

There is however a second possible relationship involving the gestation period which may prove there is increased strength of synchronisation during the fetal development, which means the synchronisation is stronger the longer the gestation period goes on.

This theoretical prediction may also follow the pattern that a positive relationship occurs until a certain stage which may be close to the time of labour at which point the synchronisation relationship then starts to get weaker.

## Chapter 2

# Literature Review

### 2.1 Blind source separation

Blind source separation is commonly achieved by applying independent component analysis (ICA) which was developed to solve a "cocktail party problem" which uses multiple microphones positioned at different places in a room to enable recording of speech from several people [46]. The sources are assumed to be mixed by a square matrix and recording positions of the individual sources has the same number of mixing coefficients and these related to the number of microphones used in the cocktail party problem. The de-mixing matrix calculates independent signals and their relation to each other.

ICA separates multiple sources from the mixing recording by the equation  $X=AS$ , where  $X$  is a multiple dimension input which is the matrix of all the source signals,  $A$  is the de-mix coefficients derived from ICA algorithm and  $S$  is the mixed signal matrix [44]. The single channel ICA (SCICA) is developed to extract a mix of multiple source signals into a single recording. SCICA takes the scalar time series to form a multi-dimension matrix as the input of ICA, it breaks the single signal into the multi-dimension vectors with a delay factor.

The principle of ICA is to maximize the non-gaussianty of the mixed sources by the weight coefficient. It is based on the statistics value to maximise joint entropy or minimise mutual information. The common ICA component calculation uses the fourth-order cumulant or kurtosis [44].

$$\text{kurt}(v)=E(v^4) - 3(Ev^2)^2 \quad (2.1)$$

The measurement of non-gaussianity can also be calculated from Negentropy as  $J(y) = H(y_{gauss}) - H(y)$  [58]. In the general process of ICA, the number of sources is assumed to be equal to or less than the number of recorded signals except for SCICA and all the source signals are assumed to be independent to each other. Also the mixing of the source signals is assumed to be linear, stationary and ideally noiseless in order to apply to independent component strategy. The variations of ICA approaches have been applied to separate fECG from the abdominal recording in a few publications and those ICA algorithms use the maximum non-gaussianity of components along with the pre-processing algorithms to increase the SNR.

Jimenez-Gonzalez demonstrated the procedures of constructing a multiple dimension matrix from a single phonogram vector with a shift variable that is dependent on the frequency ratio of the potential source components [53]. The multiple components are projected onto the subspace by a linear transformation to de-mix the source signals. ICA is also applied as a pre-processing method to remove the artefact noise from the bio-signal since the artefact component is independent from the main signal [7]. The ICA algorithms normally involve the higher-order statistical approach to maximise the independence, so the infomax in Bell-Sejnowski algorithm is the neural network gradient, and approximates the diagonalization of the eigenmatrices (JADE) [50].

The principle component analysis (PCA) and singular value decomposition (SVD) are applied at the pre-processing stage and the covariance is taken as the target variable to construct the mixing coefficient of ICA [25]. The construction functions of negentropy are:  $G(\mu) = \frac{1}{\alpha} \log \cosh(\alpha, \mu)$  and  $G(\mu) = \exp(-\frac{\mu^2}{2})$ , Fast ICA is selected as ICA algorithm [76]. PCA uses the linear projection to find the largest variation for the most information by the eigenvectors and it is based on the direction of maximal variance in Gaussian data.

## 2.2 Empirical mode decomposition

The intrinsic mode functions (IMF) from the empirical mode decomposition (EMD) use the frequency order to separate the input signal into multiple ordered elements without introducing cut-off frequency. The principle of EMD is to locate the local maxima and minima to form sinusoid waveforms, so it breaks the ECG into several segment signals. The primary element is taken as the most frequent peak with the highest amplitude. But the principle contradicts the actual property of the mECG and the fECG. In normal case, fECG peaks have higher frequency and mECG peaks have greater amplitude.

After each estimation step, the reduced frequency will not cover the complete fECG peaks. The smooth filter also extracts each component into the form of sinusoid function that is similar to the principle of empirical mode decomposition (EMD), but result from smooth filter is the superposition of multiple sinusoid functions, which is not the case for EMD. EMD is used with ICA to decompose the input signal into the subband IMFs and the IMFs are combined into multi-dimension matrix input for PCA [104]. Because EMD is noise sensitive, a noise parameter can be included to generate the multi-dimension input for FastICA with the minimised noise effect [73].

## 2.3 Singular value decomposition

The singular value decomposition (SVD) can decompose a single vector to a multi-dimension vector by applying the eigenvector. SVD takes the periodic input matrix and produces the singular values of the matrix [118]. The singular values encode the prime information of the quasi-period signal, so the ECG components are constructed into a few dominant singular triplets. The maternal ECG signal is considered to be the dominant vector in the abdominal recording, so it can be constructed as the first in the ranking matrix of the singular values [55]. The fECG is calculated as the difference between the abdominal and constructed mECG signal.

## 2.4 Adaptive filter

The adaptive filter applies the square mean error to update the filtering coefficient between the input signal and desired signal. The least mean square (LMS) algorithm feeds the difference between the processed signal and input signal back to the loop until the coefficient of the estimation factor for the reference signal reaches stable state. The adaptive filter has been applied with the noise reference signal to construct the fetal heart sound with the weight coefficients [74]. The Finite Impulse Response (FIR) adaptive filter enhances fECG by applying LMS and it can be used to estimate the fECG from abdominal mix [54]. The LMS adaptive filter is used to detect the QRS complex of the mECG that can be taken as the reference template from the abdominal signal. The subtraction result of the abdominal signal and mECG is fECG signal [2].

## 2.5 Wavelet transform

The wavelet transform is to apply decomposition to both the frequency and the time domain to separate the embedded source signals. The mother wavelet is a unity signal with zero mean and generally selected to have similar pattern feature of the estimated signal. The Discrete Wavelet Transform is used to remove the artifacts based on the spectral separation in order to break the single channel to multiple output [103].

## 2.6 Clustering

The clustering data is grouped according to the centre mean of each group in term of X-Y relationship, so each point in the vector belongs to one of the groups according to the X and Y reference. The K-nearest neighbour classifier and k-means clustering are used to identify the ECG by determining the distance from the points to the k-nearest point. In k-means clustering classifier, k is the number of prototype centre to be assigned with the outlier score and it is used to characterise the degree to the outlier. The number of clusters is calculated as the square root of the total number of sources over 2 and also the boundary curve represents the separation between two classes. The hard cluster is to separate data to only one cluster and no empty cluster, but the fuzzy cluster allows data to belong to multiple clusters with probability as  $f(x) \in 0, 1$ . The cluster is sensitive to the initial assumption and it is better to use hard cluster for ECG separation.

The Euclidean distance counts the frequency of peak and interpolates to the maximum of a polynomial to fit the position where the peaks cross below the lowest displayed contour. The objective function is the sum of the cluster error as  $L_{km} = \sum_{k=1}^k \sum_{i \in G_a} \|s_i - b_k\|^2$ , where k is the number of cluster,  $b_k$  is the representative prototype of the cluster  $G_k$ . The first step of clustering is to estimate the prototype, then the sample is assigned in an iterated loop until locating the local minimum. The different initiation can cause convergence to a different local optima. The low-dimension signal can be computed into high-dimension by the fuzzy cluster, it converts the time series vectors with delay coordinate into multi-dimension matrix. It then projects each point in the trajectory orthogonally onto the original vector to convert the processed matrix back to the scalar time domain.

$D(x,c)$  is the distance or dissimilarity between a feature vector x and cluster c, threshold q of dissimilarity is the maximum allowable number cluster. The vector is considered to be mECG signal in the case of ECG processing, the initial number of cluster m is 1 and the cluster contains the first data point. The next step is to check the distance between the next data point to the data in the different clusters, if the distance exceeds

the threshold of dissimilarity,  $m < q$ , a new cluster is created for next data, otherwise the data is grouped into the cluster with the minimum distance with all the data in the cluster.

The clustering method is used to detect the outlier and to remove the noise, which is formed by the points far away from the centroids of the major clusters that is constructed by k-mean [121]. The k-mean clustering is based on the measurement of the cost function for the dissimilarity and the fuzzy C-mean clustering groups the data based on the degree of membership [38]. The clustering approach is a self-organizing network and it is used to identify the feature of QRS complex, it maps the multi-dimensional vector onto the two-dimensional space [66]. The unsupervised learning process in clustering starts the training steps from initialising the weights till it reaches the termination criteria.

## 2.7 Neural network

In the neural network, the thoracic and abdominal signals are fed to several classification network neurons and the output signals are assigned to the output layer with the correlation coefficients to the other output components. The neural network applies the taps to the signal data at each stage to condense the signal feature into the single value, which indicates the overall feature of signal. The kernel neural network classifies the objects based on the closest training examples in the feature space, by giving a neighbour weight of  $1/d$ , where  $d$  is distance to the neighbour. The neural network is included as the pre-whitening procedure and it also can be used for the separation of sources in blind separation by deriving the total separating matrix from several steps [20]. The neural learning rules set for the pre-whitening combine the mixing and de-correlation algorithms. The Finite Impulse Response (FIR) neural network is taken for the noise cancellation to extract the fECG and the weight of the network model is a FIR linear filter [13]. The network tracks the maternal signal with the registers by training the temporal backpropagation algorithms. The FIR neural network takes the weighted sum of the delayed input signal into the multiple layers of the neurons and the learning rate and parameters are adjusted to extract fECG with thoracic signal as additional reference [14].

## Chapter 3

# Material and Method

### 3.1 Recorded database

#### 3.1.1 The recording data

There are 40 pairs of fECG and mECG recordings collected from 38 subjects included in the database, it also includes the gestation period of pregnancy. Two of the subjects are recorded repeatedly at two different gestation period. The original ECG signals are recorded with 11 abdominal electrodes non-invasively in an external institution group and only the extracted fECG and mECG signals in the duration of 1 minute are provided.

The gestation period is in the range of 16 weeks to 40 weeks with the average of 30.61 weeks and variation of 7.48 weeks. Most the of recordings have the duration of ECG in 1 minute, except for one subject at 24-week gestation period having only 50 second ECG recordings. The grouping of the subjects to analyse the gestation period is separated as below 29 weeks, 29-35 weeks and above 35 weeks in term of low gestation period ( $L_{gp}$ ), medium gestation period ( $M_{pg}$ ) and high gestation period ( $H_{gp}$ ).

#### 3.1.2 The online database

The data used to develop and test fECG separation from abdominal recording are all from an online database *PhysioNet*. *PhysioNet* was the source for 2 thoracic recordings and 3 or 4 abdominal recordings per subject (the number of abdominal recordings varies for different subjects).

The recording frequency is constantly 1kHz and the duration is all longer than 60 seconds. The processing data is selected from 60 second durations to keep the comparison

consistent. Because there are no actual recordings of fECG as a reference signal in the database to test the result of extraction, the possible validation is done by visual comparison of fECG peak in the abdominal signal. After manually checking the fECG existence in the abdominal recordings, 20 out of 55 subjects are selected from the data source to develop and test the fECG separation algorithms.

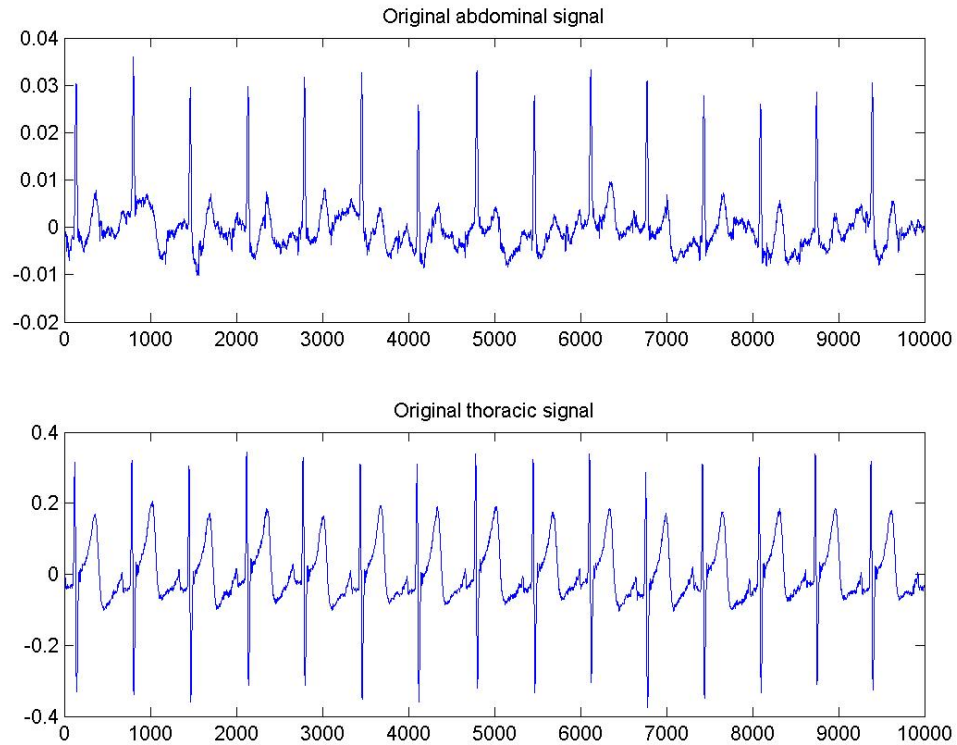


FIGURE 3.1: A pair of abdominal and thoracic recordings of one subjects from *PhysioNet*

### 3.1.3 Heart sound

The abdominal heart sound is recorded by a mobile phone, the recording is a mix of both fetal and maternal heart sound.

### 3.1.4 Mouse data

The mouse data is to analyse the fetal and maternal heart rate in various conditions. The mouse ECG database compares two groups of mother mice in different conditions. One is the control group and the other has low protein intake.

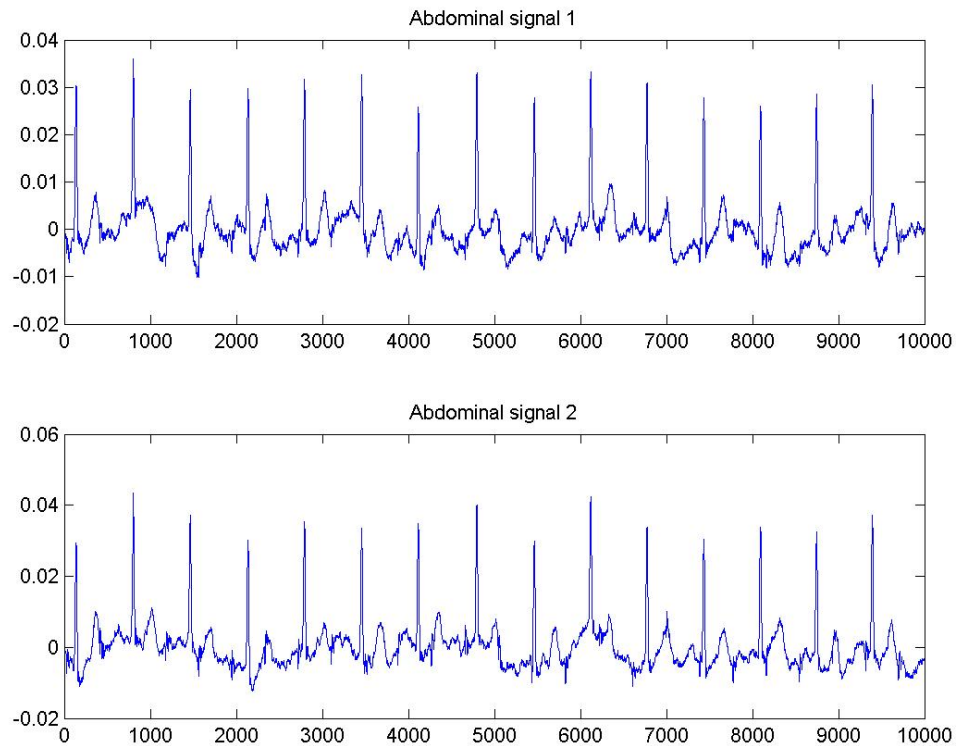


FIGURE 3.2: The abdominal recordings at two different abdominal electrodes

The recordings of the fECG and mECG are taken by the separated direct electrode contact on the fetal and maternal mice's heart and each recording contains 6 events with duration of 3 minutes in each event. Three of the events are clipping of the fetal artery and the other three is opening of the artery.

### 3.2 Measurement variables

The heart rate of fetus (fHR) and mother (mHR) are calculated from R-R interval of the individual fECG and mECG cycle as  $HR = \frac{Duration(s)}{RR} * 1000 * 60$  in the unit of beats/min. The mean and the standard deviation of fHR involved in the analysis are labelled as FM and FV, and the mean of mHR is MM, the mean value is the analysis variable for each subject.

### 3.3 Synchronisation variables

The ratio of the time interval between the mECG and the fECG is calculated from 4 time point variables, m1, m2, f1 and f2. The time duration between m1 and f1 is

$t_1$ , the interval  $t_2$  is between  $m_1$  and  $f_2$ . The ratio between the intervals  $t_1$  and  $t_2$  is not constant as the ratio of fHR and mHR is not integer. The initial design of phase between the adjacent fECG peaks within one mECG cycle is  $\frac{t_2+t_1-s}{t_2}$ . The number of synchronisation points (NP) and the time duration of synchronisation (TD) can reflect fHR by equation  $fHR = \frac{NP*N-1}{TD} * 60$ .

The synchronisation relationship is computed as the time point of the fECG peak with respect to different numbers of mECG cycles which is classified as one primary cycle. All the synchronisations are calculated in one primary cycle which can vary from 1 to 4 mECG cycles. The interval of the primary cycle reflects the synchronisation in short and long term. The time position of fECG QRS is calculated with respect to the primary cycle to analyse the synchronisation relationship between the fECG and the mECG. The number of mECG cycles in the primary cycle is defined as  $m$  and the number of fECG peaks in the primary is defined as  $n$ , so the synchronisation ratio (SR) is  $m : n$  and the high SR value reflects the fast mHR or the slow fHR. The time points of fECG peaks in the primary cycle are converted into the synchronisation coordinates. The phase of individual fECG peak  $\phi$  in the primary cycle:

$$\phi(t_i) = 2\pi \frac{t_i - T_m}{T_{m+1} - T_m} + 2\pi i \quad (3.1)$$

where  $t_i$  and  $T_j$  are the time point of fECG and mECG peak,  $i$  is the fECG peak order and  $m \in [1, 4]$ . The synchronisation coordinates of the phase  $\varphi$

$$\varphi = \frac{\text{mod}(\phi, 2\pi)}{2\pi} \quad (3.2)$$

Due to the variation of the heart rate, the synchronisation relationship may not be continuous during the entire recording time and the individual synchronisation segment is determined as synchronisation epoch (SE). The phase locking (pl) value is calculated from two adjacent synchronised primary cycles, it is the time between two synchronised fECG peaks of the same SR in the same order of the two primary cycles divided by  $n$  (as shown in Fig.3.3, phase locking value is  $b_1 - a_1$ ). The mean and the variance of the phase locking value ( $U_{pl}$  and  $V_{pl}$ ) are calculated for each individual epoch, the gradient of the phase lock value ( $S_{pl}$ ) is taken as an analysis factor for each SE. The synchronisation index (SI) is to take into account the statistical variables of fHR, mHR and SR:

$$SI = \frac{SR * MM * FV}{FM}. \quad (3.3)$$

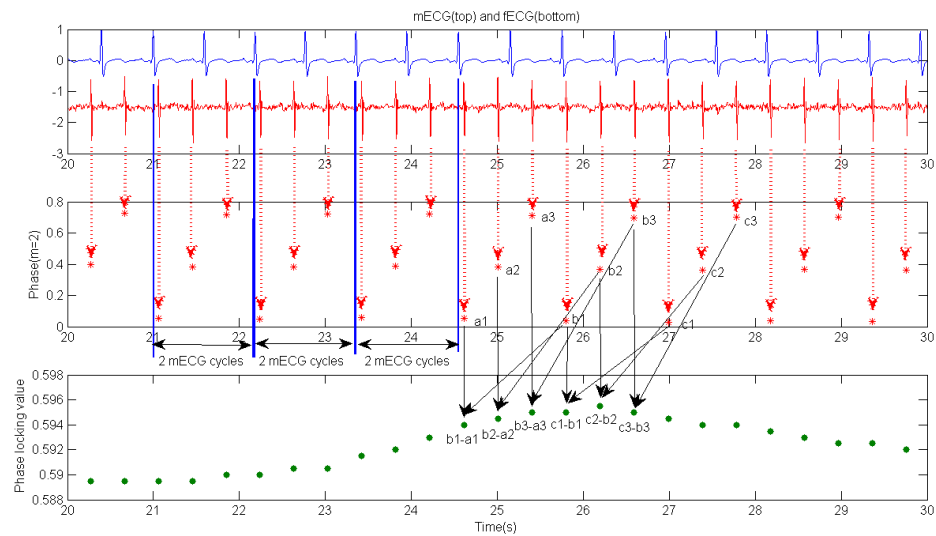


FIGURE 3.3: The fetal and maternal ECG signal forms synchronisation points and phase locking value of corresponding synchronisation points

### 3.4 Signal processing

The fECG is normally merged into the mECG signal and noise, and the pattern of the abdominal signal depends on the relative positions of electrodes. In the database recordings, the fECG is embedded in the mECG waveform which is not consistent in the three abdominal recordings. The abnormal mECG feature may not occur in every cardiac cycle, so the irregular change of the abdominal signal needs the thoracic signal as the reference to eliminate the abnormal mECG cycle from the abdominal signal first.

Heart disease will also cause inconsistent cardiac duration. The period of mECG cycle cannot be set as the reference to avoid the abnormal heart function to be taken into the algorithm development.

There are two groups of abdominal signal, one is the mECG with cycle duration referenced from the thoracic signal, the other group is the combination of the noise and the fECG signal. The abdominal recordings in most journal articles have similar pattern feature as the the gradient of the abdominal signals from *PhysioNet*.

#### 3.4.1 Preprocessing

##### 3.4.1.1 Process data selection

To develop the separation algorithm of the processing data, the input is selected to be a matrix of 3 abdominal and 1 thoracic signals. This procedure is applied to online data

as the recordings from this source have a large number of points to process. The data parameters are then set to include 1000 points to avoid any error messages *outofmemory* during the execution of functions in the MATLAB environment.

The thoracic and the abdominal signal are selected manually based on the curve feature of mECG data, the high frequency peaks with good gradients are assumed to be the fECG peaks in the abdominal recordings. The start of the analysis in the mECG cycle happens 1 second after the recording, so the calculation of the fECG phase starts from the fECG peaks in the first mECG cycle.

The cardiac cycle is calculated using the peaks in the thoracic recordings, and the distance between the peaks is set to be over a threshold variable based on the recording frequency and the normal heart rate range.

The aim of the selection is to eliminate any signal overshoot at the beginning of recording. The thoracic signal may be used with the abdominal signal for the fECG separation with the mECG cycle being selected as the start point. The start point is the first peak by the minimum threshold in both the abdominal and the thoracic signals and any fECG data that occurs before this point will be disregarded.

However, the individual cycle will not be aligned in the input matrix, because it requires a normal cycle duration. The processed data will be reconstructed into a 1-dimension vector and the length of each cardiac cycle will be extracted. The data is then processed in intervals of 3 seconds using *smooth* function. In order to avoid data exclusions during assigning the uncorrelated data to the reference signal, the data signals are constructed from a continuous point in the chain - point 1 to point 4 then point 2 to point 5 - over the entire recording.

### **3.4.1.2 Resampling and modification**

The process of taking every 10th data point to form a new data signal is similar to down-sampling the signal to a frequency of 100 Hz. During the process of down-sampling, some of the fECG peaks reduce in magnitude and this results in a smoothed waveform. Data in small windows with a similar mean and standard deviation, form the signal feature as the creation of the multi-dimension matrix for fECG separation uses a shift window.

The original ECG signals from the open source are modified to enhance the ECG peak magnitude. The square value of the original signal data will increase signal-to-noise ratio, but it removes the actual fECG pattern feature. Instead the transform function used to increase the fECG magnitude is *exp* function at the current stage, other potential

approach such as a match table for electrode position or transform function will be considered in the further work.

The cross correlation function calculates the maximum correlation variable by shifting the signal in time scale. The same mECG feature do not appear at the time in the thoracic and the abdominal recordings, and it is caused by the distance from the abdominal electrode to the maternal heart. The delayed time is calculated as the maximum correlation of the abdominal and the thoracic signal and the thoracic signal is shifted by the delayed time align the mECG feature in the two recordings. The first step to align the thoracic and the abdominal signal is to find the time point of the mECG peaks in the two signals. The delayed time( $D$ ) is calculated from the maximum correlation of one abdominal and one thoracic signal, and the thoracic signal(length  $l$ ) is shifted the delayed value( $m$ ).

$$C_{xy}(t) = E\{x_l y_{l-m}^*\}$$

$$D = i - l \quad (3.4)$$

where  $C_{xy}$  is the correlation of signal  $x$  and  $y$ ,  $C_{xy}(i) = \max(C_{xy})$ , whereas  $l \leq i \leq 2l$  and  $m > 0$  The shift of the thoracic signal to align the fECG peak is for generating the multidimension matrix for independent analysis and applying the adaptive filter to separate fECG.

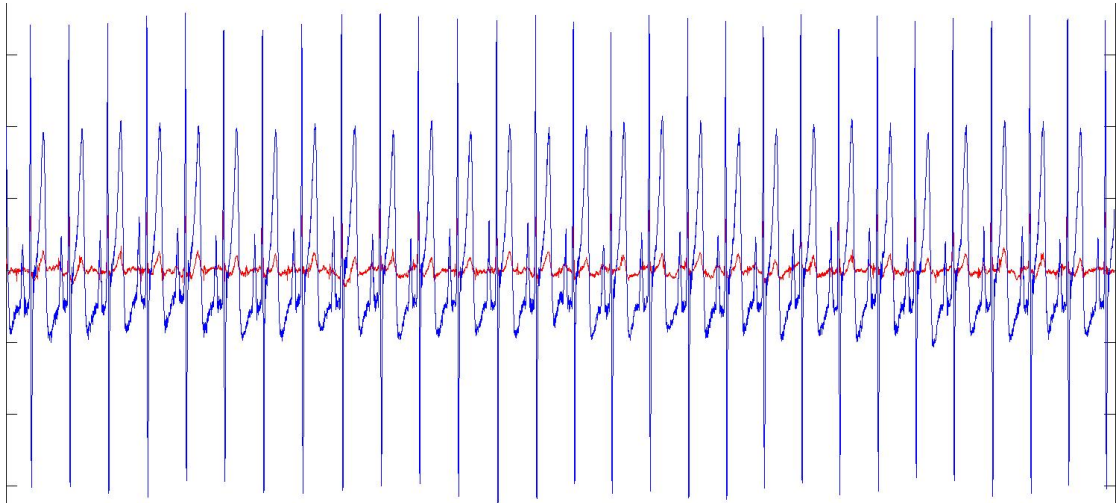


FIGURE 3.4: The alignment of mECG QRS peak in both abdominal and thoracic recordings

### 3.4.1.3 Whitening

The whitening process reduces the number of the components in the output matrix. One of the whitening strategies is to use a spherical cloud and then take the vectors of the system after shifting the centre of the data to the origin. The other whitening approach is to project the principle component analysis (PCA) mixture in the orthogonal direction of the maximum variance to rotate the matrix, and then the reduced matrix is taken as the input of independent component analysis. A long term ECG recording has a large number of data sets so PCA can reduce both the size and dimension of the processing data.

### 3.4.1.4 Baseline wander

The baseline wander is not used in the thoracic signal because the motion of the electrode at the thoracic is negligible during recording. The baseline wander is a low frequency component, the frequency range maybe overlap the low frequency segment of the cardiac cycle such as ST. The ST may be removed as part of the baseline wander by the noise filter. The spectrum of the abdominal and the thoracic signals after removing baseline wander shows the noise in low density region compared to the fECG peak and the thoracic spectrum is taken as the reference for the mECG spectrum. In the peak region, the relationship between the neighbour data points is not constant and has a minor variation around zero.

The first step is to extract all the mECG peaks in the thoracic signal using a threshold value in the recording, a moving average or a *smooth* function can remove both the peaks and noise and leave a low frequency component which relates to the baseline wander. The *smooth* function brings the signal to the zero-mean level and two main weighted scatter methods can be selected as option, *rloess* and *loess*. The *rloess* uses weighted linear least squares and  $^{nd}$  degree polynormal and *loess* applies the local weighted scatter plot smoothing. The number of data points taken for smoothing to construct the new signal is controlled by the parameter *span* which is the percentage of total number of data points, so a small sample number can construct the baseline wander smoothly with similar pattern features. The weight of function of *rloess* is

$$W(x) = (1 - |x|^3)^3 I[|x| < 1] \quad (3.5)$$

The more data used, the closer the smoothed result to the original signal. However, the baseline wander is a low frequency component which will require fewer data points to form the pattern. The weight of the adjacent data points is used to determine the

number of data points for baseline wander removal, and R-R interval of mECG is taken as the reference in order to select the neighbour points according to the time of each segment in the cardiac cycle.

Each abdominal signal is smoothed by *rloess* and the sum of the abdominal signal is smoothed after adding the original non-smooth abdominal signal to overcome the motion artifact of the individual electrode. The abdominal electrodes record the abdominal motion at different orientations during breathing and this motion artifact can be removed as part of the baseline wander. The sum of the three abdominal signals is applied afterwards because the motion artifact may partially cancel each other out.

### 3.4.2 Independent component analysis (ICA)

The assumption of applying ICA is that the source signal is noise-free and a zero mean, it uses linear transforming apply a result the correlation matrix. The source signals of the mixing input are from two separate biological systems, which are non-Gaussian so they are considered as independent sources [12][29]. The number of output signals separated from ICA process is determined by the dimension of the input matrix. The iterative weight factor is optimised based on maximising independence or the correlation of the statistical property. Even the abdominal signal is a blind source signal and both the fECG and mECG components share the similar pattern at QRS.

Prior knowledge of signal property can be introduced as the parameter of the algorithm to separate two sources. The frequency feature of the mixing signal embeds separable properties of each component as opposed to the original single signal. So applying ICA in the frequency domain may assist but adding frequency properties may not assist to identify the ECG from the separated components.

The adaptive filter with the shifted thoracic and abdominal signals as an input can generate a multi-dimension matrix which can be applied as the input for ICA (the matrix has the smaller density on mECG compared to the original abdominal signal). The recording results from the abdominal signal is a blind source mix because the three electrodes only record the mix of mECG, but both fECG and noise are present [32]. It will require the prior knowledge of the number of source component and the partial region waveform of each component to accurately apply ICA.

The fECG and noise are unknown signals with mECG being partially unknown so in total there are 2 unknown sources signals and 1 partially known source signal. To work with the partially known sources, we need to create a new BSS model. The first step of the signal separation is to convert the thoracic signal to mECG signal that matches

the pattern feature of mECG in the abdominal signal. The second step is to input the modified source signals into the BSS model. The transformation of the mECG pattern in the thoracic and the abdominal signal can be either linear or nonlinear. The transformation algorithm converts the signal pattern based on the relationship between the depolarisation peak in the signal and electrode at the heart location. The abdominal signal is taken as a semi blind source as it needs to have magnitude and shape like the ECG pattern. The mECG can span the subspace into 3 linear independent vectors and the fECG can span into 2, the abdominal signal is broken into individual cardiac cycles.

The first step of ICA is to move the input signals to the zero mean level by subtracting the row mean of the matrix vector. Then it finds the eigenvalue and eigenvector of autocorrelation and sorts the positive eigenvalue and eigenvector in a descending order to project the input signal onto the scaled eigenvector by the matrix multiply. The last step is to find the ICA direction[30].

Processing of the non-gaussianity of components in the ICA process maximises the correlation between mECG and fECG in the thoracic signal without including the high frequency components. If the mECG pattern in the thoracic and the abdominal recordings is not constant, they will be separated into two signal patterns. Two thoracic signals can be used as input for ICA to separate the segments of mECG cycle into the two components.

However, if the thoracic signal is broken into cycles, the number of input signals can be greatly increased and the number of mECG cycle components would increase too. The positions of the abdominal and thoracic electrodes is classified as "unknown information" in the entire open database, but the correlation relationship between the individual abdominal recording suggests that those electrodes are close in position and will directly affect the functionality of the multiple source independent component analysis [21].

The correlation coefficient of two abdominal signals is high and the average is above 0.8. Also, the pattern shapes of all the abdominal signals are generally the same. This indicates coefficients of the source signals are similar for each recording channel. The mixing matrix has mECG as the dominant source signal, the fECG as the other source signal is recorded with the negligible mixing coefficient at all the abdominal electrodes. In this case, the three abdominal signals cannot be considered as the input matrix for ICA because the mixing coefficients of the sources are similar across the three signals.

All three abdominal signals are combined with one thoracic signal to form embedded matrix, which is the input matrix of ICA. The single channel independent component

analysis (SCICA) separates the fetal ECG (fECG) and maternal ECG (mECG) without the alignment of the peak positions in the original abdominal signal on time scale. The embedded multi-dimension matrix is formed from a single vector by taking the segments of the original signal with a delay variable as the column of the matrix [2]. The dimension( $m$ ) and delay( $\Delta$ ) are predefined as 20 and 10, and the length of each column( $n$ ) is 60000 for 60 seconds recording.  $S_{nm}$  is the input signal with three abdominal and one thoracic signals, so the final embedded matrix has the dimension of 20x4.

The embedded matrix( $S$ ) is the combination of four multi-dimension matrixes ( $S^{(i)}$ ), where  $S^{(1-3)}$  is are formed by abdominal signals and  $S^4$  is formed by a thoracic signals.

$$S = \sum_{i=1}^4 S^{(i)} \quad (3.6)$$

$$S_{nm}^{(i)} = \begin{bmatrix} s_1 & s_{1+\tau} & \dots & s_{1+(m-1)\tau} \\ s_2 & s_{2+\tau} & \dots & s_{2+(m-1)\tau} \\ \dots & \dots & \dots & \dots \\ s_n & s_{n+\tau} & \dots & s_{n+(m-1)\tau} \end{bmatrix}$$

(3.7)

The most common approaches to extract the independent component use negentropy and maximum mutual information in the iterative loop, and the negentropy approach is applied to extract fECG in this paper. The negentropy( $J$ ) is calculated from entropy( $H$ ) in order to maximise the non-Gaussianity of each source component based on the central limit theorem,

$$H(y) = - \int f(y) \log(f(y)) dy \quad (3.8)$$

$f$  is density function

$$J(y) = H(y_{gauss}) - \mathbf{H}(\mathbf{y}) \quad (3.9)$$

And further approximation of  $J(y)$  into the following equation

$$J(y) \approx (E\{G(y)\} - E\{G(y_{gauss})\})^2 \quad (3.10)$$

where  $G$  is a nonlinear function, each mixing coefficient vector( $w$ ) is calculated in the iterative loop to maximise negentropy by Eq.(3.11)

$$w_{k+1} \leftarrow E \left\{ sG(w_k^T s) \right\} - E \left\{ G'(w_k^T s) \right\} w_k \quad (3.11)$$

The non-linear function( $G$ ) is chosen to be  $\log(\cosh(u))$  so its first derivative is  $\tanh$  and  $s$  is the embedded matrix. The mixing coefficient matrix is a square matrix of combining  $w$  of all components with the size as the column number of the embedded matrix. The mixing coefficient matrix is calculated in the iterative loop to maximise negentropy by the equation and it has same size as that of the dimension of the embedded matrix. The extracted components are the production matrix of the mixing coefficient matrix  $(\sum_{j=1}^{80} w_j^T)$  and the embedded matrix( $s$ ).

### 3.4.3 Clustering

The hard clustering takes the individual point of abdominal signal into one of the three groups whereas the fuzzy cluster separates the same point into multiple groups based on the membership to the group centres. The clustering approach groups the data into several groups according to the centre mean of each group by X-Y relationship, so each point in the signal belongs to one of the groups according to the feature of X and Y reference [3].

The abdominal ECG is the mixing of mECG and fECG. The cluster analysis considers a single data point instead of a combination of multiples in the process. The thoracic signal is designed as the cluster centre of one of the two clusters and fECG QRS will be separated from the rest signal. However it requires the alignment of the thoracic and abdominal signals in pre-processing.

The thoracic signal is reconstructed by removing the points belonging to the noise clustering in order to estimate the mECG in the thoracic signal. Then the estimated mECG is used as the individual cluster reference for the abdominal signal.

The average of the group represents the weight of the cluster and the training set takes into account the possible situation and corresponding value level to separate data points.

Once the fECG is extracted even without matching the magnitude in the abdominal signal, the two cluster templates are applied to separate the abdominal signal into three clusters. The third cluster contains all the noise data including the internal and the external interference. The fECG is then extracted by the down envelop that selects the parabolic minimum in the iterative loop.

The clustering is applied to find the mECG frequency from the thoracic signal and then the frequency component is removed from the abdominal signal by the notch filter. The most applicable approaches of clustering is k-mean and fuzzy c-mean cluster, and only

two clusters are constructed, one of those is for the mECG signal and the other one has the combination of the fECG signal and the noise.

With the thoracic signal as the reference of the mECG, any additional points from the abdominal recording changing the cluster centre within may be taken as the mECG and any other points are grouped as the fECG signal data.

### 3.4.3.1 K-mean clustering

The aim of the clustering algorithm is to locate the similarity and the difference of data points in x-axis and y-axis, where the x-axis is the thoracic signal and y-axis is the abdominal signal. The membership for the data groups is clustered as the y-axis data, one variable  $\mu_1$  is the normal clustering variable, one is the similarity  $\mu_2$  between the two axes data and the third  $\mu_3$  is the difference between the two signals. Each data point will have three membership values and they are signed to the different groups according to the combination of the three variables. The cluster members are automatically updated based on the threshold of the data distance of the new cluster, but the noise may affect the numbers of clusters. The best clustering result is at point to have the maximum  $\mu_1$  and  $\mu_3$  and minimum  $\mu_2$ . The cluster ( $S_i$ ) is generated from the data ( $x$ )

$$S_i^{(t)} = \left\{ x_p : \left\| x_p - m_i^{(t)} \right\| \leq \left\| x_p - m_j^{(t)} \right\| \forall 1 \leq j \leq k \right\} \quad (3.12)$$

The clustering equation is to minimise the sum of the square of the distance to the centroid

$$\arg \min_S \sum_{i=1}^k \sum_{x_j \in S_i} \|x_j - \mu_j\|^2 \quad (3.13)$$

The ascending membership along with the corresponding abdominal data uses the average to group the membership and data into 5 clusters. Instead of searching the centre of the cluster for individual data point, the input is set as a group of data points including the entire mECG QRS. It is similar to the moving average and the group can be generated by the overlapped data or the continuous adjacent data vector.

The k-means uses the thoracic data to generate 0 as the initial parameter vector for cluster of the fECG signal. It uses the Euclidean distance to minimise the sum of square of Euclidean distance of each data vector to its closest parameter vector. According to the basic sequential algorithm scheme, the cluster mean of the vectors is assigned to maximise the optimal Euclidean distance, the distance from the new data point to one of the existed cluster is computed to compare with the threshold of dissimilarity. The error function of individual data to the centroid of the cluster is used as the indication of the clustering group.

The parameter vector for each cluster corresponds to the point distance in one-dimension space, the points are moved into the regions that have high dense in the points of the clusters with the similar distance. The clustering starts from the initial estimation of the parameter vector, if the vector is close to the last parameter vector value, then the value is updated into the same cluster and the parameter vector is updated for the new cluster. The first step of clustering algorithm is to set up five cluster groups, then it locates the two data sets with the maximum difference at both the minimum and maximum values. The maximum value is usually at the mECG peaks without having extreme error. The difference between the data and the maximum is descended and it is applied to separate the data into 5 groups.

### 3.4.3.2 Fuzzy clustering

The fuzzy clustering initially sets the centres of the cluster from a random guess, then it assigns the degree of membership between every point in the cluster to the centre of cluster [4]. The standard function of minimising an objective function is:

$$w_k(x) = \frac{1}{\sum \left( \frac{d(\text{centre}_k, x)}{d(\text{centre}_j, x)} \right)^{\frac{2}{m-1}}} \quad (3.14)$$

The centroid of the cluster is weighted by the degree

$$c_k = \frac{\sum_x w_x(x)x}{\sum_x w_x(x)} \quad (3.15)$$

The divergence of moving the centres of cluster is based on minimising the distance between the data point and the cluster centre. The reference signals of noise can be the abdominal signal, and the thoracic signals are the reference of ECG signal [6]. The other approach is to use the thoracic signal as the weight component after aligning the mECG with the abdominal signal. The iterative clustering loop and the convergence of the correlation coefficient are used to separate the data into two groups, instead of removing the correlated region. The subtraction clustering assumes each data point is the potential cluster centre and calculates the likelihood to define the cluster centre based on the density of the surrounding data [17]. The modified algorithm takes the first RR interval as the initial cluster centre from the thoracic signal. It then calculates the mean square error within the clusters and updates the cluster centre into a new matrix that is compared the mean square error to the thoracic signal.

### 3.4.4 Beamforming

The ECG is the potential measurement of the myocardium excitation propagation. The potential signal is a dipole vector in the electrical field projecting onto 3-dimension where the body is the volume conductor. The dipole projection to the different directions can be measured by the electrodes at various locations on the body. The heart position with respect to the electrode is in 3D(x,y,z), the direction of the heart vector is known based on the physiological property of the heart and it can also be derived from the ECG segments. The weight of minimising the average power in the error signal is calculated from input signal with the angle of arrival.

$w_{mmse} = \arg \min_w (w^H R w - w^H E \{x d^*\} - E \{x d^*\}^H w + d d^*)$ , where R is covariance matrix and d is source signal (3.16)

The magnitude difference between the two thoracic signals is generally consistent in every cardiac cycle, so it may be caused only by the relative distance between the electrodes. The magnitude difference at QRS indicates the shorter radius from the origin of the heart vector with the lower magnitude in QRS. The ECG signal is used to reconstruct the heart vector map, the magnitude is the relative value to the P-wave magnitude. It is the physiological principle of being able to apply beamforming to separate the signals recorded at different locations. The beamforming links the behaviour of recorded pattern to the location of the source signal.

The beamforming is the source position orientated approach to maximize the reception of the signal based on the direction of arrival. It uses the desired angles of arrival of the dominant signal during the recording process. The original design principle is to use the position angles of the two ECG sources. It assumes the maternal heart is at the vertical position to the thoracic electrode. The same assumption is introduced to the location of the fetal heart to the abdominal electrode. However, the maternal heart is at an angle to the abdominal electrode in a practical situation.

The main difference of the mECG is the two signals are caused by the horizontal distance of electrodes and the distance is calculated from the heart to the abdomen in the general population. The approach derived from the beamforming to separate ECG takes into account the differentiated signals from the mixture. The location difference of electrodes can be seen in the pattern transformation of certain segments in the mECG recording. The pattern difference is due to the direction of the heart vector. However, the pattern transformation in different locations is only the variation of the amplitude which is not

constant for everyone. So the change in the amplitude needs to be referenced in order to connect the pattern change to the position.

In between the abdominal and the thoracic signals, there is time delay at the mECG QRS peak. The QRS peak can be applied to determine the location relationship between the abdominal and the thoracic electrodes. But the cause of the delay is uncertain. It could be due to the electrode configuration or the actual time of ECG signal propagating from the maternal heart to the abdominal electrode. If the assumption is made that the delay is based on the signal propagation, the beamforming can construct the original mECG signal from the thoracic signal with the electrode relative locations. The abdominal and thoracic electrodes are assumed to be at the corresponding positions of the 12-lead ECG placement, so the angle between the recording signal and the source signal can be used for the beamforming separation.

### 3.4.5 Transform of mECG signal in thoracic and abdominal signal

The additional thoracic signal is taken as one of the source signals for both the magnitude and the waveform modification. If the thoracic recording is used to re-construct mECG by either solving the transformation relationship or removing the partial mECG component from the abdominal according, it will leave the T-wave of mECG as part of the noise.

The first step is to use the mECG as the noise signal with the known transformation pattern from the thoracic recording, then build a transform model of mECG for the abdominal signal from the thoracic signal based on the location assumptions of the relationship between the two electrodes. The actual distance in the real application can be recorded by a sensor that can form part of the input parameter to the algorithm.

The mECG in the abdominal signal is irrelevant to the purpose of the abdominal recording so it can be removed from the segment block. The non-linear transformation function involves the distance factor between the thoracic and the abdominal electrodes, and the tissue density variation effect. However, neither of these factors is available in the open database, so the algorithm variables need to be selected or built based on this general assumption for the template. The thoracic and abdominal signals are transformed into the same magnitude interval before projecting with or without the magnitude mapping.

If the abdominal signal is considered as the echo distortion of the thoracic signal, then the ECG will be the matched component between the echo and the ordinal signal. The Q point is selected as the start point and it is compared to the 10 points on each side to locate the point with maximum difference. Instead of removing QRS by the

thoracic signal from the abdominal signal, the time interval of QRS is calculated. If the algorithms flip the downward peak and keep the ordinary QRS peak in the thoracic signal, the end point of the descent slope is the S point. The advantage of locating the S point instead of retrieving the peaks directly is the peak magnitude can be removed completely without leaving the effective magnitude which will distort the fECG in the separation process.

The conversion from ECG signal to VCG signal requires the multi-coefficients for the 12-lead configuration. It contains information on the location of electrodes and the coefficients are selected through the learning process. Then a corresponding table of electrode angles is built from the ECG and VCG information. The transform function is applied to the abdominal signal to estimate the angle between the electrodes based on the table. The assumption factors made in the method include the steady transformation factor across the electrodes at both the abdominal and the thoracic signals and the linear relationship of the delay to the source signals.

### 3.4.6 Power spectral

The power spectral density of the mECG and the fECG are different in the frequency feature, but the power distribution of the mECG should remain the same as each segment of the cardiac cycle contributes the same over the time. The power spectral density of signal  $x(t)$  is

$$P = \lim_{T \rightarrow \infty} \frac{1}{2T} \int_{-T}^T x(t)^2 dt \quad (3.17)$$

The noise reference is assumed to form the identical magnitude in the power spectral during the measurement in the reference collection. The power spectral density groups similar frequencies by using the *Welch* method of *Hanning* window and 32 coefficients with 50% overlap. The individual component in the same power group is shifted back from the delay variable and then it is averaged out to find the final result. This is similar to the cluster approach, the probability density function (pdf) of the thoracic signal is calculated as a template and is matched against the abdominal information with the same value and then grouped as the mECG signal. The pdf of the thoracic signal is compared to the extract the the points with the same pdf.

### 3.4.7 Learning iterative loop

In the learning algorithm, the clustering will use the correlation relationship to separate the ECG instead of finding the cluster centroid. The initial cluster data includes all the abdominal data points, then every 2 neighbouring data points are grouped into the test

interval and compared to the mECG component. The mECG signal is designed as the carrier of fECG in the abdominal signal and the learning algorithm uses the iterative loop to retrieve the embedded fECG. The learning process that will be compatible for the covariance function in MATLAB.

The first 3000 data points are selected as the input to the machine learning approach and the output is then filtered to remove the mECG peak in the abdominal signal. The learning approach is to extract the waveform of fECG and then use the waveform as the template to compare with the overall signal. The waveform with the most frequent appearance is taken within the selected interval. The abdominal electrode signals may change if one of the fECG waveform signals has a magnitude change, this will then shift the fECG out of scale from each other. The sum will only be applied if the individual signal contains the small magnitude of the fECG signal.

### 3.4.8 Template construction of ECG

The first step of template separation is to set up a collection of possible ECG patterns then apply "trial and error approach" to match the ECG template to the components in the abdominal signal. The weight of the selected region in the learning data interval is variable due to the additional appearance of the fECG signal. The controlled parameters in the template are derived from the peak magnitude, the duration and the spectral separation of the individual thoracic recording. The parameters can be adjusted by the number of data points in the template and the shape of the template is initialised for the general condition. The error of the template match process controls the parameter and it modifies the template in a continuous loop until it reaches the minimum level of data errors, distribution errors or energy errors. The initial template of the fECG signal is defined as a single upward peak, the length of the peak sides is adjusted by the error controlled parameter.

Template matching uses the correlation and likelihood to find a similar pattern in the two signals. It is essential to only match the pattern not the magnitude level and only match the region with the same waveform. Instead of using the template for one pattern feature, both the mECG and the fECG signals can be inputted to test the relationship to the template. The template that represents the mECG and the fECG signals can be linear or high order polynomial function.

The circle matching template has the radius as the same length as the magnitude of the fECG peak and the value only changes if the deep slope changes. The circle is set as a measurement tool to monitor slight change in the peak slope and it recognises the change in the peak magnitude in the circular area based on the percentage error. The

weighted principal includes the interpolation of the mECG QRS peak and the surface distribution and generates a template to match the mECG signal in the abdominal and the thoracic signals.

### 3.4.9 Empirical mode decomposition (EMD)

The procedure of the empirical mode decomposition (EMD) is to generate the upper and the lower envelopes by the cubic spline interpolation. It then subtracts the envelop functions from the signal and feedbacks the residual to the input until the residual is monotonic. The EMD keeps finding the minimum value after each signal update, and the parabolic minimum is found by setting the linear relationship between the adjacent three data points. The order of the intrinsic mode function reciprocally reflects the frequency of the component and the input signal is separated into ordered elements. It is similar to calculate the membership of the neighbouring data. The decomposition of the input signal  $X(t)$  into multiple  $IMF(c_i)$

$$X(t) = \sum_{i=1}^n c_i + r_n, \text{ where } r_n \text{ is residual (3.18)}$$

The mECG can be extracted from the resulted IMF but the fECG signal emerges as part of the mECG signal. Because the frequency of the fECG signal is normally higher than the frequency of the mECG signal, the fECG signal is supposed to be in the higher order IMF component. The mECG is taken as the 1st order decomposition component of the abdominal signal and then it is removed from the abdominal signal after the decomposition. The IMF components may include the baseline wander signal, because each quadratic function is only separated into one component and it may not match to the signal.

### 3.4.10 Singular value decomposition (SVD)

The singular vector decomposition (SVD) is to form the component that is considered to be the most dominant in the matrix of abdominal signals based on the eigenvalue. It can also be applied to compress the ECG signal to reduce matrix size as well. The original multi-dimension matrix (M) is factorised into the combination of the singular

values( $\Sigma$ ) and singular vector ( $V$ )[32]

$$M = U \Sigma V^* \quad (3.19)$$

### 3.4.11 Mask for fECG

When the abdominal and the thoracic signals are separated into the cardiac cycles, the thoracic signal can be used to mask the abdominal signal. The iterative process uses the individual cycle instead of the overall recording, so the coefficients are updated in each cycle. The coefficient is added to the thoracic signal to maximise the difference with the abdominal signal with the step size increment of the coefficient depending on the actual difference between the two signals.

The difference is taken over a period of 10 data points in order to avoid the removal of fECG by the single data difference. The potential error of masking the mECG peaks due to the thoracic signal occurs when the fECG peaks align with the mECG peaks. The removal of the entire mECG QRS complex results can cause the mECG peaks to be missing and it also causes an inaccurate fetal heart rate calculation.

The mask can be used to find the noise reference like the adaptive noise canceler and treats the mECG signal as associated noise because the pattern form of the mask is more closely matched to the mECG signal in the abdominal recording than the mECG in the original thoracic signal. Both the mask and the thoracic signal are introduced with shape only to eliminate the error caused by the magnitude. The covariance between the difference and the sum of the abdominal recordings can form the mECG signal with the minor magnitude in the P-wave and can be used as the mask to remove the mECG signal in the abdominal recording.

### 3.4.12 Adaptive filter

The adaptive filter uses the thoracic signal as the reference of the mECG signal and it removes the mECG signal from the abdominal recording. The adaptive filter reconstructs the desired signal  $d(t)$  from the input signal  $x(t)$  based on the reference signal  $v(t)$ , where  $w_t$  is the weight coefficient controlled by the error between  $d(t)$  and  $v(t)$ .

$$d(t) = w_t * x(t) \quad (3.20)$$

Because the principle of least mean square (LMS) is to minimise the difference between the reference and the input signal based on the thoracic and the abdominal signals, the variation of the mECG pattern in the thoracic signal is left as a part of the fECG signal.

It is caused by the transformation function of the conversion that is not applicable in the abnormal cases. Both the magnitude and the period of mECG are extracted as the reference from the thoracic and abdominal signals.

### 3.4.13 Frequency filter

In the thoracic recording, the mECG has a relatively high magnitude compared to the one in the abdominal recording in the same frequency range. The bandstop filter is only applied to the thoracic signal to indicate the frequency range of the mECG component that is in the same frequency range in both the abdominal and the thoracic signals [8]. The abdominal signal can be considered to be the combination of one high and one low frequency data, and every signal data point as a sum of two source signals. The frequency filter and wavelet transformation may be applied to enhance the fECG peak in the ICA component or to separate the high frequency noise.

### 3.4.14 Other approaches

There are other algorithms apart from the above approaches that have been developed and tested to separate the fECG from the abdominal signal or to enhance the SNR. The difference between the two abdominal recordings is used as a reference of the fECG signal offset to remove the remaining T-wave or P-wave of the mECG component.

Instead of using a single order algorithm, the relationship between the thoracic and the abdominal signal is reconstructed by several mathematical models with logarithm, summation, exponential, power and sinusoid functions. The QRS in the abdominal signal is symmetrical but it is asymmetric in the thoracic signal, so forward and the backward checking is applied for the symmetric property and it detects the unmatched mECG QRS complex region. But if the downward peaks disappear in the thoracic signal, the function cannot find the QRS complex. The magnitude subtraction is applied to the same cardiac cycle, after removing the time delay of the mECG in the abdominal signal.

The gradient of the abdominal signal indicates the time point of the fetal QRS more clearly than the original abdominal signal. The mECG QRS can be removed first from the abdominal signal, then the gradient function can be applied to the rest signal to locate the fetal QRS. The number of data points forming the peak is proportional to the magnitude of the peak, so a line segment is used to approximate the peak by the algorithm  $y = Ax + B$ . The linear regression is to estimate the slope and the intercept of

the line by minimising the least squares function, it may be applied as a segmentation tool to separate the mECG from the fECG components based on the linear relationship.

The kernel function in the neural network takes the thoracic and the abdominal signals as the input to several classification processors and the outputs are assigned to the multiple layers based on the correlation between each output component [11]. The neural network applies the taps to the signal data at each stage to condense the signal feature into the single value that indicates the overall feature of the signal [13]. The Karhunen-Loeve(KL) function reconstructs the R-wave of the ECG signal, it then projects the pattern vector onto the ordered eigenvector.

The feature space uses the second-order temporal decorrelation to reduce the dimensions of the abdominal signal, the size is only up to the number of data covering one mECG cycle. The wavelet transform (WT) is to separate the components with the different frequencies in time domain, it groups the components in the high and the low frequency ranges respectively [7]. The mother wavelet is selected depending on the signal pattern of the desired signal.

The relationship between the abdominal and the thoracic signals adjusts the parameters of fECG extraction equation, and the noise filtered by WT is considered to be the maxima of the recording. The components separation in each subband should be correlated to each other because the subband signals are filtered into the same source and the different segments of ECG are in the different frequency range.

The non-linear relationship between the mECG and the fECG signals can be re-arranged by the non-linear operation such as trigonometry, log, exp and power, but it requires further testing on the relationship to build up the algorithms. The threshold of the peaks location in the abdominal and the thoracic signals is calculated in the iterative loop and the threshold value should result the same number of peaks in the two signals. The initial setting of the duration threshold of the mECG cycle is 10 milliseconds to avoid the double mECG peaks detection.

The last peak in the abdominal may be the baseline wander or the motion artifact and it is not in the thoracic signal, so the number of mECG peaks is determined by the thoracic signal instead of the abdominal signal even the time point is extracted from the abdominal signal. The function  $\exp(\cosh A)$  is used to extract the mECG component, then it is used to work backward to reconstruct another ECG component from other recordings.

When the signal is plotted as a graphic pattern, the magnitude of ECG peaks is converted to the vector in the image, and the vector data is interpreted into two sets of data. When the two sets are linked together in the algorithms, the same feature can be extracted

by the cross section of the two sets of information. The common noise in the image is the sudden change in peaks magnitude and both fECG and mECG signals form those changes.

### 3.4.15 Heart sound processing

The fetal heart beat tone can be separated by the envelope function into the sound block. The first few seconds of the sound recording is used as the reference for external noise because the recording started before placing the microphone on the target position Fig.3.5. The white noise data can be removed by the adaptive filter and the maternal heart beat needs an additional reference to use the adaptive filter. The FPCG is passed to the bandpass filter to remove components in the range of 35-200 Hz. The possible extended noise is analysed in the frequency domain and the filtered signal is shown in Fig.3.6.

The abdominal PCG is processed as a single channel signal and the delay time variable results in the maximum correlation coefficient which is used to generate the embedded matrix. The mixed signals have similar properties due to the frequency overlap and one source signal may be assumed as the attenuation signal. So the fetal heart signal is considered to be the main source and the maternal heart signal is the secondary source and is treated as the delayed reflection of the main source from different directions. The magnitude threshold and parameters are set manually for processing. The process can be developed into an automatic procedure by modifying the variables according to the data distribution.

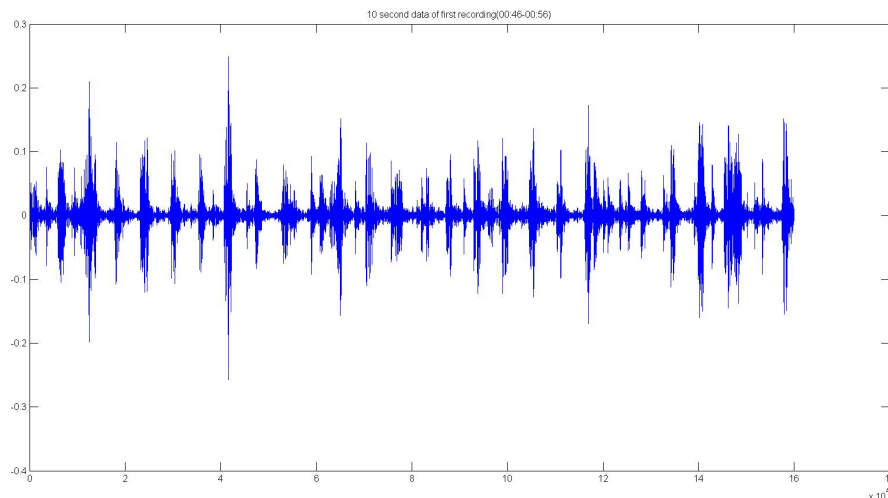


FIGURE 3.5: The first minute recording of heart sound with heart sound peaks

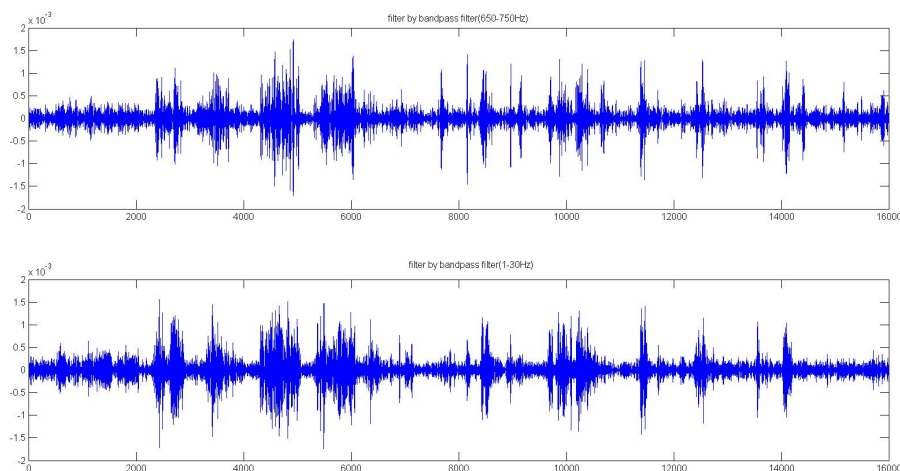


FIGURE 3.6: The heart sound recording filtered by high and low frequency filters

### 3.4.16 Mouse data

The first step of extracting the heart rate of mouse data is to remove the power line noise by a notch filter, the cut-off frequency is then selected to be 50Hz (the data was collected in Japan). The next step is to remove the random noise and enhance the SNR of the ECG signal by a bandpass filter at cut-off frequencies of 20 and 200 Hz. The interval of the processed data is selected as a section of the entire recording to avoid certain dominant noise.

The selected interval includes all the analysis events, but the events are missing in the recording of one subject. The event duration for the mouse data is selected to be 2 minutes from the overall 5 minutes recording, and the region is chosen to have the best continuous signal with the maximal SNR. The associated noise with the significant peak amplitude is removed manually in the ECG pattern before calculating the heart rate. The ECG QRS complex is processed first with a general threshold value, then a boundary is set to test the accuracy of peak extracting by limiting the heart rate within a reasonable fluctuation Fig.3.7.

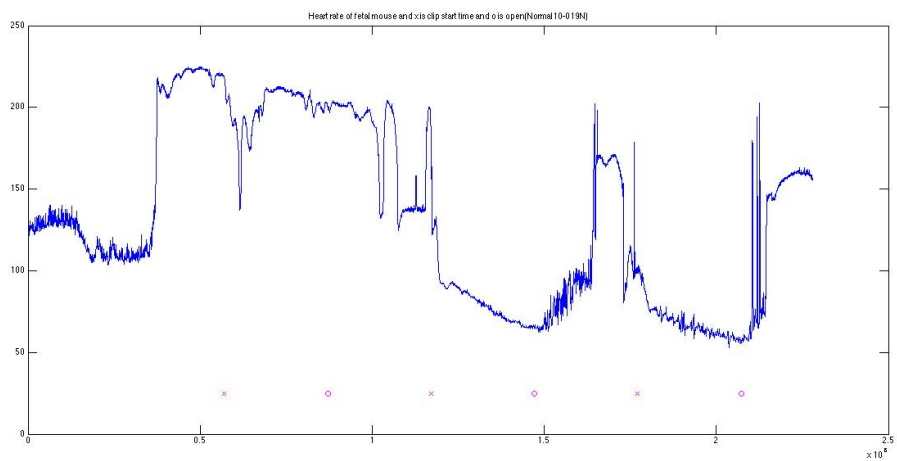


FIGURE 3.7: The fetal ECG from normal mouse including events of clipping and opening

# Chapter 4

## Result

### 4.1 Signal processing

The mECG peaks of the abdominal signal from the open source *PhysioNet* are located using 0.8 as the threshold value after normalizing the signal magnitude to the interval [0,1]. The magnitude of fECG peaks in the abdominal signals have slightly greater slopes than the associated noise. The gradient function of the abdominal signal has more obvious fECG peaks and is applied to select pairs of signals to extract the fECG and the mECG signals.

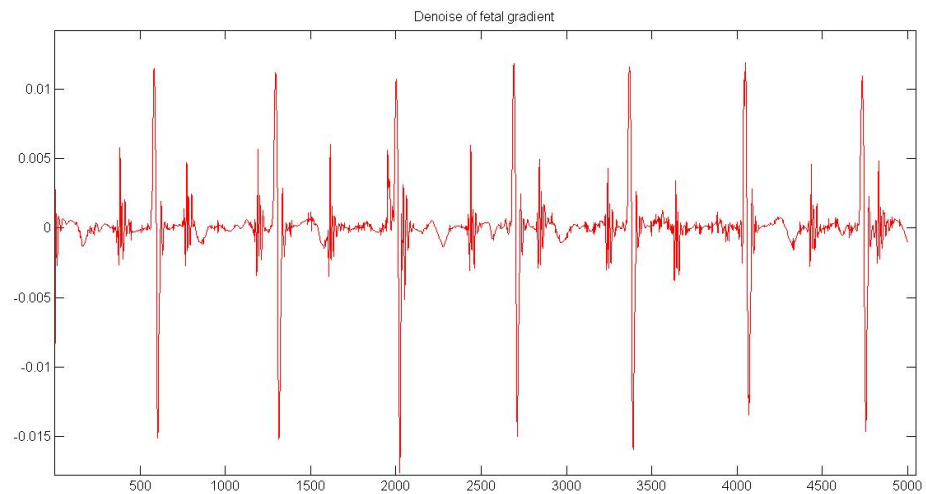


FIGURE 4.1: The gradient of abdominal signal after removal of white noise

### 4.1.1 Noise

The SNR of the fECG signal is improved by taking the product of two abdominal signals and both the magnitudes of the mECG and fECG QRS peaks are increased. The square root function reduces the magnitude of the mECG peaks more effectively compared to its effect on the amplitude of the fECG peaks.

### 4.1.2 Baseline wander

The baseline wander results in different patterns in the individual abdominal signal as in Fig. 4.2 as it is caused by abdomen movement and can change when breathing. The

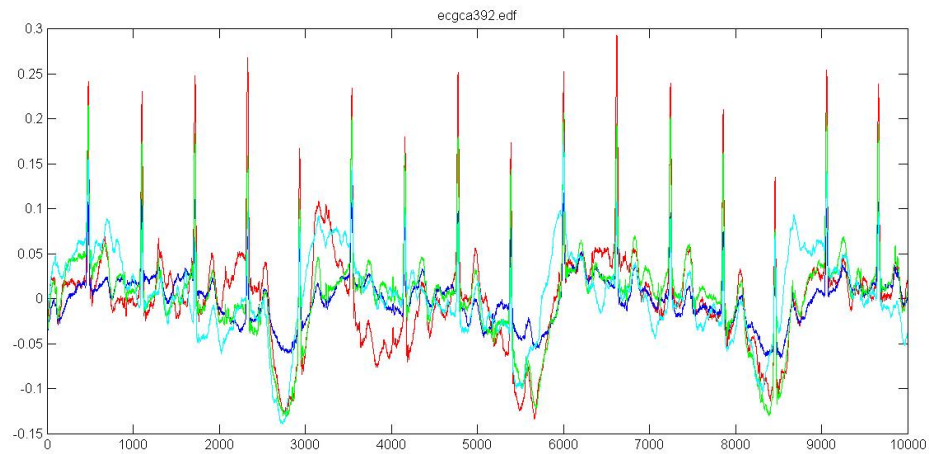


FIGURE 4.2: The three original abdominal recording with visible potential fECG peaks from *PhysioNet*

baseline wander is low frequency noise, so both a butterworth highpass filter of  $N=8$  at cutoff frequency of 2 Hz and *smooth* function can remove the baseline wander.

#### 4.1.2.1 Smooth

The *roess* process uses 10% of the original data as the single input, but is considered to be a time consuming process in MATLAB as the result is not instantaneously calculated. Processing time is shorter with improved *roess* as it has the specific data number upfront and works with a quadratic function to fit to the data points smoothly. The smooth procedure modulates the thoracic to a similar pattern as the abdominal signal with existed downward mECG peaks. The longer the data interval, the less accurate the mECG component reference in the *smooth* function is. The *smooth* process can also remove both the motion artefact and the mECG QRS complex at the beginning and end

of the signal interval. The *smooth* function is robust without tuning the cut-off frequency for different subjects or affecting the low frequency component of the fECG signal. The baseline wander is constructed first and subtracted from the original abdominal signal in Fig. 4.3.

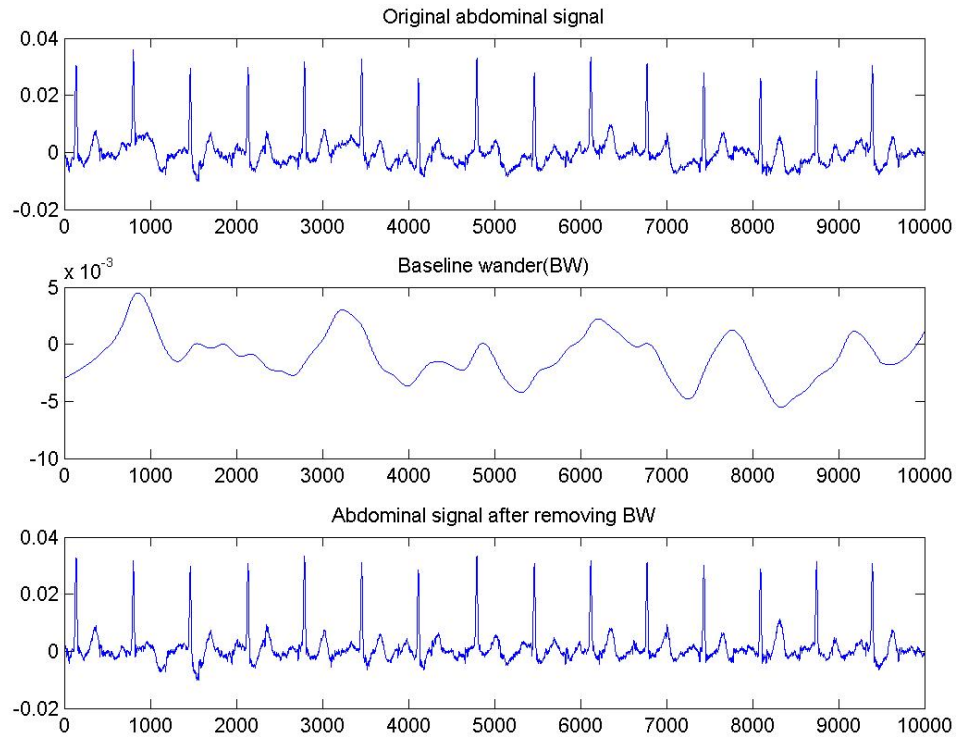


FIGURE 4.3: The baseline wander signal and result abdominal signal after removal of baseline wander

### 4.1.3 Cross correlation variables

The cross correlation coefficient is initially introduced to align the mECG peaks in the abdominal and the thoracic signals in order to construct the multi-dimensional matrix as the input of the independent component analysis (ICA). The time delay is calculated using difference of the cross correlation coefficient and the duration of the data recording and it is chosen as the start point of the vector interval in the abdominal signals for the matrix . The delay variable is the same for the three abdominal signals. Then it is developed to locate the fECG in the two adjacent mECG cycles however this approach was deemed unsuccessful due to the variation in the duration of the mECG cycles. The correlation coefficient decreases with the increased number of the data intervals regardless of the correlation relationship. If the correlation coefficient between the two

mECG cycles exceeds the length of data intervals, it indicates that there is no correlation between the mECG cycles.

#### 4.1.4 Independent component analysis

The ICA is applied to the open source data to separate the fECG signal, the extracted fECG signal has peaks aligning to the points of the predicted fECG peaks in the original abdominal signal in Fig.4.4. The component matrix from ICA has the same dimen-

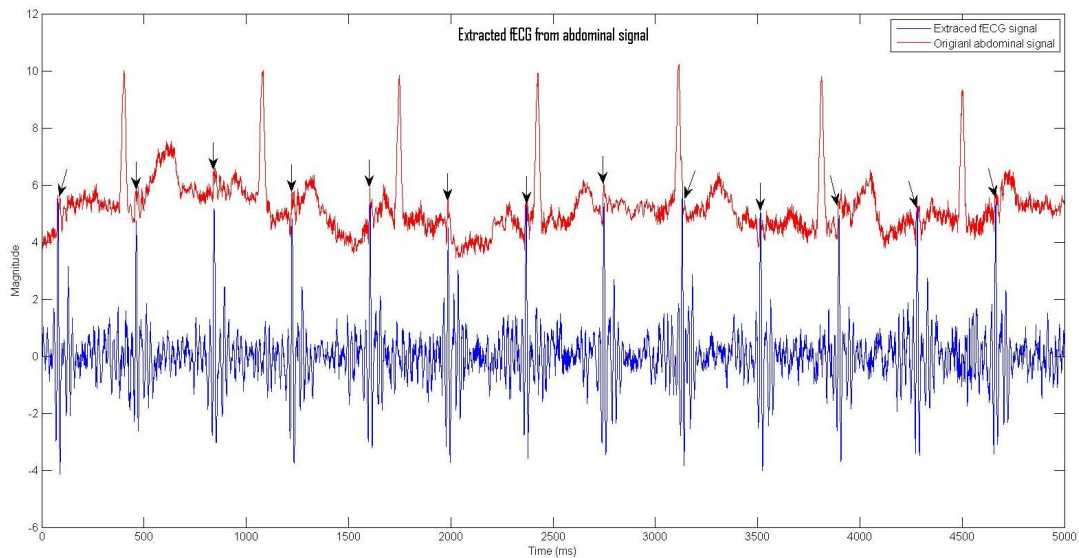


FIGURE 4.4: The extracted fECG is compared to the potential fECG peak in abdominal recording

sions as the size of the embedded matrix, and the fECG signal is extracted into several components. The fECG signal could not be filtered out with highest SNR in a learning processing, the potential fECG signals are selected manually based on the observation of noise influence in the component signal. The selected fECG signals for the synchronisation analysis need post-processing to enhance the peak amplitude before the peak detection Fig. 4.5. Because all the recordings are assumed are from healthy subjects with a normal fetus condition, the cardiac cycle is reasonably consistent. Due to the relative low SNR of fECG in the original abdominal recording, only the QRS segment of the fECG is extracted with accurate time point. Some of the subjects have R-R intervals over 50ms which may be caused by the associated significant noise such as the random peaks in the extracted fECG component. Because the mixing matrix of ICA is a square matrix, adding more input sources will result in more accurate components. The ICA has been tested successfully on simulate signal to separate the mixed sources with the weight coefficients.

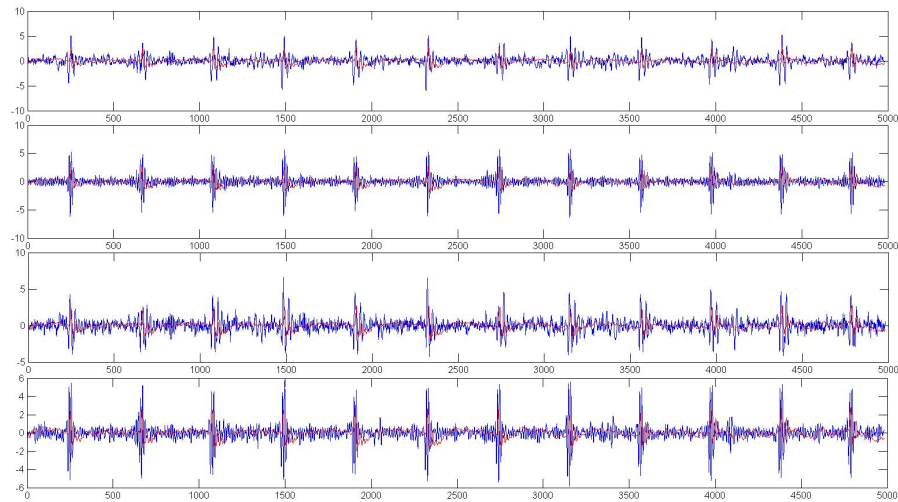


FIGURE 4.5: The ICA separated component corresponding to fECG signal (blue) and filtered signal for peak detection signal (red)

#### 4.1.5 Frequency domain

After applying 50 Hz notch filter and one lowpass filter, a cutoff frequency of 100 Hz is added to the original signals. The fECG QRS in the gradient of the signal is clearer as the minor partial magnitude in both the mECG and the fECG peaks is removed. The power spectral in the frequency domain of the thoracic and the abdominal signals has two peaks within the 10 Hz range. The indication of the mECG position in the abdominal signal is based on the thoracic recording and the frequency of the mECG component should remain the same in both the abdominal and the thoracic signals. Clustering finds the mECG frequency in the thoracic signal and removes the frequency component from the abdominal signal in the frequency domain by the notch filter. The frequency component of the abdominal and the thoracic signals have similar mECG pattern and the corresponding thoracic frequency component is used as the mask to remove mECG in the abdominal signal. The frequency component enhances the fECG in the abdominal signal, but it is not observable in the original recordings around 80-110 Hz.

#### 4.1.6 Clustering

Clustering can find mECG peaks because they are not influenced by the other segments of the cardiac cycle. The cluster with the minimum number of points is the group of mECG complex and it can be located by *min* function. The cluster components of the fECG and the mECG signals are not in constant order after each clustering process with the same input matrix. The input signal of the sum of the three abdominal signals and

one thoracic signal results in 20 clusters, two of which could be combined together to represent the fECG signal and the noise can be removed by using the threshold value.

There is no direct relationship between the accuracy of the fECG component and number of clusters. It can extract fECG with removable errors with generally only 10-20 clusters. The mECG QRS peaks are clear in one of the clusters but the fECG signals are embed in the mECG signal in some of the clusters with relatively small magnitude. The clustering algorithm does not have equal distribution of the difference along the x-axis, most of the different values are in the range of -0.6 to -1. The difference range indicates most signals are far from the maximum and show sharp increases from -0.6 to 0 at the peak regions in both the mECG and the fECG signals. The cluster centre of the noise signal is zero and the mean values of the fECG and the mECG QRS complex are also around zero. The peaks in the cluster group are the QRS complex which is shifted by the delay between the two signals, so the resulted peak cluster group is delayed as well.

The k-means function of clusters separates the signal into 3 groups, one is corresponding to noise, one is the fECG signal and the third one is the mECG signal and it also uses the gradient of the abdominal signal as the input. Both the abdominal and thoracic signals have to be normalised using the mean and the standard deviation, to set the cluster centre. When apply clustering to the abdominal signal, the fECG peaks in the mECG peak are separated into the mECG groups as they are too close to the mECG cycle instead of separating into individual fECG cluster.

#### **4.1.7 Singular value decomposition**

The SVD algorithm can break down the matrix of 3 abdominal recordings into 3 components, the second and last component will have mECG QRS removed from the signal but none of them kept the shape of original abdominal signal. The mECG is separated from abdominal signal as the singular component with relative high coefficient but the extracted signal is not identical to the mECG component in the abdominal signal in magnitude and pattern. Because fECG is not considered as singular component in the abdominal signal, SVD will not extract any information regards fECG.

The output matrix of SVD is similar to the abdominal ECG and first component has negative peak. The result signal has QRS complex align with that in abdominal signal which suggests that only mECG complex were found.

### 4.1.8 Empirical mode decomposition

The EMD applies to the sum of the abdominal signals. The first IMF which has the highest frequency is supposed to be the fECG signal, but the peaks at the corresponding time point does not match the time point of the fECG peak in the actual abdominal recording.

### 4.1.9 Adaptive filter

The adaptive filter is tested with the mECG signal as the additive noise in the abdominal recording and having the thoracic signal as the reference. The error signal of LMS, which is supposed to contain the fECG signal in the design of the adaptive filter, has the thoracic pattern with the modified amplitude. This is due to the magnitude and pattern difference of the mECG component in the abdominal and the thoracic signals.

### 4.1.10 Other approaches

The *exp* function brings the abdominal and the thoracic signals to the same baseline level which is the essential step for applying the adaptive filter. The function  $\log(\cosh(\text{cov}(\text{abd1} - \text{abd2})))$  can remove the relatively low magnitude component such as the ripple at the fECG component or the T-wave of the mECG signal. The function also cuts down the width of the mECG peak by reducing the interval of QRS, which leaves the partial mECG in the subtraction result. The enhancement of the fECG signal may also increase the magnitude of the noise ripple if the target is the entire signal pattern. The location mask is used to remove the mECG QRS component from the abdominal signal, but it also removes the fECG peaks that are embedded in the surrounding mECG QRS. The mask matrix is converted from the mask template by logarithm and hyperbolic cosine algorithm. The hyperbolic cosine removes some of segments in the mECG signal.

## 4.2 Heart rate

### 4.2.1 *PhysioNet* recordings

The mHR of the extracted mECG components for the *PhysioNet* data are more accurate than the fHR pattern, but the mHR signals are still in oscillation in the pattern Fig. 4.6. Most of extracted fHR and mHR are in the normal, 4 subjects have larger standard

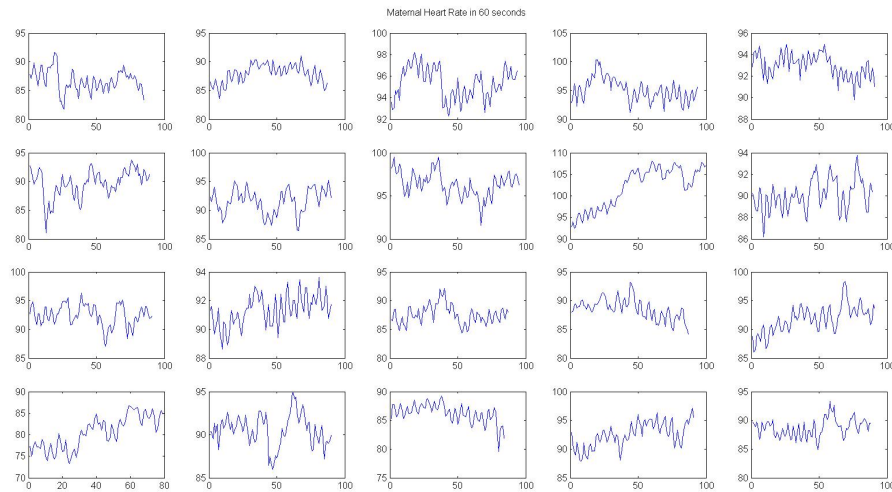


FIGURE 4.6: The maternal heart rate in the overall analysis interval for subjects from *PhysioNet*

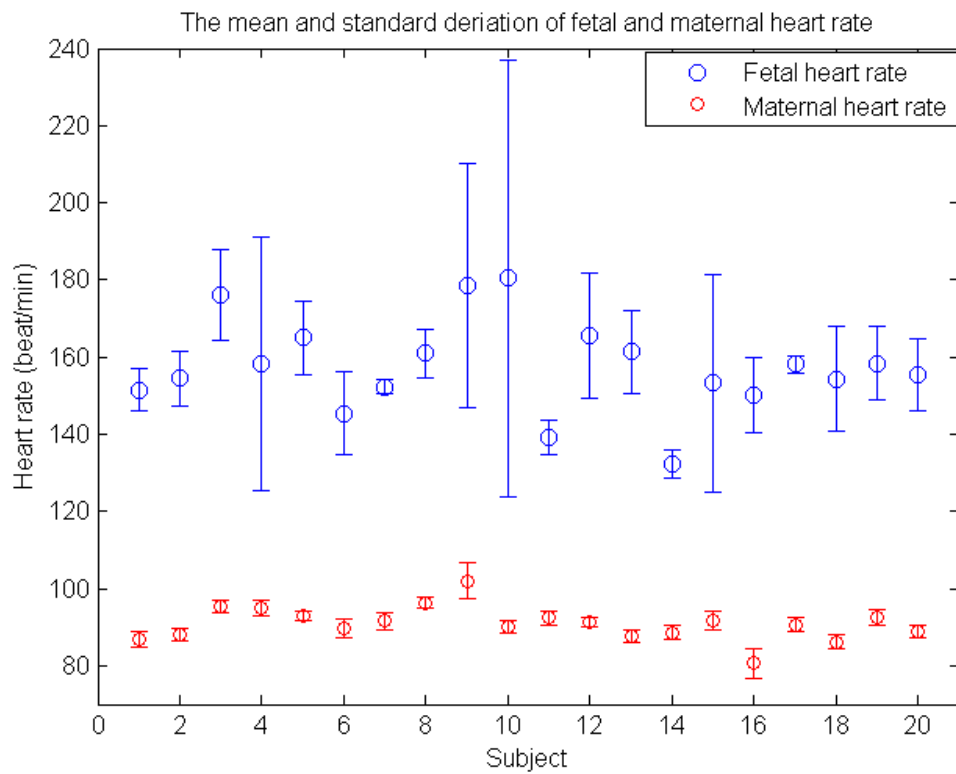


FIGURE 4.7: The mean and standard deviation of fetal and maternal heart rate for subjects from *PhysioNet*

derivation of fHR which may be out of the normal fHR range as in Fig. 4.7. The gestation period is analysed with respect to the fHR feature instead of using the synchronisation behaviour Fig.4.8. In the *PhysioNet* database the RR ratios of the fECG signal to the

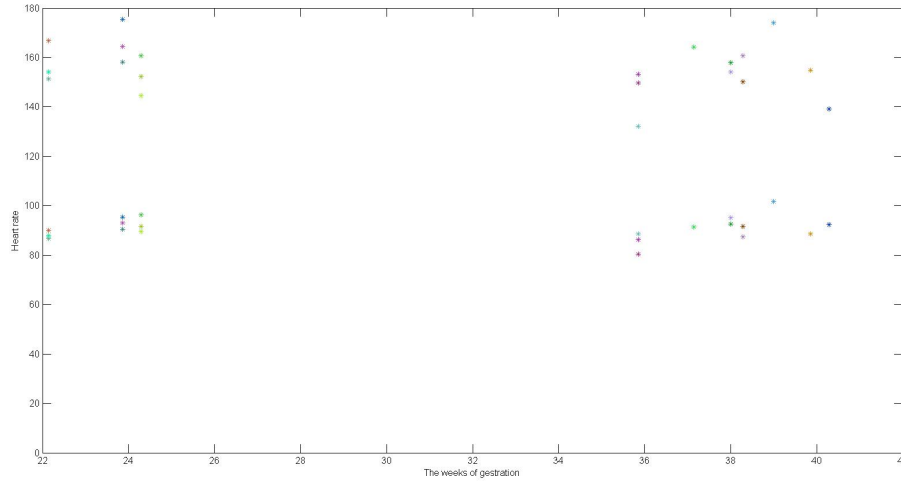


FIGURE 4.8: The fHR at corresponding gestation period for subjects from *PhysioNet*

mECG signal is 5:3 so the repeated duration of the fECG signal is 15 cycles. The RR duration of the fECG signal is 0.4 second, so the minimum time to have the repeated fECG cycle at the same respect time point to the mECG cycle is about  $15 \times 0.4 = 6$  seconds.

#### 4.2.2 Subjects at various gestation period recordings

The mean values of the fHR of all the recordings are in the normal range of 120-180 bpm except one subject at 28 gestation weeks having fHR below 110 bpm. The mean values of the mHR are in the range of 60-110 bpm but do not show the consistent variation pattern with the increased gestation week.

At the same gestation period of 30 weeks, the standard deviation of mean values of the mHR is 15.73 which it is much higher than the standard deviation of mean values of the fHR which is 8.16. The general statistical property of the heart rate across the different gestation groups is summarised in Tab. 4.1. There is no direct correlation between the heart rate and the gestation weeks or between the mHR and the fHR. The p-value of the correlation relationship between the fHR and the mHR across all three gestation groups is  $4.64 \times 10^{(-36)}$ , so the fHR does not significantly correlate to the change of the mHR in each gestation group. Comparing the data of the open source *PhysioNet*, the fECG R-R interval directly affects the shape of phase pattern but the mECG R-R interval may not be in linear relationship to the fECG R-R interval. When the average difference between the R-R interval of the fECG and the mECG decreases from 300 to

TABLE 4.1: The mean and standard deviation of heart rate at three gestation groups, where red is low gestation period, blue is median and green is high

Heart Rate(beats/min)		Gestation period		
		$L_{gp}$	$M_{gp}$	$H_{gp}$
fHR	Mean( $\pm$ STD)	150.83 $\pm$ 4.73	141.77 $\pm$ 14.33	144.76 $\pm$ 10.68
mHR	Mean( $\pm$ STD)	84.49 $\pm$ 11.13	86.91 $\pm$ 14.91	85.00 $\pm$ 12.21

250, the ripples feature disappears and the pattern becomes continuously smooth when the number of stripes drop and stay at 3. According to the research across 20 subjects from *PhysioNet* database, if the interval difference of the mECG signal and the fECG signal is below 245, the number of strips is 3 in general without oscillating ripples and the number of strips is 4 if the difference is above 345.

The fHR and mHR of the actual recording is also analysed across three gestation periods but there is no significant linear relationship between fHR and mHR in overall three gestation period Fig. 4.9.

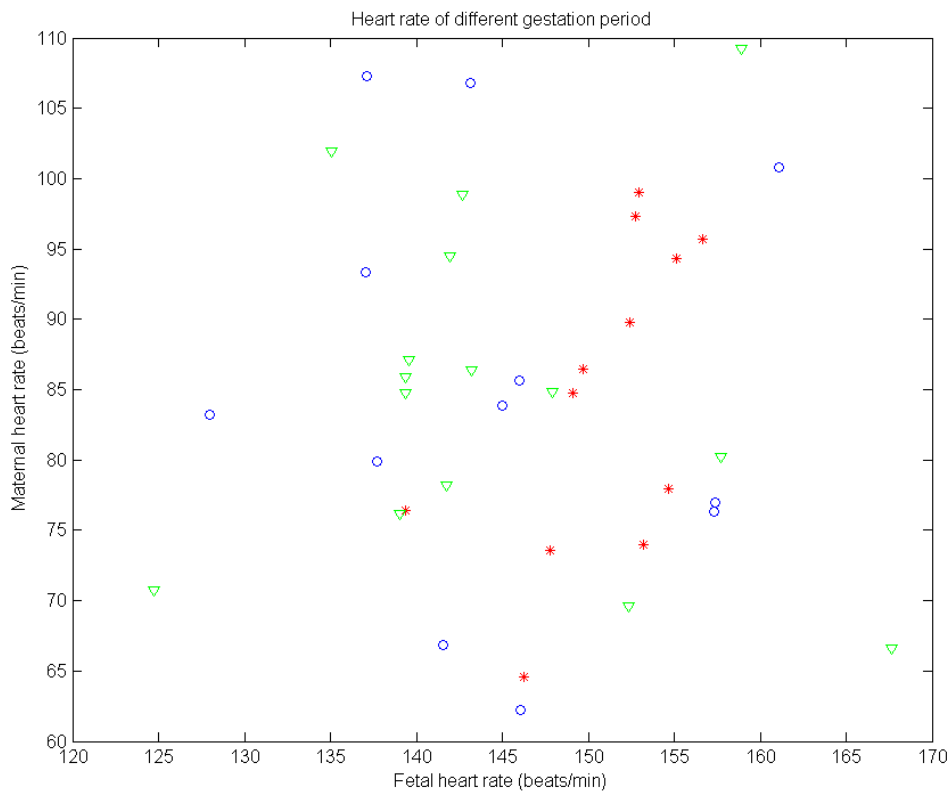


FIGURE 4.9: The relationship between maternal and fetal heart rate at corresponding gestation period, red is low gestation period, blue is median and green is high

### 4.3 Synchronisation

The synchronisation correlation converts the different mECG intervals into the normalised scale  $[0,1]$  and has the fECG peak positions in the corresponding points in the new interval  $[0,1]$ . Because the number of synchronisation coordinates for the shorter primary cycle is more than the number in the longer primary cycle, the spread density in the same time scale decreases by  $N_{f_{ecgpeak}}$  and  $m$ ,  $N_{f_{ecgpeak}}$  is the total number of fECG peak in 60 seconds recording where  $m$  is the number of mECG cycles in one primary cycle. In this situation, the synchronisation coordinates have less gap in time scale in the shorter primary cycle in Fig.???. Some of the phase points spread in the horizontal

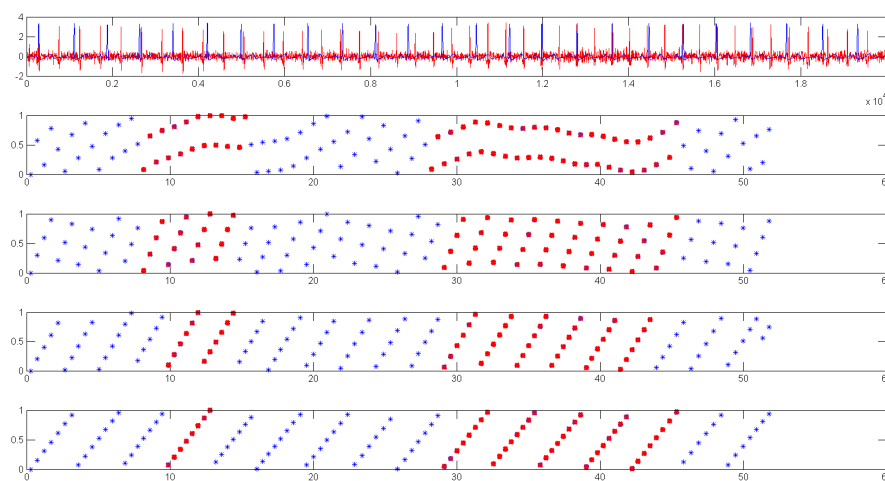


FIGURE 4.10: The fECG and mECG extraction from abdominal and thoracic signals and synchronisation relationship between the two signals at various primary cycles

direction and the gaps between them are too large to consider them for the continuous synchronisation. The epoch of the synchronisation is not calculated from the duration in the time scale, because the phases of the fECG signal are calculated from the time point of peaks instead of the whole ECG cycle. So the epoch is calculated from the number of synchronisation points (NP) and the duration of synchronisation (TD) that is converted into the time scale as the time difference between the start and the end point of the synchronised region. The synchronisation coordinates of the two subjects are analysed in 4 different primary cycle intervals, the time interval is the same for all the analysis. But as the interval of the primary cycles increases, the time interval between the neighbouring synchronisation coordinates increases too.

The synchronisation ratio may not be steady across the 60 second recording. Four subjects showed variations in the synchronisation ratio in 4 mECG cycles and 2 of these subjects also had variations in 3 mECG cycles. The number of strips corresponds

to the number of fECG peaks in the primary cycle and the slope of strips reflects the variation of the fHR such that the higher the variation shown, the greater the slope. The frequency of the ripples relates to the space between each strip, the higher frequency corresponds to the bigger space. The number of points is quite consistent with respect to the time duration in the synchronisation ratio of 7:4 and 5:3, but the correlation coefficient between the time duration (TD) and number of point (NP) does not match in Fig.4.11.

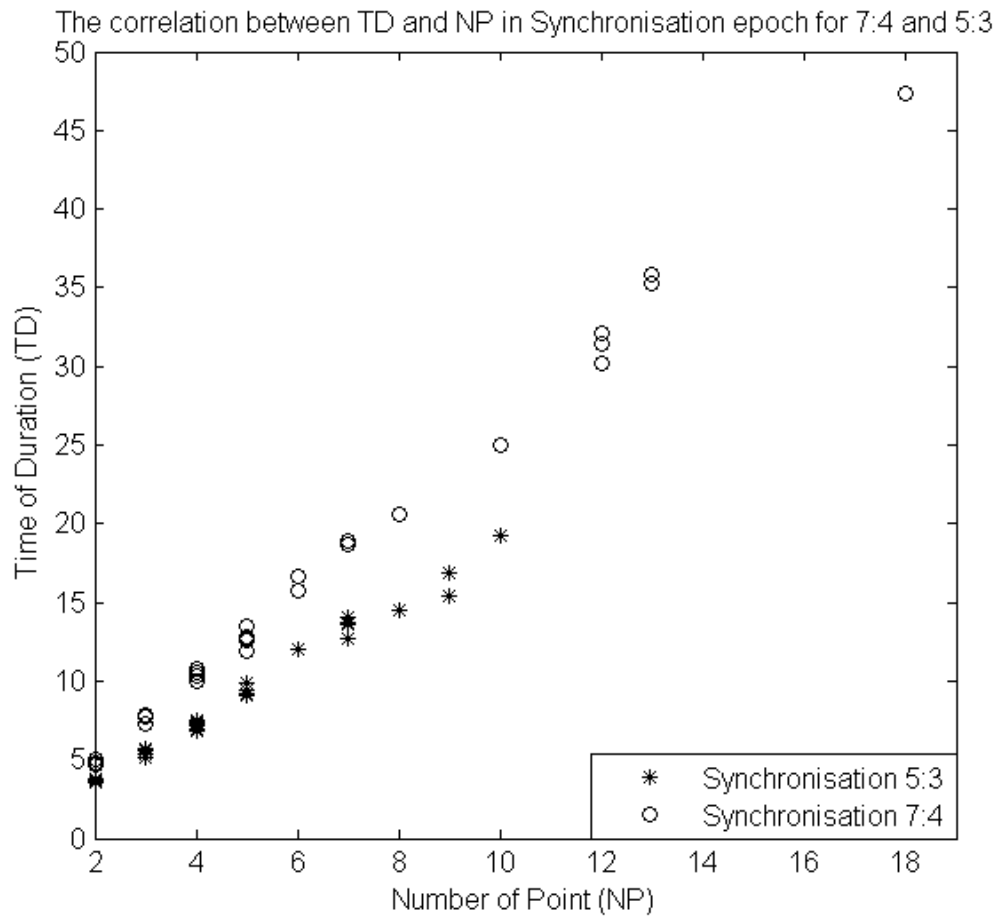


FIGURE 4.11: The corresponding relationship between the number of synchronisation points and duration of synchronisation at synchronisation ratio 3:5 and 4:7

The ratio of the mean values of the heart rate is taken as the indirect parameter of the gestation period to analyse the relationship with the synchronisation behaviour. The low gestation period group results show an inverse relationship and the variation of the relationship increases with the increased gestation period Fig.4.12. The sudden change in the heart rate signals form a rising peak, but it does not affect the synchronisation behaviour unless the magnitude variation of heart rate occurs frequently Fig.4.13.

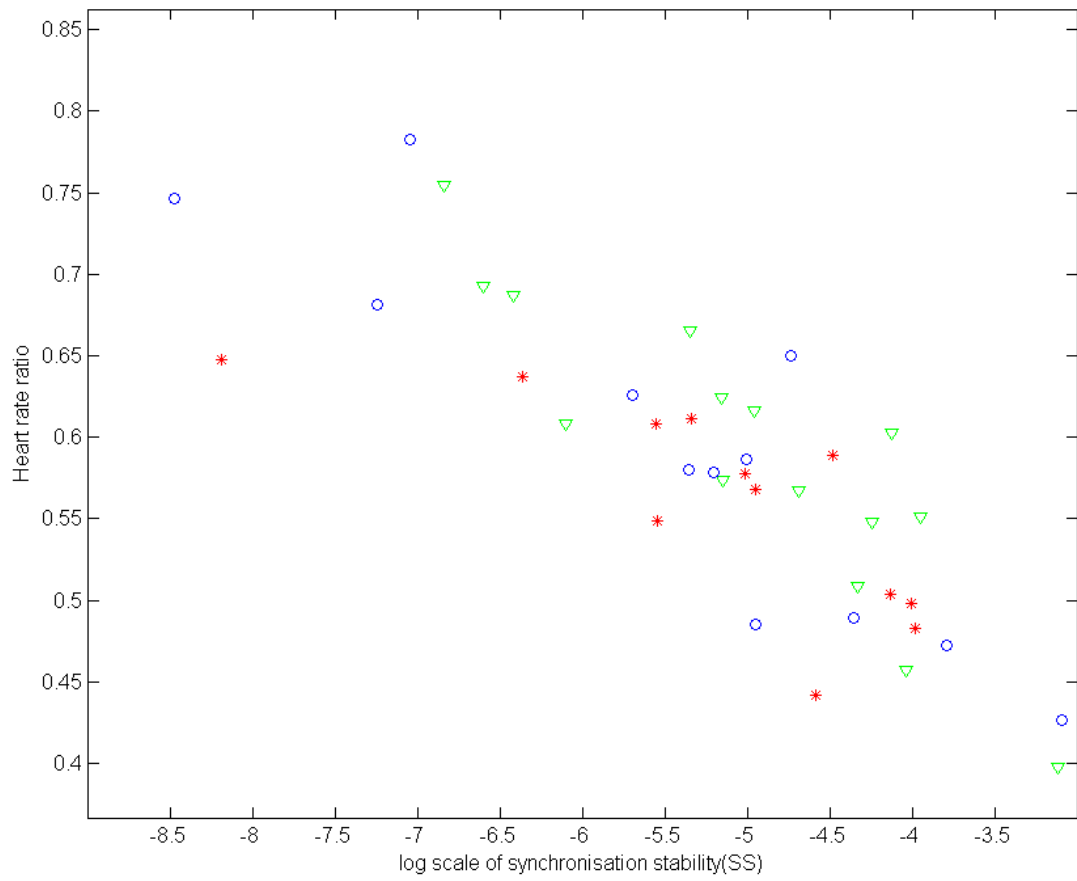


FIGURE 4.12: The synchronisation stability at corresponding heart rate ratio in log scale

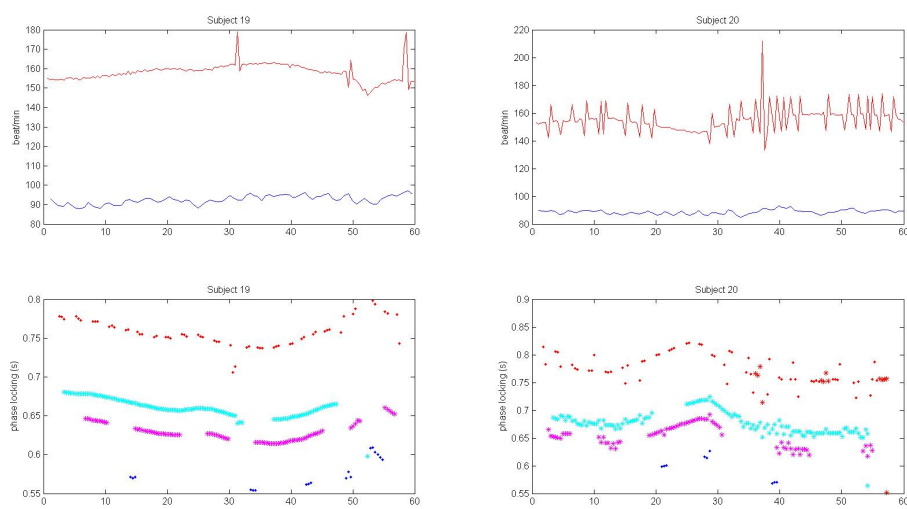


FIGURE 4.13: The effect on the variation of synchronisation by the variation of mHR

### 4.3.1 Synchronisation ratio

The general synchronisation ratio is 7:4 for the data from the *PhysioNet* database and if the mHRs are in a similar range for all of the subjects, the synchronisation of 7:4 may still exist with the a different combination of pairs of fECG and mECG. The synchronisation ratio 3:2 is dominant for the high mHR subjects.

In the overall 20 subjects, there are 4 synchronisation ratios: 2:1, 3:2, 5:3 and 7:4. 4 of the subjects with the synchronisation ratio of 5:3, also have the synchronisation ratio of 7:4. The ratio 3:5 exists at the great increase in the mHR or the decrease in the fHR. If the change in the mHR is mono-direction, it results in a constant ratio of 3:5. But if fHR decreases then increases again, the pattern of ratio of 3:5 would follow the increase of the fHR.

The synchronisation ratio at the different primary cycles overlaps in the time scale but does not have to exist in the same duration. The synchronisation ratio ranges in the recording data are from 1:3 to 1:1 including 1:1, 4:5, 3:4, 2:3, 3:5, 4:7, 1:2, 4:9, 3:7, 2:5, 3:8, 4:11 and 1:3. The synchronisation ratio is not constant during the processed interval of data from the *PhysioNet* database. It may decrease from the high ratio to the low ratio within the 1 minute recording Fig.4.14. The phase locking value is in the range of

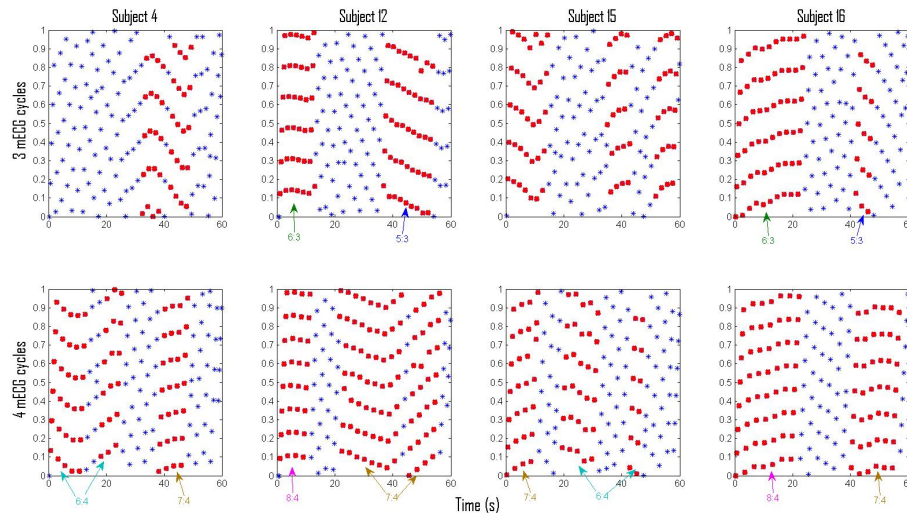


FIGURE 4.14: The synchronisation of fECG at primary cycle 3 and 4 mECG cycles results various synchronisation ratio for 4 subjects from *PhysioNet*

0.5 to 1.2, the higher phase locking value corresponds to the higher synchronisation ratio, which reflects faster fHR. The synchronisation ratio of 1:2 exists for all the subjects in the primary cycle of 1 mECG cycle with a short epoch duration. The synchronisation behaviour is most distinguishable between the low and high gestation period, where the median gestation period behaves as the transient between the two groups Fig.4.15.

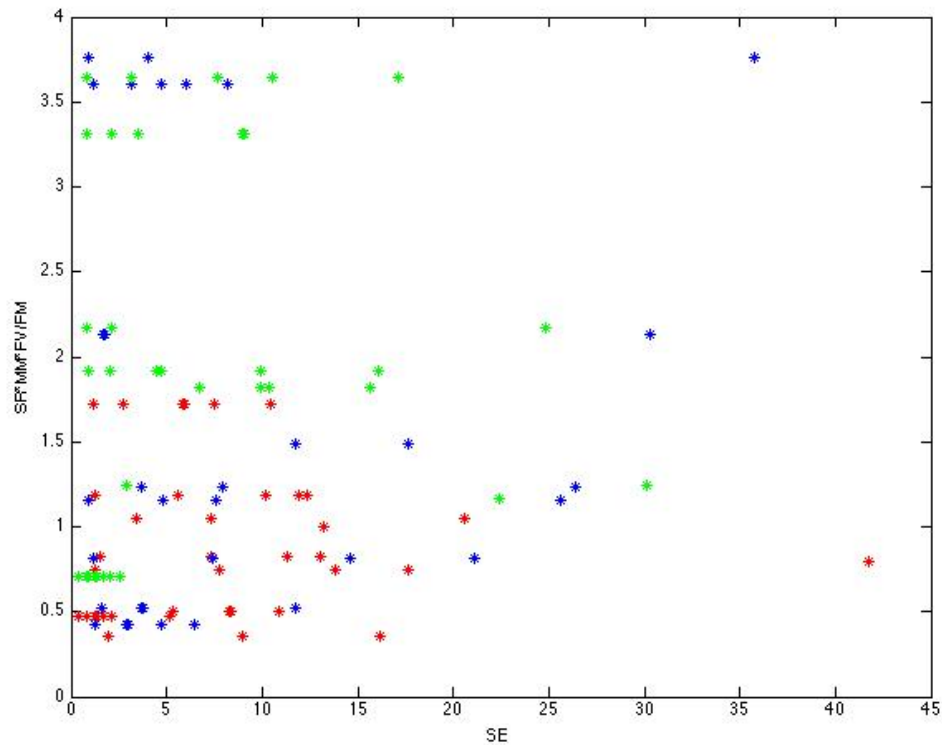


FIGURE 4.15: The synchronisation ratio with effect from heart rate variables at corresponding synchronisation epoch, red is low gestation period, blue is median and green is high

### 4.3.2 Phase locking value

The discontinuous epochs do not change the pattern of  $S_{pl}$  if the phase locking value is generally steady during the entire recording. However,  $S_{pl}$  may vary within the individual epoch and the different phase locking values can result the same variance. The phase locking values are overlapping for same SR at the different primary cycle, but the gradient is not identical. The phase locking values also can be overlapping at the different SR but with the relatively large  $S_{pl}$ . The phase locking value reciprocally relates the fHR because the phase locking value is the time duration between two the fECG QRS peaks at the synchronised state in Fig.4.16.

The synchronisation with the large primary cycle analyses the long term relation between the fECG and the mECG signal, so the heart rate variation may not break the synchronisation epoch but it may affect the phase locking value to result the significant  $S_{pl}$  due to the large amplitude change of the fHR. The variance of the gradient of the phase locking value increases rapidly once the gestation weeks are over 30 weeks in the long-term synchronisation in Fig.4.17.

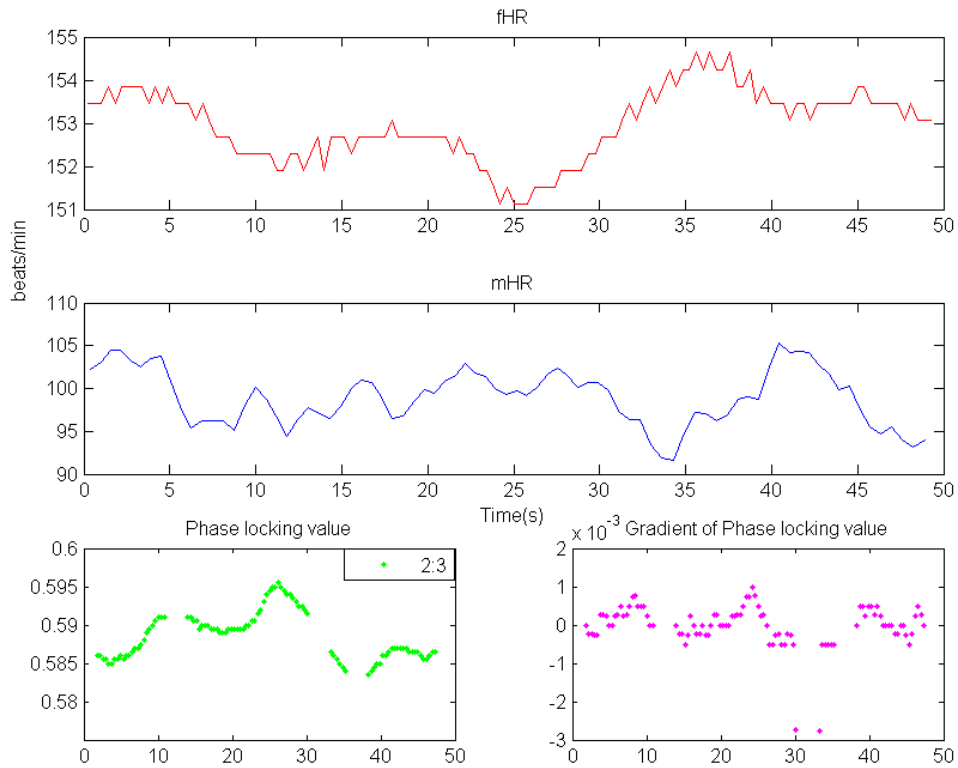


FIGURE 4.16: The fetal and maternal heart rate, synchronisation phase locking value and gradient of phase locking value

Also the SR is reduced with the gestation period across 30-week and it is increased when the gestation period beyond 37-week. The stability of  $S_{pl}$  is better at higher SR for the same gestation period. The pattern of phase locking follow fHR, and sudden change in fHR as peaks can cause discontinuity in phase locking pattern. The phase locking pattern was represented by mean ( $U_{pl}$ ) and the standard deviation ( $V_{pl}$ ) value of the epoch. As it is calculated from the single epoch, the multiple pairs of  $U_{pl}$  and  $V_{pl}$  can be generated for the same synchronisation ratio in the same primary cycle. However, neither of the mean or the standard deviation is constant as the heart rate is not steady to form the constant phase locking pattern. The value of the three variables in the phase locking pattern,  $V_{pl}$ , synchronisation epoch (SE) and  $S_{pl}$  reflect different synchronisation behaviour characteristics, the smaller value of  $V_{pl}$ , the sum of  $S_{pl}$  and the large value of SE establish a steady synchronisation relationship. The gradient of the phase locking value shows the variation of the phase locking value as one of the synchronisation behaviour characteristics in Fig.4.18. The high gestation group shows more fluctuation in the gradient of phase locking value across time Fig.???. The phase locking value range remains the same for the same synchronisation ratio in the different primary cycles, and the range is reciprocal to the

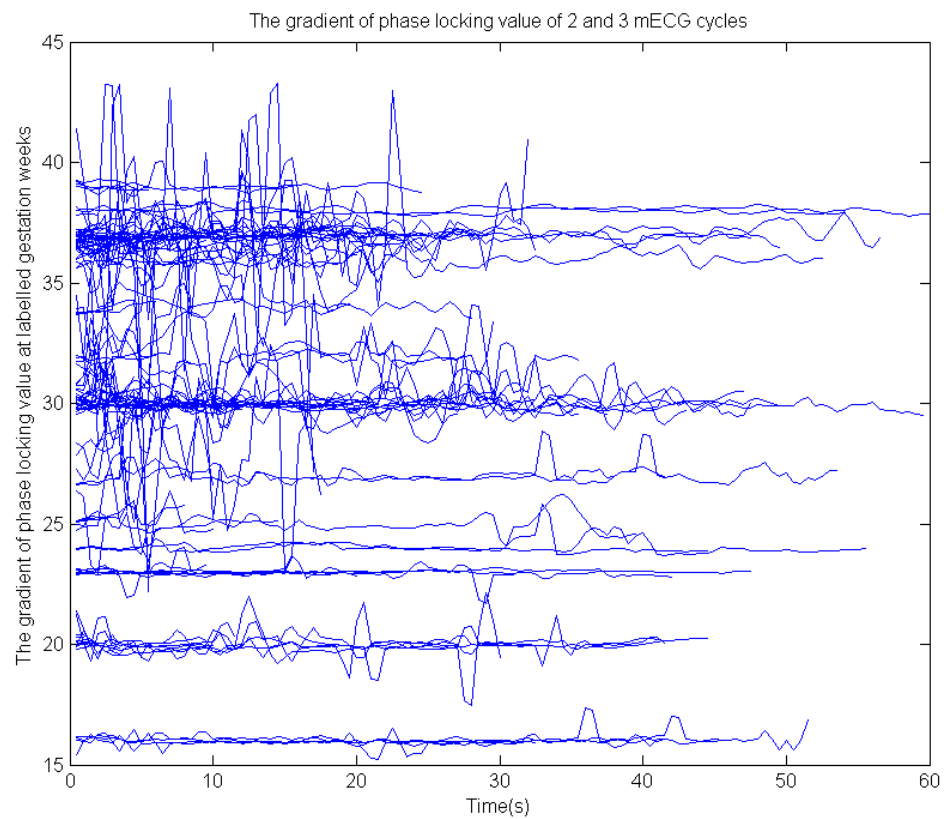


FIGURE 4.17: The gradient of phase locking value at primary cycle 2 and 3

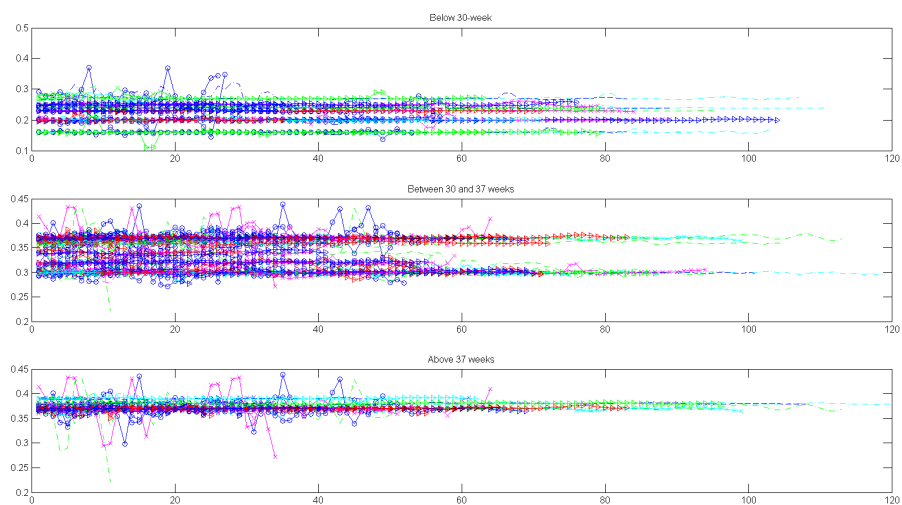


FIGURE 4.18: The gradient of phase locking value at three different gestation groups of data in 120 seconds

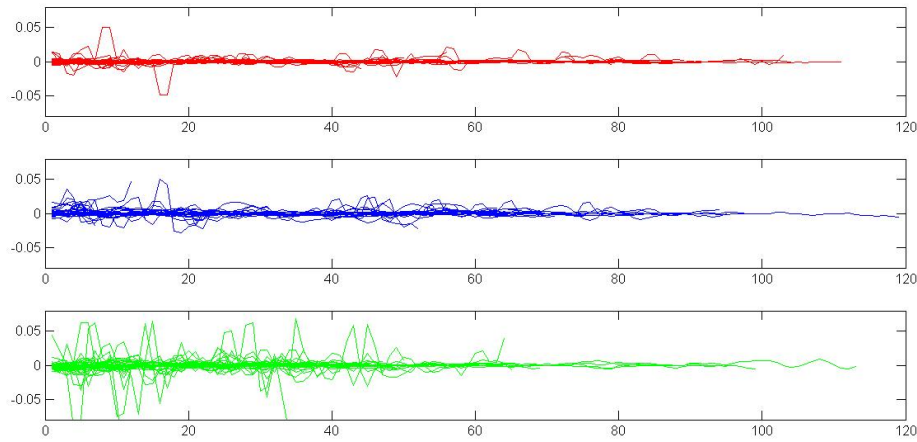


FIGURE 4.19: The gradient of phase locking value of subjects in individual gestation groups in 120 seconds (Top: Low gestation group, Middle: Median gestation group, Bottom: High gestation group)

synchronisation ratio.

### 4.3.3 Synchronisation epoch

The normalised synchronisation epoch duration (nSE) is the ratio ( $SR_{ms}$ ) between SE and  $U_{pl}$ , and is used to normalise the epoch duration from the fHR as  $U_{pl}$  when related to the fHR. The ratio is the one with the overall longest synchronisation epoch of each recording, so SE and  $U_{pl}$  are taken for the longest epoch at the corresponding SR. Most of the group subjects with the gestation period below 30 weeks or above 37 weeks have nSE within the range of 2:3 to 1:2 but the subjects in the gestation period between 30-37 weeks, the ratio varies in a wide range and most synchronisation concentrates at the ratio of 2:3. The comparison of the synchronisation epoch between the gestation groups is focused on the major synchronisation ratios Fig.4.20. The duration of the synchronisation epoch is normalised based on the processing interval of the signal at major synchronisation ratios in Fig.4.21.

TABLE 4.2: The p-value of statistical property of synchronisation behaviour at 6 major synchronisation ratios between the three gestation groups

	1:2	4:7	3:5	2:3	3:4	4:5
Synchronisation epoch (SE)	0.11	0.3706	0.11	0.23	0.75	0.18
Normalised Synchronisation epoch (nSE)	$6.72 \times 10^{-6}$	0.1923	0.0154	0.0167	0.8863	$2.89 \times 10^{-4}$
Mean value of phase locking value ( $U_{pl}$ )	0.04	0.15	0.11	0.23	0.59	0.17
Variance of phase locking value ( $V_{pl}$ )	$3.68 \times 10^{-12}$	0.09	$7.43 \times 10^{-8}$	$1.07 \times 10^{-9}$	0.37	$4.98 \times 10^{-12}$
Gradient of phase locking value ( $S_{pl}$ )	0.90	0.27	0.77	0.44	0.88	0.97

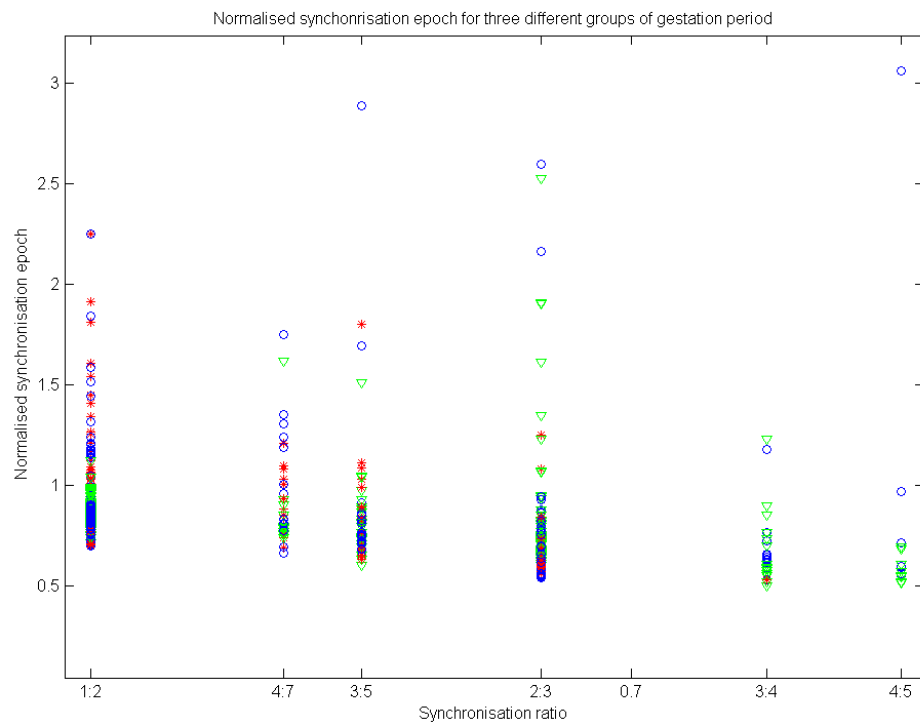


FIGURE 4.20: The normalised synchronisation epoch at major synchronisation ratio for the three gestation groups

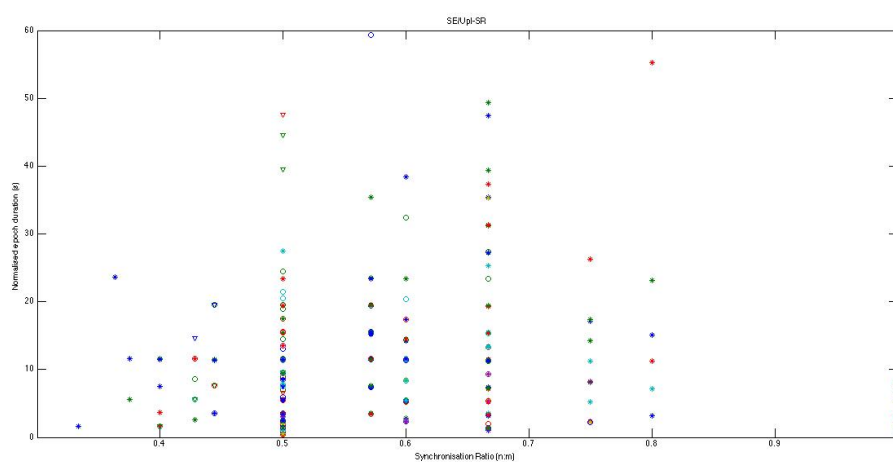


FIGURE 4.21: The normalised synchronisation epochs at corresponding synchronisation ratios

### 4.3.4 Same subject

One of subjects has signals recorded at both 27 weeks and 30 weeks, the SR are consistent with the ratio of 1:2 at the two gestation periods Fig.4.22 . The correlation between the fHR of the two gestation period is -0.22 and it is 0.27 for mHR, they still form the same synchronisation relationship at the overlapped time point.

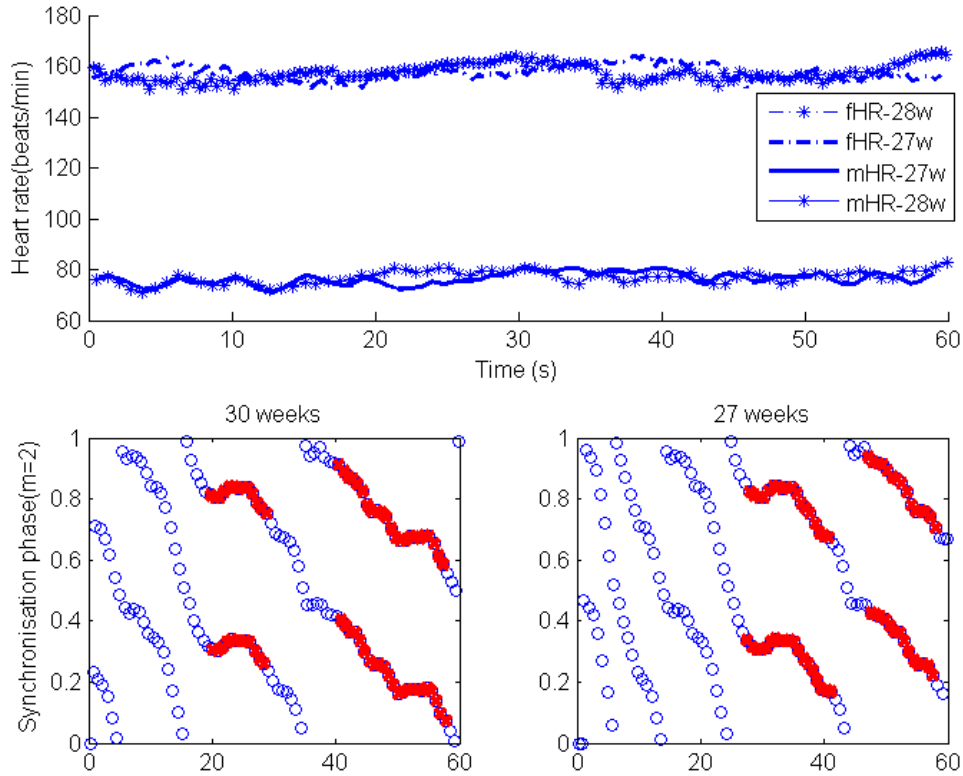


FIGURE 4.22: The heart rate and synchronisation behaviour of same subject at different gestation period

## 4.4 Fetal heart sound

The first recording has clear fetal heart beat (FHB), most work is applied on the second data as FHB is recorded as the background signal. The recording is preprocessed in order to extract the fetal heart sound Fig.4.23 The frequency component is not significant in the FHB sound with the sample frequency of 16000Hz, so the signal is separated into different spectrum by the short time Fourier Transform. The bandpass filter with the cut-off frequency 2 and 30 Hz extracts the envelop of signal and the bandpass filter of cut-off frequency 630 - 750 Hz obtains the significant FHB signal Fig.4.24. The low

frequency range should be above 100 Hz and it forms the least correlation coefficients. The bandpass filter of cut-off frequency range 400-500 Hz results the slight increased the correlation coefficient but the possible FHB sound is removed significantly. The duration of the processing data interval affects the frequency range of FHB sound, so the interval is selected to be 10 seconds. The adaptive filter with least mean square algorithm is more efficient to separate the noise from heart beat sound, but the periodic signal with the great magnitude is more likely to be the mother heart beat sound. The Independent Component Analysis is used to extract fetal heart sound and the result is shown in Fig.4.25.

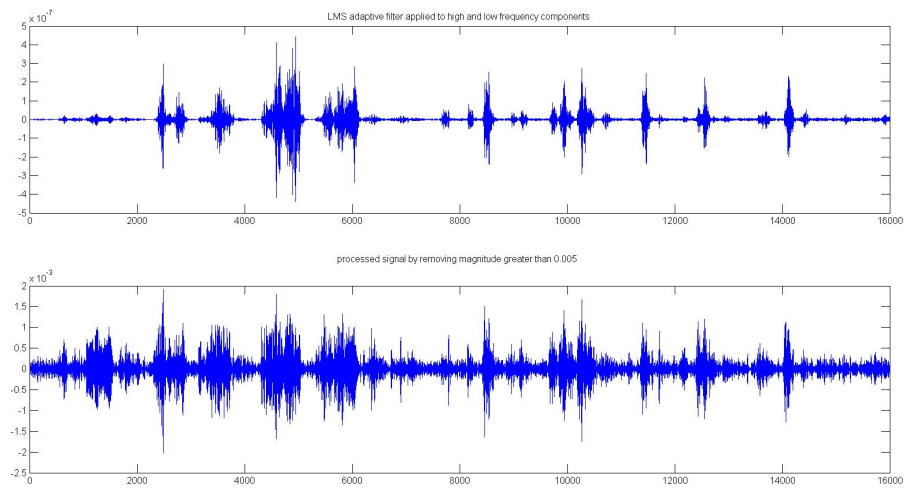


FIGURE 4.23: The preprocessing stage of heart sound recording to enhance the peaks of ECG signal

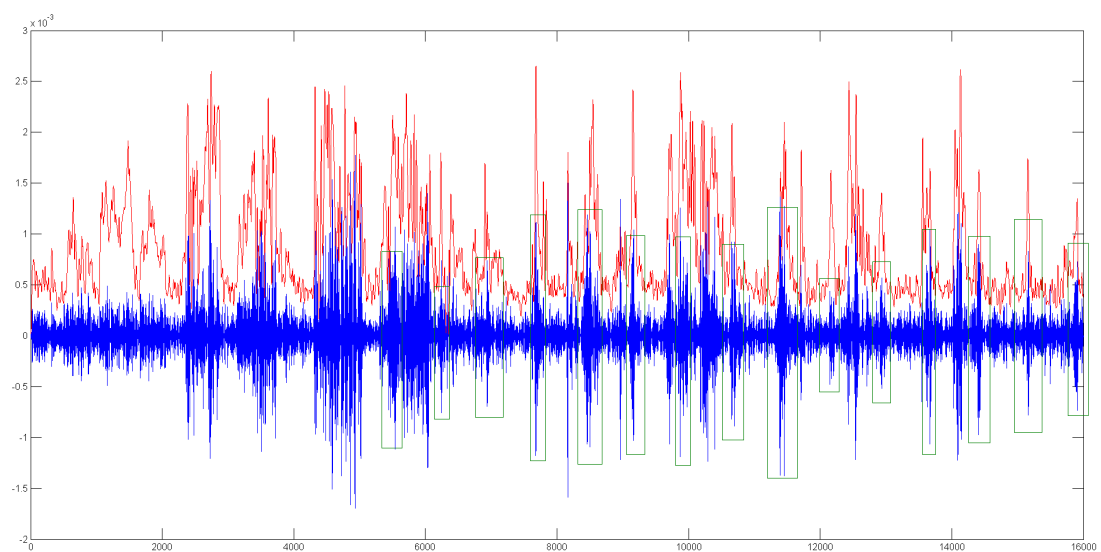


FIGURE 4.24: The envelope of heart sound signal with manual selected potential heart sound region

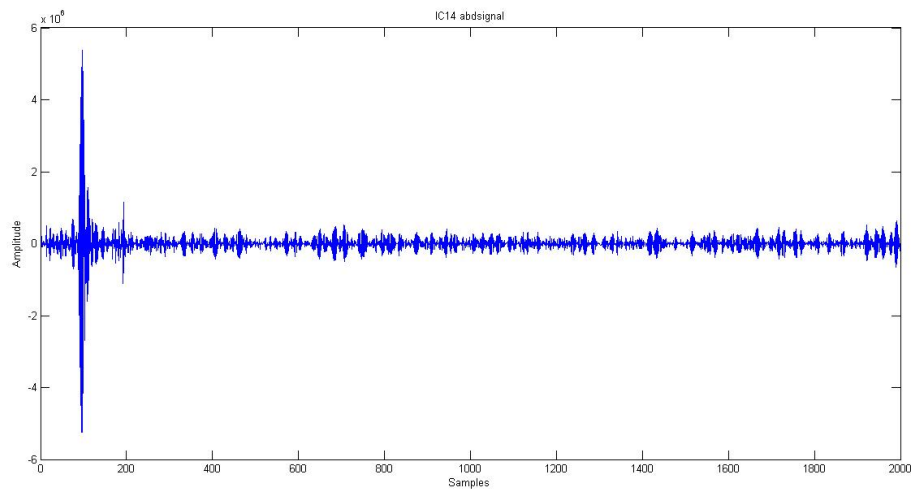


FIGURE 4.25: The ICA component of heart sound recording for best representation of heart sound signal

## 4.5 Mouse data

The mouse data is processed to extract the best pattern information across the different experiment stages. The raw signal is preprocessed to remove the noise, the heart rate of mouse with low protein at each event is manually detected in Fig.4.26. The heart rate of normal mouse is separated to the individual event period in Fig.4.27.

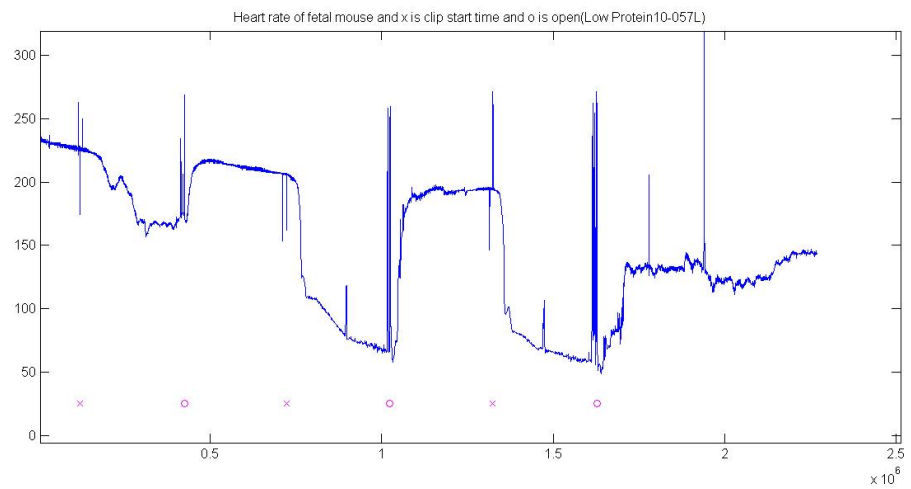


FIGURE 4.26: The fetal ECG from low protein intake mouse including events of clipping and opening

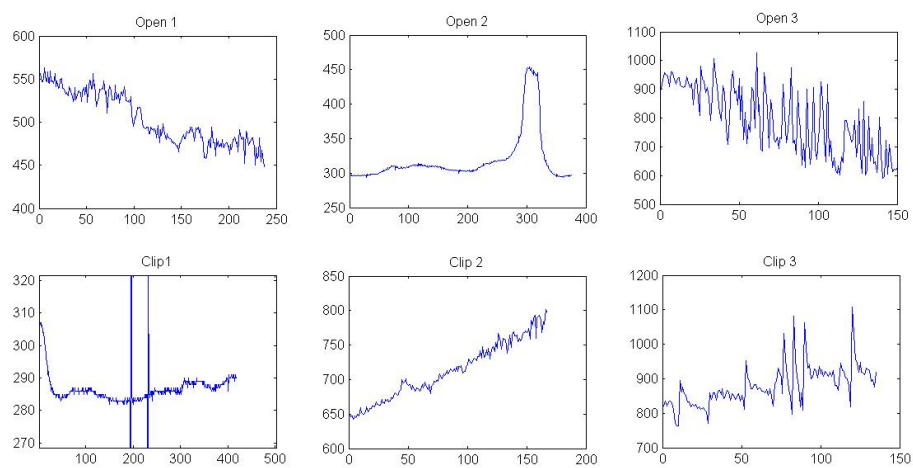


FIGURE 4.27: The fetal heart rate from normal mouse at individual event interval

# Chapter 5

## Discussion

### 5.1 Signal selection

The database of *PhysioNet* is assumed to only have the normal cases so this data is used to design the fECG separation algorithm and to derive the synchronisation relationship between the fECG and the mECG signals. The processing of fECG in the individual abdominal signal has both an advantage and disadvantage over processing the three abdominal signals as one input matrix. On the positive side, the noise associated in the individual ECG cycle of the abdominal signal such as the breath motion artefact, does not affect the accuracy of extraction in the other abdominal recordings, so the mECG variation is limited locally instead of using the average function globally to reduce the error. The disadvantage is that the separation of the mECG cardiac cycle requires either the thoracic or the abdominal signal as the reference to distinguish the mECG from the rest signal data. As the thoracic signal is less likely to be affected by the noise, especially the breath motion artefact, the reference of the mECG cycle can be located in the thoracic signal. The positions of the fetal and the maternal heart source signals are different and is encountered in both the sound and the electrical information.

### 5.2 ECG pattern

The direction of the fECG peak depends on the relative direction between the fetal heart and the abdominal electrode, so the direction may vary in different recordings as the fetus is non-stationary. The thoracic signal is the stationary signal however the abdominal signal is not due to the effect of the motion artefact. The fECG pattern also varies at the different gestation stages.

The extraction principle of the fECG signal cannot be based on the pattern feature or the pattern difference between the fECG and the mECG signal. The weight of the mECG QRS complex varies in between the abdominal and the thoracic signals due to the fECG variation.

The thoracic signal does not have an identical mECG pattern as the pattern recorded in the abdominal signal due to the electrode positions and the heart vector. The QRS peaks may occur at the different time points of the mECG signal depending on the location of the thoracic electrode. The option is to either manipulate the mECG waveform to match the pattern in the abdominal signal or develop the algorithms to only extract the mECG peak.

The most similar region between the abdominal and the thoracic signals is the upward mECG QRS complex. Differences are found in the extra downward peaks of the mECG QRS in the thoracic signal and the relative increase in the T-wave compared to the abdominal signal. The removal of the similarity between the two signals tends to remove the mECG signal entirely from the abdominal signal if the extra downward peaks do not occur in the mECG QRS complex in the abdominal signal.

The longer distance from the maternal heart to the electrodes does not result in a smaller magnitude in the signal or more attenuated waveform. The indication of the mECG locations in the abdominal signal is based on the thoracic recording and there is a delay of mECG in the abdominal signal compared to the thoracic signal in time-domain.

The pattern of the thoracic signal from the database cannot represent the general pattern of all the possible thoracic recording, so the S point cannot be considered as the end of the downward peak, but the Q point is consistent in both the thoracic and the abdominal signals as the start of the high gradient.

The mECG P-wave is not significant in the abdominal signal and may be removed during the baseline wander removal process. The transformation of the mECG signal between the thoracic and the abdominal signals is not linear as the ECG changes both the magnitude and the waveform pattern. The maximum number of fECG peaks within one mECG cycle is two in the recording data set, but more fECG may occur in abnormal conditions. The fECG peaks may sometimes be within the mECG QRS complex, so the removal of the mECG QRS complex by mask may also remove the fECG. However, the possibility of removing the fECG component is low and it can be regenerated by averaging the entire recording once all the processed cycles are linked together.

The peak finding approach is affected by the sudden magnitude changes caused by the abdominal motion. The relationship between the mECG component and the abdominal signals is 4th degree polynomial, but the higher the results the lower the residual and

using the 6th degree is accurate enough. The waveform of the thoracic signal is not used for the relationship of mECG between the abdominal and the thoracic signals because it is inconsistent in all the recordings. The thoracic signal is only used to locate the time points of the mECG QRS complex and number of mECG cycles in the selected interval.

### 5.2.1 Normalisation of ECG interval

The normalisation of the number of input data affects the duration of the actual fECG cycle as none of the ECG cycles have the identical duration, so it is inappropriate to use the normalisation as it would affect the synchronisation relationship. When the cycles are cropped into the same interval as the shortest mECG cycle in the abdominal signal, it directly changes the length of the fECG interval. The correlation between the thoracic and the abdominal signals is not affected by the amplitude normalisation.

## 5.3 Signal processing

The common processing domains are the frequency and the time domain. The analysis unit is either the single point or the group of data depending on the feature representation. The histogram balance is applied for both the single point and group operation, but both the averaging and the template are only applied to the group.

### 5.3.1 Assumption

The assumption of the fECG and the mECG signals is that the properties of the two signals are independent to each other in order to apply ICA. The abnormal mECG and fECG signals may result in similar frequencies, but the signals are still from independent sources. The vector relationship of the abdominal and the thoracic signals is assumed to be derived from a healthy adult case. The period of the ECG signal is determined by delaying the data with the time variable however this is based on the assumption that all the ECG cycles are periodic. There is no assumptions applied to both the pattern and magnitude of the fECG and the mECG signals in order to design the robust separation algorithm to extract the fECG signal from the abdominal recording including in abnormal cases. The last peak of the mECG component in the abdominal signal is disregarded for all the recordings.

### 5.3.2 Error

The additional peak in the gradient signal due to the sudden change in the mECG signal may be correlated to the abnormal feature of the fECG component. The result from the gradient data cannot be used directly to calculate the heart rate, it has to be filtered by the abdominal ECG. The separation of the abdominal signal into segments may cause the loss of the fECG QRS complex due to different HRs of the fetus and the mother. The algorithm of extracting the fECG component from the abdominal signal should be a general process for abnormal mECG and fECG cases, but the algorithm can only be designed to target the feature of the abdominal with prior information which is unknown in the abnormal cases.

### 5.3.3 Effect

The movement of the abdominal electrode caused by respiration affects the measurement of the projection direction of the heart vector in the cardiac cycle. The thoracic and abdominal signals are recorded with the same instruments so the noise sensitivity and the filter tolerance are the same for the two recordings. The physiological feature of the maternal cardiac system has a direct effect on the synchronisation relationship as it is measured by the ECG signal. If the signal is processed in the normalised interval of  $[0,1]$ , the separated ECG signals cannot be converted back to the original magnitude range. The result is that the signals only present a waveform pattern unless the mean and minimum or maximum of the original data is saved. The equalisation of histogram of the abdominal signal will enhance the fECG but also increase the effect of other sources in the abdominal signal.

Due to the significant assumptions for the transform function, it is not an effective approach for the abnormal cases those may have various conditions including the abnormal tissue density or the ECG pattern.

#### 5.3.3.1 Noise

The variation of the ECG recording is unpredictable, the configuration of the electrodes can minimise the external noise but it is ineffective on internal noise such as the EMG signal. The unknown variables for the ECG separation algorithms include the noise signal statistical feature, the number of noise signals, the distribution range and the density. The accuracy of the noise baseline estimation is dependent on the various recording environments and the individual ECG situation. Because the information of fECG magnitude is unknown before it is separated from the abdominal signal, there is

no unsupervised signal selection based on the threshold of the SNR in the preprocessing stage.

The removal of the Gaussian mix which is the white noise, should not affect the probability density of the signal. The noise signal is the unknown source in the abdominal signal, it may be either separated as an individual component or embedded into the fECG and the mECG components. The distribution of the noise is normally assumed to be white noise with zero mean and unity standard deviation. Special cases such as the embedded EMG and the abdomen movement may contribute to the abdominal noise signal as they are not white noise.

### **5.3.3.2 Motion artifact**

The breath motion artefact is an effective factor of extracting the fECG signal accurately, it has to be eliminated from the abdominal signal before the extraction process. Because the motion artefact results in a significant magnitude change in every ECG cycle in the abdominal signal, the range of fECG can be changed from the minimum to the maximum value over the entire recording. The magnitude of the first point of the fECG peak varies as it emerges in different segments of the mECG component. The mECG signal is at a different baseline level due to the motion artefact. The abdominal motion changes the magnitude of the baseline level as the gradient of the abdominal signal cannot distinguish the motion change from the slope change of the mECG peak. The chest movement is a relatively significant motion as well, but the baseline of the mECG pattern in the thoracic signal is consistent at each cycle.

The respiratory cycle is not proportional to the heart rate without intentional control and there is no distortion in any of the mECG patterns in the thoracic signal, so there is no respiratory effect recorded. The fetus movement attenuates the baseline of the abdominal signal, which causes the larger magnitude of the individual mECG QRS peak. The fetus rotation is not a uniform motion, it might be triggered by certain physiological events however it is abnormal to have frequent position changes.

### **5.3.3.3 Cardiorespiratory**

The cardiorespiratory movement is embedded in the mHR signal as a low frequency component, the continuous oscillation does not affect the synchronisation relationship regardless of the amplitude of oscillation ripples [24].

### 5.3.4 Independent component analysis

The key point of FastICA is to achieve the convergence of the weight vector and find the maximum independence and the minimum nongaussianity. The mECG signal cannot be removed from the matrix of the abdominal signals using ICA, the reason is that the fECG peak is considered a part of the mECG signal during maximisation of non-gaussian.

The magnitude of the fECG peak cannot be separated by ICA, so it is not considered as an analysis variable. The time shift of the extracted fECG component from the original time point in the abdominal signal cannot be retrieved by cross correlation. Cross correlation is applied to re-align the mECG peaks in the thoracic and the abdominal recordings.

The P-wave and Q-wave of mECG cycle are disregarded in the separation procedures because they may distort the pattern and none of the signal analysis is based on the amplitude level of these segments.

### 5.3.5 Clustering

Clustering is used to find the membership between data points in the signal, more clusters means more accurate membership. The fuzzy c-mean and k-means are both clustering approaches to group data points with a similar statistical property. They aim to achieve the steady state of the centre of the clusters. Clustering separates data points according to the relationship to the cluster centre. As the shape extraction is used for the fECG component instead of the magnitude, the original clustering method cannot separate the fECG component from the abdominal signal.

Clustering provides the QRS time points and can only be used to separate the ECG components into the cardiac cycle, not to remove the mECG component from the abdominal signal. The cluster is applied to the matrix by combining the abdominal and the thoracic signals, because the single input does not extract the mECG peaks, it only separates the T-segment into the cluster group.

The cluster function can also enhance the SNR of the fECG component in the abdominal signal. The processing relates to and effects the number of clusters defined for separating data points.

The mixing process of the fECG and the mECG components in the abdominal signal is unknown. It can be additive, linear or non-linear. Hard clustering is better approach for the additive process as the fuzzy clustering is not suitable for additive mixing because

one point of the abdominal signal may be the combination of both the mECG and the fECG signal points in the unknown ratio.

### 5.3.6 Empirical mode decomposition

It may be more accurate to design the EMD based on the ECG feature instead of using the maxima and the minima points of the signal. Because mECG has a large peak value, it can be used for the upper envelope.

### 5.3.7 Adaptive filter

The transformation of the mECG QRS complex between the thoracic and the abdominal recordings affects the result accuracy when applying the adaptive filter to remove the mECG signal from the abdominal recordings. The adaptive algorithms reduce both the mECG and the fECG magnitudes in the output signal and the magnitude of the fECG signal should remain unaffected if the adaptive filter is only focused on removing the mECG signal.

### 5.3.8 Learning algorithm

The mECG signal of healthy adults is generally uniform in each cycle, so the learning algorithm between the thoracic and the abdominal signals can be used to find the transform of the mECG pattern in between the two signals. The noise in the abdominal signal may affect the result of the learning process when the algorithms try to fit every mECG cycle into the target feature. In the network training process, if the noise signal is not stationary, the algorithm cannot reach the optimal convergence point. The average of the abdominal signal is subtracted from the individual cycle to bring the abdominal signal to the zero-mean level.

### 5.3.9 Wavelet transform

The mECG component of the thoracic signal is taken as the weight coefficient of the wavelet transform (WT). The advantage of using WT is to break down the signal that has large amounts of data into small data sets according to the frequency range. However, there is no data compression of the mECG cycle in the WT process.

Both the WT and the EMD decompose the input to sub-levels and the output pattern is controlled by the mother wavelet in WT, but the EMD is the sinusoid output. The

normal WT algorithm cannot extract the mECG QRS complex straight from the abdominal signal due to the fECG peaks, but they can be removed from the abdominal signal as a noise component of the mECG cycles.

### 5.3.10 Frequency domain

The frequency range of the fECG component may overlap with the range of the mECG component in abnormal signals. Separating this in the frequency-domain is not successful because it is impossible to extract either the mECG signal or the fECG signal without involving each of the other outputs.

The thoracic signal does not record much high frequency noise unlike the abdominal signal and the adaptive filter can remove the isolating noise. The overlapping of the fECG and the mECG frequency ranges directly affects the accuracy of removing the mECG frequency component as part of the mECG component is embedded in the fECG frequency component.

The main issue is the frequency overlap of the fECG and the mECG components as both components have high and low frequency groups and are composed by the partial mECG and fECG signals. The time delay is applied before using the bandpass filter which takes the same frequency range for each delay as the analysis matrix.

### 5.3.11 Beamforming

According to the dipole model, the delay of the mECG QRS complex between the abdominal and the thoracic signals is caused by the distance between the electrodes. As the depolarisation is along the myocardium in dimension sequence, the muscles further down will be depolarised later which results in the delay of the QRS. So the delay in time relates to the relative physical location of the electrodes.

Once the signal is recorded in the numerical data, the angle of arrival is no longer available and the beamforming is not applicable to analyse these signals. Beamforming targets the signals from the sources in the different direction, but the path of the heart vector to the abdominal electrodes may not be in a straight line. It also requires the data to be processed with directional information which is inaccessible for the current data set.

### 5.3.12 Other approaches

The difference between the neighbour data points in the group can represent the fECG better than the gradient as the change in a group of mECG QRS points is sharp but it does not last long. The magnitude of the difference is much greater than the magnitude of the noise ripple.

A few approaches are under consideration. One is to convert the heart vector based on the difference in abdominal and thoracic signal patterns to the electrode positions. The beamforming is applied afterwards to separate the signals from the sources at different angles to the electrodes. The other method is to increase the SNR in the abdominal signal before ICA by applying the adaptive filter with the thoracic signal as the reference signal.

### 5.3.13 Selection of the algorithms

Not all the algorithms proposed in the method section have been tested with the open source data. A few of the approaches such as the beamforming are initiated in the algorithm design because of the similarity of the signal recording process of the thoracic and the abdominal signal and the pattern feature. The strategy of beamforming is to use the recorded pattern and the angle of arrival of the source to construct the source signal and is introduced to estimate the mECG component in the abdominal signal. However, the angle of arrival to the electrode is an unknown variable during the recording so it would be not successful to develop the algorithms based on the principle of beamforming.

Some of the algorithms are aimed to extract the fECG and the mECG signal, but they can only improve the SNR of the fECG signal, with the partial mECG signal left in the result signal. The only approach that succeeds to separate the fECG and the mECG signals from the input matrix is the independent component analysis with pre-processing, however the separation algorithm is not robust enough for all the data from the open source due to the different signal features.

### 5.3.14 Cross correlation

The cross correlation between the selected abdominal and thoracic signals should give the distance to the next peak with a view to aligning ECG between the two signals again. By running a loop of cross correlation of the two signals, all the peaks should be allocated. If the peak point of the mECG cannot be allocated by cross correlation, the signal is separated into the square matrix. The correlation between the abdominal and

thoracic signals is used to find the mECG component region in the abdominal signal and the missing mECG data points from the output component can be retrieved by checking the neighbouring data around the peak region.

Template matching is a special way of cross correlation. It obtains the time point of the maximum value of the shifted input data to find the similar region across the two input data's.

The correlation coefficient of the mHR and the fHR signal is generally low. The correlation coefficient analyses the attenuation of the patterns, but the synchronisation indicates the existence of the coupling relationship of the fHR signal with respect to the mHR signal instead of considering the two signals as two separate variables.

### 5.3.15 Very low frequency component

The very low frequency (VLF) component of the maternal heart rate is calculated after converting the signals by the Fourier Transform in frequency domain and it is selected as the most dominant peak in the low frequency range. Even if there is a correlation between the synchronisation ratio to the range of the maternal VLF component in the subject recordings from the *PhysioNet* database, it may not directly connect the coupling between the maternal and the fetal cardiac systems.

In a few publications, the VLF is linked to the oxygen consumption or the temperature. The temperature is directly affected by the oxygen consumption as the metabolism process requiring the presence of oxygen will vary the body temperature. The actual relationship of VLF to either the temperature or the oxygen consumption is not illustrated so the value of the VLF does not demonstrate a possible link to the fetal temperature or the oxygen consumption.

## 5.4 Demographic information

TABLE 5.1: The demographic information of recorded subjects

Low gestation period				Medium gestation period				High gestation period			
GP(weeks)	Age(year-old)	Height(cm)	Weight(kg)	GP(weeks)	Age(year-old)	Height(cm)	Weight(kg)	GP(weeks)	Age(year-old)	Height(cm)	Weight(kg)
16				29	24	156	55.7	36	31		
16	30			29	30	156	56.6	36	30	157	55.76
20	30	148.5	46.7	30.29	35	157	52	37	40	153	58.2
20	38	155	55.5	30.86	34	159	56	37	36	155	53
20	31	148.4	46	32	29		50.2	37.43	18	155	61.8
20	35	164	60	32		155		38	34	157	64.5
23				32	21		54	38	24	164	68.45
24	26	161.8	65.9	34	34	159	55.2	38.86	36	153	47.9
25	31	148.4	46	34	21	152		39	27	155	51.6
27	25	163	52.5	34	27	157	55.2	39	35	158	64.3
27				34		162	48	39.14	20	157	60.6
28	30	153	52.1	34.29	25	152.7	56.2	39.71			
				34.86	29	154.9	47	40	37	155	60.8
								40			

Not all the subject demographic information is collected. The information includes the age, height, weight and the gestation period, but some information may not be released due to a confidentiality policy.

## 5.5 Synchronisation

The horizontal line of the synchronisation epoch needs to be evenly distributed to be considered as synchronised data point. The synchronisation is not time-dependent, it is event dependent analysis and the absence of synchronisation indicates the unstable fHR.

When the synchronisation of the fetal and the maternal cardiac systems is analysed by projecting the fECG QRS onto the mECG cycle on the time scale, it focuses on the heart rate variable instead of the ECG component. The synchronisation coordinates are discontinued in the primary cycle with of 3 or 4 mECG cycles due to the limited number of fECG peaks in the 60-second recording interval. The longer recordings may show the complete continuity of the synchronisation coordinates.

The synchronisation phase is based on the single time point of the fECG peak with respect to the different mECG cycle durations. The synchronisation can be interpreted into the short term and the long term behaviour. When the primary cycle composes less than or equal to two mECG cycles, it is considered to be short term analysis and the long term analysis has a number of mECG cycles equal to or over 3. The short term synchronisation is sensitive to the change of the fHR signal but it can also show the synchronisation in the single mECG cycle event. The long term synchronisation with up to 4 mECG cycles in the primary cycle is not sensitive to the change within each mECG cycle and the alternated increase or decrease of the fHR signal may not be detected in longer term cycles.

Individual sudden changes will not affect the overall pattern behaviour unless it is continuous for a period. The ripple or the continuous shape in synchronisation is not controlled by the individual interval of the fECG or the mECG signals.

The last synchronisation point is disregarded as it may not result from a complete primary cycle. The synchronisation may disappear in the longer primary cycle if the number of synchronisation points cannot be divided by the factor. The difference between the synchronisation of the fetal and maternal systems and cardiorespiratory synchronisation is that the synchronisation uses the interval of mECG cycle and time point of the fECG R peaks instead of the phase of the patterns, so the variation in the mECG pattern feature will not be taken into the analysis.

All the variables are added to the combinations in the equation to represent the feature of synchronisation instead of using individual variables. The time point of the fECG peak in the fECG component extracted from ICA may not be identical to the original time point in the abdominal signals as it may shift the time point of the synchronisation. It will result in different synchronisation ratios only if there is a large variation in the mHR signal.

The synchronisation between the two systems does not consider the magnitude of the ECG, so the strength of myocardium polarisation is not analysed but it does not exclude possibility of the relationship at the strength level.

The potential synchronisation force is the oxygen supply to the fetal system totally relies on the oxygenated level in the maternal cardiovascular system. The status of the maternal cardiac functionality may indirectly link to the fetal cardiac system. In this case, it is important to improve the fECG extraction approach to increase the accuracy of the synchronisation relationship analysis. However, the comparison between the gestation periods and the synchronisation relationship is not based on the control group as the recordings are collected from the different patients with different gestation period and the synchronisation ratio for each gestation period is not constant.

### 5.5.1 Synchronisation ratio

The synchronisation ratio may stay the same for the same subject but it is not conclusive from the current dataset. As the synchronisation ratio is based on the fECG peaks and mECG cycles, the error in the extraction of fECG peak will be carried to the calculation of the synchronisation ratio. The decrease of the synchronisation ratio can be caused by either the increase of the mHR or the decreased fHR, the change factor cannot be determined if no control subjects are included.

Different from the cardiorespiratory synchronisation, once the synchronisation ratio changes from the constant 4:2 to 3:2, it does not return back to the previous ratio. Based on the current database, the range of synchronisation ratios of the healthy subjects is within the range of 3 : 2 to 2 : 1, but the ratios out of the range can be caused by the abnormalities in either the fetus or maternal or both systems.

The overlap region of the synchronisation ratio 4:7 and 3:5 on time scale indicates the primary cycle controls the synchronisation analysis duration. The less mECG cycles included in the primary cycle results the shorter term synchronisation. The synchronisation ratio of 1:2 at one mECG cycle is a rare case and presents normally when the gestation period is in the third trimester. The ratio 1:2 appears in various numbers of

the mECG cycles, and it leads to a continuous ratio of 2:3. In this circumstance, the short term synchronisation should not be included to draw conclusion and the size of the primary cycle needs to be 2 or above to be considered for the synchronisation behaviour.

### 5.5.2 Phase locking value

The gap of the phase locking value between each strip represents the value level of the fHR which is reciprocal to the fECG interval. The greater the gap, the longer the fECG interval.

The phase locking value indicates the stability of the synchronisation between the fECG and the mECG signals and it is inversely correlated to the fHR but independent to the mHR. The increased fHR leads to a decrease in the phase locking value and the synchronisation relationship would be broken at certain fHR and mHR ratios.

The increased variance of  $S_{pl}$  corresponds to the discontinuous synchronisation between fetal and maternal cardiac systems. The discontinuity of the synchronisation does not necessarily lead to changing synchronisation ratios. The continuous changing in the slope with a discontinuous synchronisation epoch indicates the consistent increase or decrease of the fHR without the mHR variation. In most cases, multiple synchronisation epochs (SE) occur in each primary cycle due to the variation of the heart rate and the duration of each SE is not consistent for the same SR.

The duration of the phase locking value epoch is measured from the first to the end points of the synchronisation phase. Unlike the fHR, the variation of the mHR does not affect the phase locking value however it directly affects the synchronisation ratio. The extended variables from the phase locking value,  $V_{pl}$ ,  $U_{pl}$  and  $S_{pl}$  represent the feature in the synchronisation condition at each individual epoch. The difference between  $V_{pl}$  and  $U_{pl}$  from  $S_{pl}$  is that the first two variables are single values for each epoch and the last one keeps track of every point in the epoch.

### 5.5.3 Same subject

In the recording database, two subjects are recorded twice at different gestation periods. They are identified according to a subject label which is unique for every subject and one of them has recorded age and height in the demographic information table. One of the subjects with recordings at the gestation period of 20 week and 24 weeks has a short recording less than 30 seconds at 24 weeks and about 60 seconds recording at 20 week. This subject is excluded from the analysis due to the short recording. The

relationship between the synchronisation and the gestation period is analysed separately for one subject with recordings at 27 and 28 weeks.

#### **5.5.4 Statistical comparison analysis across the gestation groups**

The mean and the standard deviation of the normalised synchronisation epoch at the individual synchronisation ratio are compared across the low, median and high gestation period groups. However, the numbers of the synchronisation epoch for each subject are not consistent and the numbers of subjects in each gestation period group are not the same, so only the analysis of variance (ANOVA) is applied to compare across the different gestation groups.

### **5.6 Heart rate**

Neither the fHR nor the mHR are distinguishable in between the different gestation periods because the individual subject has different baseline heart rates and the ratio of the mHR over the fHR has a tendency to increase in the longer gestation period.

The pairs of the maternal and the fetal heart rates do not show the correlation between each other or to the gestation period based on the mean value. The synchronisation relationship is analysed with respect to the gestation period as the mHR feature may have a unique feature at the different gestation period.

The mHR and the fHR are extracted from the same recording but they have different signal length due to the various duration of the ECG cycle. When the correlation coefficient is applied to analyse the similarity between the two signals patterns, the length of the vectors needs to be the same. So the mHR is stretched to the same vector length as the length of the fHR. The process uses the value distribution of the pattern from dividing the point value equally into the length of the fHR signal. The single mHR and fHR mean value only covers the overall average range of the signal.

### **5.7 Gestation period**

The separation of the subjects into the groups regarding the gestation period is tested in two strategies, first is to separate the subjects into three groups, below 26 weeks, between 26 and 33 weeks and above 33 weeks. The other separation strategy considers two groups based on the trimester stages and the overall recording database only includes second

(13-28 weeks) and third (29-40 weeks) trimesters. Only the first strategy is applied in the analysis.

The initial separation uses the three gestation period groups, the middle gestation period group is assumed as the transient group and it may have a decreased synchronisation ratio, but the significant variation of the slope of the phase locking value is not for all subjects.

The first data analysis result is concluded from the gestation period labelled in the files of each subject, but the gestation periods are not recorded correctly for some of the subjects. After regrouping the subjects by the correct gestation period, one of the subjects is moved from the middle gestation group to the high gestation group and the rest of the subjects remained in the previous groups.

## 5.8 Oxygenation level

The oxygenation level in the mothers cardiovascular system is not monitored during the ECG recording but in under general health conditions. The increased heart rate normally is caused by a reduced oxygenation level. However, neither respiratory nor oxygenation level can be taken as a controlled variables as it may affect fetal development.

## 5.9 Proposed relationship

The possible relationship between the fetal and the maternal cardiac systems may be caused by the oxygen saturation level in the maternal cardiovascular system as oxygen exchange of the fetus occurs in the placenta. The low level of the oxygen in the maternal blood system may trigger a change in the maternal heart rate to supply more efficient oxygen for the fetal metabolism.

In the comparison of the synchronisation ratios distribution with the gestation period, the longer gestation periods tend to have lower synchronisation ratios which represent as the increased mHR with respect to the fHR. It correlates to the fact that the fetus may require an increased amount of oxygen for the cell development in the later stage of pregnancy. The variance of  $S_{pl}$  may indicate the complex development of the fetus which disrupts the steady synchronisation to the maternal cardiac system and may be caused by the shortage of oxygen supply from the mother so then alters both systems. Also, the synchronisation relationship is strong at the early stage of gestation and stays in a reasonable ratio of between 2:3 and 1:2 during stable oxygen supply.

Further questions raised relating to the proposed interaction force and the direction of regulation are whether the oxygenation level affects the fetal oxygen exchange behaviour by reducing the fHR or the low oxygenation level in the fetal blood triggers the increase of the mHR. It is also possible that the interaction force is dual-directional so the fHR and the mHR may affect each other in relation to the oxygenation variation. Another factor that may also cause synchronisation differences is that the foetus is isolated from the air so it is not easy for them to adapt the change of oxygenation level.

## 5.10 Heart sound

The generated multi-dimension signal is considered to be recorded from the microphones located extremely close to each other. The creation of the matrix by the delay variable only influences the high frequency component due to the heart function. Since the same mixing matrix is applied to the maternal heart sound, the new row vector can be created by shifting the signal in the time scale based on the method of the delay generated matrix. The frequency is not a distinguishable tool to separate the FHR in the sound wave.

## 5.11 Mouse data

The mouse data is used to analyse the effect of different events on the heart rate by comparing a controlled group to a group with a low protein intake. The original data is recorded with a significant noise level which causes the signal to have the low signal-to-noise ratio. One subject with fECG amplitude in the range of 40 has a sudden drop to -20, which results in the failure of the QRS extraction by the peak detection. The bandpass filter shifts the signal consistently for every data point, but the data applied for analysis is time sensitive as the time related events are variables in the recording.

## Chapter 6

# Conclusion

The research takes two different sources of the abdominal recording to analyse the synchronisation relationship between the fetal and the maternal cardiac systems. The multiple abdominal and the thoracic signals from one online source are implemented as the input to separate fECG and mECG. The pairs of fECG and mECG recordings for the subjects at the different gestation periods are recorded and extracted by an external institute. That data is then applied to analyse the synchronisation relationship behaviour with respect to the gestation periods.

### 6.1 fECG signal separation from abdominal signal

The abdominal and thoracic signals from the online source does not include information on the maternal health condition or the reference signals of the fECG patterns. The multiple recordings of the ECG signal at the maternal abdomen are processed by independent component analysis (ICA) to extract the fECG and the mECG signals.

An approach is developed for the signals from the online open source *PhysioNet* and an extraction strategy is applied by using ICA after testing the separation results of various algorithms including clustering, wavelet transform, singular value decomposition, empirical mode decomposition, adaptive filter and beam-forming.

The input signal of the fECG and mECG signals is a matrix of three abdominal and one thoracic recordings. The pre-processing is also included in the algorithms development with the first step being to remove the baseline wander from the abdominal signal by using a smooth function to construct the baseline wander signal in the form of the sinusoid wave.

The next step is to align the abdominal signal to the thoracic signal according to the time point of the mECG peaks by finding the cross correlation variable. The multi-dimensional input matrix of ICA is constructed by continuously taking a shifted vector from the single vector as the columns of the matrix. The shift variable is 20 data points for each recording signal and in total three abdominal signals and one thoracic are used to construct the matrix with the size of 20 by 4.

The number of separated components is the same as the number of columns in the matrix and both the fECG and mECG patterns are separated into several components. The components are separated by the demix coefficients which is a square matrix. The coefficients matrix maximises the non-gaussianity between the extracted components and the algorithm is designed with the non-quadratic function and the derivative of the function. The threshold of optimising the demix coefficients in the iterative loop is in the level of  $10^{-5}$ .

The separated fECG and mECG signals with the highest SNR are selected from the resultant components and those components are compared to the estimated fECG peaks in the original abdominal signal to confirm the correct peak extraction.

## **6.2 The synchronisation analysis between fetal and maternal cardiac system**

The synchronisation equation is developed from the extracted fECG and mECG signals which are separated from the abdominal and thoracic signals in the online open source. But the synchronisation is irrelevant to the ECG pattern feature as it only considers the time point of the ECG peaks when calculating the synchronisation relationship.

The synchronisation takes the mECG cycles as the new time scale for each fECG peak within the mECG cycle. The constant number of fECG peaks in the analysis of the mECG cycles is defined as the synchronisation point in the synchronisation phase and they form the continuous horizontal strips in the plots. The number of strips indicates the synchronised number of fECG peaks.

The duration of synchronisation epoch is not constant at the same synchronisation ratio for the same gestation period, but the duration for a high synchronisation ratio is reduced in the high gestation group. The heart rate signals are not a control factor in the synchronisation relationship, but it indirectly affects the synchronisation ratio because it is derived from the combination of the both fHR and mHR.

The synchronisation ratio compares the number of mECG cycles with the number of fECG peaks in those cycles and the synchronisation phase points with the same synchronisation ratio form a block of synchronisation epoch which represents one of synchronisation behaviour characteristics.

When the synchronisation behaviour is analysed against the gestation period, there is a decrease of the synchronisation ratio in the longer gestation period. The synchronisation analysis is based on various variables and the combination of the variables, but none of them shows the absolute relationship between the stability of the synchronisation and the gestation period.

# Bibliography

- [1] S. Abboud and S.and Sadeh D. Alaluf, A.and Einav. Real-time abdominal fetal ecg recording using a hardware correlator. *COMPUTERS IN BIOLOGY AND MEDICINE*, 22(5):11, 1992.
- [2] R. Arias-Ortega and M.J. Gaitlén-González. Single channel abdominal ecg algorithm for real-time maternal and fetal heart rate monitoring. *ARTÍCULO DE INVESTIGACIÓN ORIGINAL*, 31(2):8, 2010.
- [3] M. Arif, M. UsmanAkram, and Fayyaz ul AfsarAmirMinhas. Pruned fuzzy k-nearest neighbor classifier for beat classification. *JOURNAL OF BIOMEDICAL SCIENCE AND ENGINEERING*, 3(4):10, 2010.
- [4] K. Assaleh. Extraction of fetal electrocardiogram using adaptive neuro-fuzzy inference systems. *IEEE TRANSACTIONS ON BIOMEDICAL ENGINEERING*, 54(1):10, 2007.
- [5] K. Assaleh and H. Al-Nashash. A novel technique for the extraction of fetal ecg using polynomial networks. *IEEE TRANSCATIONS ON BIOMEDICAL ENGINEERING*, 52(6):5, 2005.
- [6] K.A.K. Azad. Fetal qrs complex detection from abdominal ecg: A fuzzy approach. *IEEE NORDIC SIGNAL PROCESSING SYMPOSIUM*, page 4, 2000.
- [7] B. Azzarboni, M. Carpentien, E.L. Foresta, and E.C. Morabito. Neural-ica and wavelet transform for artifacts removal in surface emg. 4:6, 2004.
- [8] A.K. Barrosa. Extracting the fetal heart rate variability using a frequency tracking algorithm. *NEUROCOMPUTING*, 49(1-4):10, 2002.
- [9] R. Bartsch, J.W. Kantelhardt, T. Penzel, and S. Havlin. Experimental evidence for phase synchronization transitions in the human cardiorespiratory system. *PHYSICAL REVIEW LETTERS*, 98(5):4, 2007.
- [10] S.C. Bera, B. Chakraborty, and J.K. Ray. A mathematical model for analysis of ecg waves in a normal subject. *MEASUREMENT*, 38(1):8, 2005.

- [11] O. Boiman and M. Irani. Similarity by composition. *ADVANCES IN NEURAL INFORMATION PROCESSING SYSTEMS*, (19):8, 2007.
- [12] J.L. Camargo-Olivares, R. Martín-Clemente, S. Hornillo-Mellado, and Román I. Elena, M.M. The maternal abdominal ecg as input to mica in the fetal ecg extraction problem. *IEEE SIGNAL PROCESSING LETTERS*, 18(3):4, 2011.
- [13] G. Camps-Valls, M. Martínez-Sober, and E. Soria-Olivas. Fetal ecg extraction using an fir neural network. page 4, 2001.
- [14] G. Camps-Valls, M. Martínez-Sober, E. Soria-Olivas, R. Magdalena-Benedito, J. Calpe-Maravilla, and J. Guerrero-Martinez. Foetal ecg recovery using dynamic neural networks. *ARTIFICIAL INTELLIGENCE IN MEDICINE*, 31(3):13, 2004.
- [15] J. Cardoso. Source separation using higher order moments. 4:3, 1989.
- [16] J. Cardoso. Multidimensional independent component analysis. 4:4, 1998.
- [17] R. Ceylan and Y. Ozbay. Comparison of fcm, pca and wt techniques for classification ecg arrhythmias using artificial neural network. *EXPERT SYSTEMS WITH APPLICATIONS*, 33(2):10, 2007.
- [18] R. CHAOUI, J. HOFFMANN, and K.S. HELING. Three-dimensional (3d) and 4d color doppler fetal echocardiography using spatio-temporal image correlation (stic). *ULTRASOUND OBSTETRICS GYNECOLOGY*, 23(6):11, 2004.
- [19] J. Chee, R. Acharya, K. Er, W. Tan, and C.K. Chua. Visualization of cardiac health using vector cardiogram. *INGÉNIERIE ET RECHERCHE BIOMÉDICALE*, 29(4):10, 2008.
- [20] A. Cichocki, J. Karhunen, W. Kasprzak, and R. Vigario. Neural networks for blind separation with unknown number of sources. *NEUROCOMPUTING*, 24:55, 1999.
- [21] G.D. Clifford. Fetal maternal ecg blind source separation lab. *BIOMEDICAL SIGNAL AND IMAGE PROCESSING SPRING*, page 10, 2005.
- [22] G.D. Clifford, R. Sameni, J. Ward, J. Robinson, and A.J. Wolfberg. Clinically accurate fetal ecg parameters acquired from maternal abdominal sensors. page 26, 2011.
- [23] D. Cysarz, H. Bettermann, S. Lange, D. Geue, and P. Van Leeuwen. A quantitative comparison of different methods to detect cardiorespiratory coordination during night-time sleep. *BIOMEDICAL ENGINEERING ONLINE*, 3(1):44, 2004.
- [24] D. Cysarz and A. Bussing. Cardiorespiratory synchronization during zen meditation. *EUROPEAN JOURNAL OF APPLIED PHYSIOLOGY*, 95(1):15, 2005.

- [25] L. De Lathauwer, B. De Moor, and J. Joos Vandewalle. Fetal electrocardiogram extraction by blind source subspace separation. *IEEE TRANSACTIONS ON BIOMEDICAL ENGINEERING*, 47(5):6, 2000.
- [26] L.D. Devoe. Fetal eeg analysis for intrapartum electronic fetal monitoring: A review. *CLINICAL OBSTETRICS AND GYNECOLOGY*, 54(1):10, 2011.
- [27] G.R. Devore, P. Falkensammer, M.S. Sklansky, and L.D. Platt. Spatio-temporal image correlation (stic): New technology for evaluation of the fetal heart. *ULTRASOUND OBSTETRICS GYNECOLOGY*, 22(4):8, 2003.
- [28] J.A. DiPietro. Maternal influences on the developing fetus. *NEURODEVELOPMENT: CLINICAL AND RESEARCH ASPECTS*, Chapter 3:14, 2010.
- [29] T. Eichele, S. Rachakonda, B. Brakedal, R. Eikeland, and V.D. Calhoun. Eegift: Group independent component analysis for event-related eeg data. *COMPUTATIONAL INTELLIGENCE AND NEUROSCIENCE*, 2011:9, 2011.
- [30] M. Elsabrouty, M. Bouchard, and T. Aboulnasr. A new on-line negentropy-based algorithm for blind source separation. *2003 IEEE 46TH MIDWEST SYMPOSIUM ON CIRCUITS AND SYSTEMS*, 2:4, 2003.
- [31] A.G. Favret. Computer matched filter location of fetal r-waves. *MEDICAL AND BIOLOGICAL ENGINEERING*, 6(5):11, 1968.
- [32] P. Gao, E. Chang, and L. Wyse. Blind separation of fetal eeg from single mixture using svd and ica, 15-18 December 2003 2003.
- [33] H.M. Gardiner, C. Belmar, L. Pasquini, S. Seale, M. Thomas, W. Dennes, M. Taylor, E. Kulinskaya, and R. Wimalasundera. Fetal eeg: A novel predictor of atrioventricular block in anti-ro positive pregnancies. *HEART*, 93(11):7, 2007.
- [34] D.B. Geselowitz. On the theory of the electrocardiogram. *PROCEEDINGS OF THE IEEE*, 77(6):20, 1989.
- [35] L. Gindes, J. Hegesh, B. Weisz, Y. Gilboa, and R. Achiron. Three and four dimensional ultrasound: A novel method for evaluating fetal cardiac anomalies. *PRENATAL DIAGNOSIS*, 29(7):9, 2009.
- [36] M. Girolami and C. Fyfe. Negentropy and kurtosis as projection pursuit indices provide generalised ica algorithms. *INFORMATION SYSTEMS JOURNAL*, 8, 1996.
- [37] L.F. Goncalves, W. Lee, T. Chaiworapongsa, J. Espinoza, M.L. Schoen, P. Falkensammer, M. Treadwell, and R. Romero. Four-dimensional ultrasonography of the

- fetal heart with spatiotemporal image correlation. *AMERICAN JOURNAL OF OBSTETRICS AND GYNERCOLOGY*, 189(6):11, 2003.
- [38] K. Hammouda and F. Karray. A comparative study of data clustering techniques. *UNIVERSITY OF WATERLOO, ONTARIO, CANADA*, 13(2-3):11, 1997.
- [39] M. A. Hasan, M. B. I. Reaz, M. I. Ibrahimy, M. S. Hussain, and J. Uddin. Detection and processing techniques of fecg signal for fetal monitoring. *BIOLOGICAL PROCEDURES ONLINE*, 11(1):33, 2009.
- [40] M.A. Hasan, M.I. Ibrahimy, and M.B.I. Reaz. Fetal eeg extraction from maternal abdominal eeg using neural network. *JOURNAL OF SOFTWARE ENGINEERING AND APPLICATIONS*, 2(5):5, 2009.
- [41] T. Hata, S. Dai, E. Inubashiri, K. Kanenishi, H. Tanaka, T. Yanagihara, and S. Araki. Four-dimensional sonography with b-flow imaging and spatiotemporal image correlation for visualization of the fetal heart. *JOURNAL OF CLINICAL ULTRASOUND*, 36(4):4, 2008.
- [42] D. Hoyer, R. Bauer, B. Walter, and U. Zwiener. Estimation of nonlinear couplings on the basis of complexity and predictability—a new method applied to cardiorespiratory coordination. *IEEE TRANSACTIONS ON BIOMEDICAL ENGINEERING*, 45(5):8, 1998.
- [43] <http://www.fetaldopplerfacts.org/facts/dopplers/fetal-heart-rate-facts.php>.
- [44] A. Hyvarinen, P. Hoyer, and E. Oja. A fast fixed-point algorithm for independent component analysis. *NEURAL COMPUTATION*, 9:10, 1997.
- [45] A. Hyvarinen, P. Hoyer, and E. Oja. Sparse code shrinkage: Denoising by nonlinear maximum likelihood estimation. *ADVANCES IN NEURAL INFORMATION PROCESSING SYSTEMS*, 11(1):7, 1999.
- [46] A. Hyvarinen and E. Oja. Independent component analysis: Algorithms and applications. *NEURAL NETWORKS*, 13(4-5):31, 2000.
- [47] M.I. Ibrahimy, F. Ahmed, M.A.M. Ali, and E. Zahedi. Real-time signal processing for fetal heart rate monitoring. *IEEE TRANSACTIONS ON BIOMEDICAL ENGINEERING*, 50(2):5, 2003.
- [48] P.C. Ivanov, Q.D.Y. Ma, and R.P. Bartsch. Maternal and fetal heartbeat phase synchronization. *PNAS*, 106(33):2, 2009.
- [49] M.G. Jafari and J.A. Chambers. Fetal electrocardiogram extraction by sequential source separation in the wavelet domain. *IEEE TRANSACTIONS ON BIOMEDICAL ENGINEERING*, 52(3):11, 2005.

- [50] C.J. James and C.W. Hesse. Independent component analysis for biomedical signals. *PHYSIOLOGICAL MEASUREMENT*, 26:25, 2005.
- [51] R. Jane, P. Laguna, N.V. Thakor, and P. Caminal. Adaptive baseline wander removal in the ecg: Comparative analysis with cubic spline technique, 11-14 Oct 1992 1992.
- [52] S. Janjarasjitt. *A NEW QRS DETECTION AND ECG SIGNAL EXTRSCTION TECHNIQUE FOR FETAL MONITORING*. Doctor of philosophy, 2006.
- [53] A. Jimenez-Gonzalez and C.J. James. Extracting sources from noisy abdominal phonograms: A single-channel blind source separation method. *MEDICAL BIOLOGICAL ENGINEERING COMPUTING*, 47:10, 2009.
- [54] A. Kam and A. Cohen. Detection of fetal ecg with iir adaptive filtering and genetic algorithms, 15-19 March 1999 1999.
- [55] P.P. Kanjilal, S. Palit, and G. Saha. Fetal ecg extraction from single-channel maternal ecg using singular value decomposition. *IEEE TRANSACTIONS ON BIOMEDICAL ENGINEERING*,, 44(1):9, 1997.
- [56] C. Kezi Selva Vijila and P. Kanagasabapathy. Intelligent technique of canceling maternal ecg in fecg extraction. *IRANIAN JOURNAL OF FUZZY SYSTEMS*, 5(1):19, 2008.
- [57] A. Khamene and S. Negahdaripour. A new method for the extraction of fetal ecg from the composite abdominal signal. *IEEE TRANSACTIONS ON BIOMEDICAL ENGINEERING*,, 47(4):10, 2000.
- [58] A. Khaparde, M. Madhavilatha, M.B.L. Manasa, P.A. Babu, and S.P. Kumar. Fastica algorithm for the separation of mixed images. *WSEAS TRANSACTIONS on SIGNAL PROCESSING*,, 4(5):8, 2008.
- [59] S. Kharabian, M.B. Shamsollahi, and R. Sameni. Fetal r-wave detection from multichannel abdominal ecg recordings in low snr, September 2-6, 2009 2009.
- [60] D. Kim, J. Choi, and J. Kim. Adaptive motion estimation based on spatio-temporal correlation. *SIGNAL PROCESSING: IMAGE COMMUNICATION*, 13(2):10, 1998.
- [61] J.A. Kors, G. Vanherpen, A.C. Sittig, and J.H. Van Bommel. Reconstruction of the frank vectorcardiogram from standard electrocardiographic leads: Diagnostic comparison of different methods. *EUROPEAN HEART JOURNAL*, 11(12):10, 1990.

- [62] E.J. Kostelich and T. Schreiber. Noise reduction in chaotic time-series data: A survey of common methods. *PHYSICAL REVIEW-C- NULCEAR PHYSICS*, 48(3):14, 1993.
- [63] M. Kotas. Projective filtering of time-aligned ecg beat. *IEEE TRANSCATIONS ON BIOMEDICAL ENGINEERING*, 51(7):11, 2004.
- [64] M. Kotas. Projective filtering of time-aligned beats for foetal ecg extraction. *BULLETIN OF THE POLISH ACADEMY OF SCIENCES*, 55(4):9, 2007.
- [65] .M Kotas. Combined application of independent component analysis and projective filtering to fetal. *BIOCYBERNETICS AND BIOMEDICAL ENGINEERING*, 28(1):19, 2008.
- [66] M. Lagerholm, C. Peterson, G. Braccini, L. Edenbrandt, and L. Sornmo. Clustering ecg complexes using hermite functions and self-organizing maps. *IEEE TRANSACTIONS ON BIOMEDICAL ENGINEERING*, 47(7):11, 2000.
- [67] P. Langley, E.J. Bowers, and A. Murray. Principal component analysis as a tool for analyzing beat-to-beat changes in ecg features: Application to ecg-derived respiration. *IEEE TRANSACTIONS ON BIOMEDICAL ENGINEERING*, 57(4):9, 2010.
- [68] C. Li, C. Zheng, and C. Tai. Detection of ecg characteristic points using wavelet transforms. *IEEE TRANSACTIONS ON BIOMEDICAL ENGINEERING*, 42(1):8, 1995.
- [69] A. Lombard, T. Rosenkranz, H. Buchner, and W. Kellermann. Multidimensional localization of multiple sound sources using averaged directivity patterns of blind source separation systems, 19-24 April 2009 2009.
- [70] S. Loncaric and Z. Majcenic. Optical flow algorithm for cardiac motion estimation, 23 Jul-28 Jul 2000 2000.
- [71] Y. Lu and M.N. Do. Multidimensional directional filter banks and surfacelets. *IEEE TRANSACTIONS ON IMAGE PROCESSING*, 16(4):14, 2007.
- [72] S.M.M. Martens, C. Rabotti, M. Mischi, and R.J. Sluijter. A robust fetal ecg detection method for abdominal recordings. *PHYSIOLOGICAL MEASUREMENT*, 28:17, 2007.
- [73] B. Mijovic, M. De Vos, I. Gligorijevic, J. Taelman, and S. Van Huffel. Source separation from single-channel recordings by combining empirical-mode decomposition and independent component analysis. *IEEE TRANSACTIONS ON BIOMEDICAL ENGINEERING*, 57(9):9, 2010.

- [74] A.K. Mitra and N.K. Choudhari. Development of a low cost fetal heart sound monitoring system for home care application. *JOURNAL BIOMEDICAL SCIENCE AND ENGINEERING*, 2(6):10, 2009.
- [75] F. Mochimaru, Y. Fujimoto, and Y. Ishikawa. Detecting the fetal electrocardiogram by wavelet theory-based methods. *PROGRESS IN BIOMEDICAL RESEARCH*, 7(3):9, 2002.
- [76] F. Mochimaru, Y. Fujimoto, and Y. Ishikawa. The fetal electrocardiogram by independent component analysis and wavelets. *JAPANESE JOURNAL OF PHYSIOLOGY*, 54:7, 2004.
- [77] R. Mrowka, A. Patzak, and M. Rosenblum. Quantitative analysis of cardiorespiratory synchronization in infants. *INTERNATIONAL JOURNAL OF BIFURCATION AND CHAOS (IJBC) IN APPLIED SCIENCES AND ENGINEERING*, 10(11):10, 2000.
- [78] J. Nagel and Joachim H. Progresses in fetal monitoring by improved data acquisition. *IEEE ENGINEERING IN MEDICINE AND BIOLOGY MAGAZINE*, 3(3):5, 1984.
- [79] J. Nagel and M. Schaldach. Processing of abdominal lead eeg and emg in perinatal monitoring, AUGUST 19-24, 1979 1979.
- [80] J. Nagel and M. Schaldach. Processing the abdominal fetal eeg using a new method. *FETAL AND NEONATEAL PHYSIOLOGICAL MEASUREMENTS*, page 7, 1980.
- [81] M. Nii, R.M. Hamilton, L. Fenwick, J.C.P. Kingdom, K.S. Roman, and E.T. Jaeggi. Assessment of fetal atrioventricular time intervals by tissue doppler and pulse doppler echocardiography: Normal values and correlation with fetal electrocardiography. *HEART*, 92(12):7, 2006.
- [82] S. Ogata. Improved spatio-temporal correlation method for velocity field measurements. *MEASUREMENT*, 32(1):11, 2002.
- [83] N.J. Outram, E.C. ifeachor, P.W.J. Van Eetvelt, and J.S.H. Curnow. Techniques for optimal enhancement and feature extraction of fetal electrocardiogram. *IEE PROCEEDINGS SCIENCE, MEASUREMENT AND TECHNOLOGY*, 142(6):8, 1995.
- [84] N.R. Pal, K. Pal, J.M. Keller, and J.C Bezdek. A possibilistic fuzzy c-means clustering algorithm. *IEEE TRANSACTIONS ON FUZZY SYSTEMS*, 13(4):14, 2005.

- [85] Y.C. Park, K.Y. Lee, D.H. Young, N.H. Kim, W.K. Kim, and S.H. Park. On detecting the presence of fetal r-wave using the moving averaged magnitude difference algorithm. *IEEE TRANSACTIONS ON BIOMEDICAL ENGINEERING*, 39(8):4, 1992.
- [86] S.D. Parmar and B. Unhelkar. On the performance analysis of the ica algorithms with maternal and fetal ecg signals inputs and contaminated noises. *INTERNATIONAL JOURNAL OF COMPUTER APPLICATIONS*, 2(7):5, 2010.
- [87] A.j. Patterson. *BLIND SOURCE SEPARATION OF SPEECH SIGNALS USING FILTER BANKS*. PhD thesis, 2002.
- [88] K. Papat. Cluster-based probability model and its application to image and texture processing. *IEEE TRANSACTIONS ON IMAGE PROCESSING*, 6(2):17, 1997.
- [89] M. Richter, T. Schreiber, and D.T. Kaplan. Fetal ecg extraction with nonlinear state-space projections. *IEEE TRANSACTIONS ON BIOMEDICAL ENGINEERING*, 45(1):5, 1998.
- [90] M. Riedl, P. Van Leeuwen, A. Suhrbier, H. Malberg, D. Gronemeyer, J. Kurths, and N. Wessel. Testing foetal-maternal heart rate synchronization via model-based analyses. *PHILOSOPHICAL TRANSACTIONS OF THE ROYAL SOCIETY A: MATHEMATICAL, PHYSICAL AND ENGINEERING SCIENCES*, 367(1892):16, 2009.
- [91] J. Rychik. Fetal cardiovascular physiology. *PEDIATRIC CARDIOLOGY*, 25(3):10, 2004.
- [92] R. Sameni and G.D. Clifford. A review of fetal ecg signal processing; issues and promising directions. *THE OPEN PACING, ELECTROPHYSIOLOGY THERAPY JOURNAL*, 3:17, 2010.
- [93] R. Sameni, C. Jutten, and M.B. Shamsollahi. Multichannel electrocardiogram decomposition using periodic component analysis. *IEEE TRANSACTIONS ON BIOMEDICAL ENGINEERING*, 55(8):6, 2008.
- [94] R. Sameni, M.B. Shamsollahi, C. Jutten, and G.D. Clifford. A nonlinear bayesian filtering framework for ecg denoising. *IEEE TRANSACTIONS ON BIOMEDICAL ENGINEERING*, 54(12):14, 2007.
- [95] S. Saranya and S. Priyadharsini. A novel hybrid soft computing technique for extracting fetal ecg from maternal ecg signal. *INTERNATIONAL JOURNAL OF COMPUTER APPLICATIONS*, 3(8):7, 2010.

- [96] A.V. Sazonov, C.K. Ho, J.W.M. Bergmans, J.B.A.M. Arends, P.A.M. Griep, E.A. Verbitskiy, P.J.M. Cluitmans, and P.A.J.M. Boon. An investigation of the phase locking index for measuring of interdependency of cortical source signals recorded in the eeg. *BIOLOGICAL CYBERNETICS*, 100:18.
- [97] M. Shao, K.E. Barner, and M.H. Goodman. An interference cancellation algorithm for noninvasive extraction of transabdominal fetal electroencephalogram (tafeeg). *IEEE TRANSACTIONS ON BIOMEDICAL ENGINEERING*, 51(3):13, 2004.
- [98] Z. Shi, H. Zhang, X. Tan, and Z. Jiang. Blind source separation using quadratic form innovation. *NEURAL PROCESS LETTER*, 33:15, 2011.
- [99] B.H. Smaill, I.J. LeGrice, D.A. Hooks, A.J. Pullan, B.J. Caldwell, and P.J. Hunter. Cardiac structure and electrical activation: Models and measurement. *PROCEEDINGS OF THE AUSTRALIAN PHYSIOLOGICAL AND PHARMACOLOGICAL SOCIETY*, 34(12):9, 2004.
- [100] R. Swarnalatha and D.V. Prasad. Interference cancellation in fecg using wavelet-adaptive filtering technique. *JOURNAL OF ENGINEERING AND APPLIED SCIENCES*, 4(5-6):5, 2009.
- [101] R. Swarnalatha and D.V. Prasad. Maternal eeg cancellation in abdominal signal using anfis and wavelets. *JOURNAL OF APPLIED SCIENCES*, 10(11):10, 2010.
- [102] A. Ta-Shma, Z. Perles, S. Gavri, J. Golender, S. Tarshansky, C. Shlichter, H.B. Tov, and A.J.J.T. Rein. Analysis of segmental and global function of the fetal heart using novel automatic functional imaging. *JOURNAL OF THE AMERICAN SOCIETY OF ECHOCARDIOGRAPHY*, 21(2):5, 2007.
- [103] J. Taelman and S. Van Huffel. Wavelet-independent component analysis to remove electrocardiography contamination in surface electromyography. In *PROCEEDINGS OF THE 29TH ANNUAL INTERNATIONAL CONFERENCE OF THE IEEE EMBS*, page 4, 2007.
- [104] J. Taghia and M.A. Doostari. Subband-based single-channel source separation of instantaneous audio mixtures. *WORLD APPLIED SCIENCES JOURNAL*, 6(6):9, 2009.
- [105] L. Tapobrata, K. Upendra, M. Hrishikesh, S. Subrata, and R. Arunava Das. Analysis of eeg signal by chaos principle to help automatic diagnosis of myocardial infarction. *JOURNAL OF SCIENTIFIC INDUSTRIAL RESEARCH*, 68:5, 2009.
- [106] P. Tass, M.G. Rosenblum, J. Weule, J. Kurths, A. Pikovsky, J. Volkmann, A. Schnitzler, and H.J. Freund. Detection of n:m phase locking from noisy

- data: Application to magnetoencephalography. *PHYSICAL REVIEW LETTERS*, 81(15):4, 1998.
- [107] N.V. Thakor and Y. Zhu. Applications of adaptive filtering to ecg analysis : Noise cancellation and arrhythmia detection. *IEEE TRANSACTIONS ON BIOMEDICAL ENGINEERING.*, 38(8):10, 1991.
- [108] M. Unguranu and W.M. Wolf. Basic aspects concerning the event-synchronous interference canceller. *IEEE TRANSCATIONS ON BIOMEDICAL ENGINEERING*, 53(11):8, 2006.
- [109] G.M. Ungureanua, J.M. JBergmansb, S. GuidOeic, A. Ungureanua, and W. Wolfd. The event synchronous canceller algorithm removes maternal ecg from abdominal signals without affecting the fetal ecg. *COMPUTERS IN BIOLOGY AND MEDICINE*, 39(6):6, 2009.
- [110] P. Van Leeuwen, D. Geue, and Gronemeyer D.H.W Lange, S. Modeling fetal-maternal heart-rate interaction. *IEEE ENGINEERING IN MEDICINE AND BIOLOGY MAGAZINE*, 28(6):5, 2009.
- [111] P. Van Leeuwen, D. Geue, S. Lange, D. Cysarz, H. Bettermann, and D.H.W. Gronemeyer. Is there evidence of fetal-maternal heart rate synchronization? *BMC PHYSIOL*, 3(2):11, 2003.
- [112] A. Van Oosterom. Spatial filtering of the fetal electrocardiogram. *JOURNAL OF PERINATAL MEDICINE*, 14(6):9, 1986.
- [113] V. Vigneron, A. Paraschiv-Ionescu, A. Azancot, C. Jutten, and O. Sibony. Fetal electrocardiogram extraction based on non-stationary ica and wavelet denoising, 2003.
- [114] R. Vullings, B. De Vries, and J.W.M Bergmans. An adaptive kalman filter for ecg signal enhancement. *IEEE TRANSACTIONS ON BIOMEDICAL ENGINEERING.*, 58(4):10, 2011.
- [115] R. Vullings, C. Peters, M. Mischi, G. Oei, and J. Bergmans. Maternal ecg removal from non-invasive fetal ecg recordings, Aug 30-Sept 3, 2006 2006.
- [116] R. Vullings, C. Peters, M. Mischi, R. Sluijter, G. Oei, and J. Bergmans. Artifact reduction in maternal abdominal ecg recordings for fetal ecg estimation, August 23-26, 2007. 2007.

- [117] R. Vullings, C.H.L. Peters, M.J.M. Hermans, P.F.F. Wijn, S.G. Oei, and F.W.M. Bergmans. A robust physiology-based source separation method for qrs detection in low amplitude fetal ecg recordings. *PHYSIOLOGICAL MEASUREMENT*, 31:18, 2010.
- [118] J. Wei, C. Chang, N. Chou, and G. Jan. Ecg data compression using truncated singular value decomposition. *IEEE TRANSACTIONS ON INFORMATION TECHNOLOGY IN BIOMEDICINE*, 5(4):10, 2001.
- [119] B. Widrow, J.R.Jr. Glover, J.M. Mccool, J. Kaunitz, C.S. Williams, R.H. Hean, J.R. Zeidler, E.Jr. Dong, and R.C. Goodlin. Adaptive noise cancelling: Principles and applications. *PROCEEDINGS OF THE IEEE*, 63(12):26, 1975.
- [120] J.D. Wilson, R.B. Govindan, J.O. Hatton, C.L. Lowery, and H. Preissl. Integrated approach for fetal qrs detection. *IEEE TRANSACTIONS ON BIOMEDICAL ENGINEERING*, 55(9):8, 2008.
- [121] H. Xiong, G. Pandey, M. Steinbach, and V. Kumar. Enhancing data analysis with noise removal. *IEEE TRANSACTIONS ON KNOWLEDGE AND DATA ENGINEERING*, 18(3):16, 2006.
- [122] Y. Ye, Z. Zhang, J. Zeng, and L. Peng. A fast and adaptive ica algorithm with its application to fetal electrocardiogram extraction. *APPLIED MATHEMATICS AND COMPUTATION*, 205(2):8, 2008.
- [123] V. Zarzoso and A.K. Nandi. Noninvasive fetal electrocardiogram extraction: Blind separation versus adaptive noise cancellation. *IEEE TRANSACTIONS ON BIOMEDICAL ENGINEERING*, 48(1):7, 2001.
- [124] V. Zarzoso, A.K. Nandi, and E. Bacharakis. Maternal and foetal ecg separation using blind source separation method. *IMA JOURNAL OF MATHEMATICS APPLIED IN MEDICINE AND BIOLOGY*, 14(3):12, 1997.

# Appendix

The normalise of various signal value range to the same level

```
maxV=max(input);  
minV=min(input);  
output(:,1)=(input-minV)./(maxV-minV);
```

The normalisation of length of comparing vector

```
check=int32(n/num*i);  
output(i,1)=input(check);
```

The smooth function to remove baseline wander, where *bw* is the estimated baseline wander signal

```
bw = smooth(si1,0.1,'rloess');  
sigp(:,i)=si1-bw;
```

The alignment of the abdominal and the thoracic signal before constructing the multi-dimension matrix for SCICA is by calculating the cross correlation between the two signals, where *absg* and *sig2* are the abdominal and the thoracic signals

```
X1=xcorr(absg,sig2);  
[nou,dis] = max(X1);  
delay = dis - max(length(absg),length(sig2));
```

The generation of multi-dimension matrix from a single vector, where *tor* is the delay in time scale

```
snt(i,j)=sig2(i-(j-1)*tor);
```

The independent component analysis is in the iterative loop to optimise the demixing coefficient *wk*,

```

y=z'*wk;
G=(1/a1).*log(cosh(a1.*(y)));
g=tanh(a1.*(y));
wk1=((z)*(G))-sum(g)'*(wk))/sz(1,2);

```

The fECG and mECG peaks are extracted by function *findpeaks* where *h* and *d* are parameters for various ECG pattern feature

```
[mp,lp] = findpeaks(x,'minpeakheight',h,'minpeakdistance',d);
```

The heart rate of fECG, where *lfk* is the fECG peaks in time scale

```
dm{lp1,1} = 60000./diff(lfk);
```

The synchronisation phase of fECG peaks in different primary cycle, where *lkf* is fECG peak and *mc* is primary cycle

```

mc=mulC(lkm,ml);
[nphas,nphas1] = multC(lkf,mc);
dpha1 = mod(nphas,2*pi)/(2*pi);
dpha2 = mod(nphas1(:,1),2*pi)/(2*pi);

```

Function *mulC* is to generate the time point of the primary cycle by finding the peak location of mECG as start and end of the primary cycle. The original synchronisation phase without normalisation into  $[0, 2\pi]$

```
phasm = 2*pi*(sig1(k) - sig2(m))/(sig2(m+1) - sig2(m)) + 2*pi*k;
```

The phase locking value of synchronisation point is calculated from neighbour synchronisation epoch as difference in time points

```

mt2(dl3,dl2)=(len(ps)-len(mt(dl3,(dl2-1)*2+1)))/((intv-1)*1000);
mtt2(dl3,dl2)=(len(ps))/1000;

```

The bandpass filter to remove excessive noise

```

hs = fdesign.bandpass('n,fc1,fc2',30,(i1-1)*10+1+50,i1*10+50,1000);
Hd = design(hs);
mt(:,i1)=filter(Hd,pr);

```

The adaptive filter to separate ECG signals from abdominal recording

```
P0 = 10*eye(100);  
lam = 32;  
ha = adaptfilt.rls(100,lam,P0);  
[y, e] = filter(ha, nmtf1, nmtm);
```

The notch filter to remove power line noise, where the frequency is set to 50 Hz

```
Wo = 50/(1000/2); BW = Wo/35;  
[b, a] = irrnotch(Wo, BW);  
sign3 = filter(b, a, sig1);
```



**Minerva Access is the Institutional Repository of The University of Melbourne**

**Author/s:**

Wang, Qianqian

**Title:**

The synchronisation relationship between fetal and maternal cardiovascular systems

**Date:**

2015

**Persistent Link:**

<http://hdl.handle.net/11343/55635>

**File Description:**

The Synchronisation Relationship Between Fetal and Maternal cardiovascular systems